UNIVERSIDADE FEDERAL DO RIO GRANDE DO SUL
INSTITUTO DE CIÊNCIAS BÁSICAS DA SAÚDE
PROGRAMA DE PÓS-GRADUAÇÃO EM CIÊNCIAS BIOLÓGICAS: BIOQUÍMICA

RAFAEL TEIXEIRA RIBEIRO

ALTERAÇÕES NEUROQUÍMICAS E NEUROCOMPORTAMENTAIS CAUSADAS PELA ADMINISTRAÇÃO *IN VIVO* DO ÁCIDO L-2-HIDROXIGLUTÁRICO EM RATOS NEONATOS E DISFUNÇÃO ENERGÉTICA PROVOCADA PELO ÁCIDO D-2-HIDROXIGLUTÁRICO *IN VITRO* EM CORAÇÃO DE RATOS ADOLESCENTES

Porto Alegre
2023

Rafael Teixeira Ribeiro

ALTERAÇÕES NEUROQUÍMICAS E NEUROCOMPORTAMENTAIS CAUSADAS PELA ADMINISTRAÇÃO *IN VIVO* DO ÁCIDO L-2-HIDROXIGLUTÁRICO EM RATOS NEONATOS E DISFUNÇÃO ENERGÉTICA PROVOCADA PELO ÁCIDO D-2-HIDROXIGLUTÁRICO *IN VITRO* EM CORAÇÃO DE RATOS ADOLESCENTES

Tese apresentada ao Programa de Pós-Graduação em Ciências Biológicas: Bioquímica do Instituto de Ciências Básicas da Saúde da Universidade Federal do Rio Grande do Sul como requisito parcial para a obtenção do título de doutor em Bioquímica.

Orientador: Prof. Dr. Moacir Wajner

Porto Alegre

2023

CIP - Catalogação na Publicação

Ribeiro, Rafael Teixeira
ALTERAÇÕES NEUROQUÍMICAS E NEUROCOMPORTAMENTAIS CAUSADAS PELA ADMINISTRAÇÃO IN VIVO DO ÁCIDO L-2-HIDROXIGLUTÁRICO EM RATOS NEONATOS E DISFUNÇÃO ENERGÉTICA PROVOCADA PELO ÁCIDO D-2-HIDROXIGLUTÁRICO IN VITRO EM CORAÇÃO DE RATOS ADOLESCENTES / Rafael Teixeira Ribeiro. -- 2023.
102 f.
Orientador: Moacir Wajner.

Tese (Doutorado) -- Universidade Federal do Rio Grande do Sul, Instituto de Ciências Básicas da Saúde, Programa de Pós-Graduação em Ciências Biológicas: Bioquímica, Porto Alegre, BR-RS, 2023.

1. Acidúria L-2-Hidroxiglutárica. 2. Acidúria D-2-Hidroxiglutárica. 3. Erros Inatos do Metabolsimo. 4. Homeostase Redox. 5. Bioenergética. I. Wajner, Moacir, orient. II. Título.

Elaborada pelo Sistema de Geração Automática de Ficha Catalográfica da UFRGS com os dados fornecidos pelo(a) autor(a).

“She had studied the universe all her life, but had overlooked its clearest message: For small creatures such as we the vastness is bearable only through love.”

- Carl Sagan, Contact.

AGRADECIMENTOS

À Universidade Federal do Rio Grande do Sul por me proporcionar formação gratuita e de excelência.

Aos órgãos de fomento, CNPq, CAPES e FAPERGS, pelo apoio financeiro.

Ao Departamento e ao PPG Bioquímica, por fornecer todo o suporte necessário para o desenvolvimento desse trabalho e aos funcionários e professores por todo o profissionalismo e competência.

Ao meu orientador professor Moacir Wajner que sempre me incentivou a realizar um bom trabalho e proveu os meios para que minha tese virasse realidade, mas principalmente por todo incentivo, ensinamentos, carinho e respeito que venho recebendo ao longo de quase uma década de trabalho conjunto.

À Bianca Seminotti, ou simplesmente Bi, pelo acolhimento no laboratório 38 quando eu tinha acabado de ingressar na faculdade de farmácia e não sabia nem pipetar, e que através de sua a ajuda, paciência, trabalho duro e por partilhar da sua experiência de bancada, conhecimento e amizade foi essencial na minha formação como pesquisador.

Ao professor Alexandre Amaral, pela contribuição fundamental em "questões mitocondriais" e por estar sempre disposto a ajudar.

À professora Simone Magagnin Wajner, que disponibilizou a estrutura e recursos de seu laboratório viabilizando as investigações nas células H9c2.

Ao professor Carlos Alexandre Netto e aos colegas do laboratório 35, pela parceria inestimável para realização das avaliações comportamentais.

Ao professor Guilhian Leipnitz, pela amizade e por estar sempre disponível a boa discussão científica que contribui muito para a qualidade das nossas investigações.

Ao Rafael Palavro, aluno de iniciação, que auxiliou de forma imensurável na realização deste trabalho.

Aos muitos colegas que passaram pelos laboratórios 38 e 34 durante a minha jornada, em especial a Ânge, Cris, Mateus e Bel, que juntamente com a "nova geração" de pós-graduandos formados pela Ângela, Júlia, Manuela e Josy tornam nosso grupo competente e com fortes vínculos de amizade.

Aos meus melhores amigos cientistas por todo aprendizado, leveza e companheirismo que eles demonstraram ao logo desses quase 4 anos. À Ana Cristina, por todo auxílio com as mitocondrias cardíacas e corridas de oroboros e que mesmo estando um continente de distância, se mantem presente em pensamentos e no coração. Ao querido amigo e colega Rafael Marschner, pela energia contagiante, colaboração e tratamento das células às 5h da manhã, o qual sei que posso contar em todos os momentos. Às minhas amadas, Morgana e Camila, por todo aprendizado, risadas, viagens de férias coletivas e amizade que foram fundamentais pra eu conseguir superar com leveza e muitas risadas os desafios impostos por longos anos de pandemia.

Ao Andrey, meu companheiro e colaborador científico, por todo carinho, apoio, amizade e principalmente amor ao compartilhar sua vida comigo. Além é claro, do auxílio fundamental para execução e análise dos parâmetros comportamentais.

À minha vó Fátima, segunda mãe, que jamais mediu esforços para que eu realizasse meus sonhos.

À minha tia Léia, cujo acolhimento em Porto Alegre e as demonstrações diárias de carinho tornaram possível o início dessa longa jornada.

Aos meus pais, que sempre acreditaram e incentivaram todos meus sonhos.

SUMÁRIO

RESUMO

As acidúrias D-2-hidroxiglutárica (D-2-HGA) e L-2-hidroxiglutárica (L-2-HGA) são distúrbios neurometabólicos caracterizados bioquimicamente pelo acúmulo tecidual e elevada excreção urinária dos ácidos D-2-hidróxiglutárico (D-2-HG) e L-2-hidroxiglutárico (L-2-HG), respectivamente. A D-2HGA tipo 1 (D-2-HGA1) é causada por mutações patogênicas no gene que codifica a enzima mitocondrial D-2-hidroxiglutarato desidrogenase (D-2-HGDH), enquanto mutações de ganho de função da enzima isocitrato desidrogenase 2 (IDH2) são a causa da D-2HGA2. As manifestações clínicas da D-2HGA1 e D-2-HGA2 são predominantemente neurológicas tais como convulsões, hipotonia e atraso no desenvolvimento psicomotor, devido a isso são consideradas acidemias orgânicas cerebrais. No entanto, a D-2HGA2 é mais severa, manifestando-se no período neonatal com alto risco de vida causada pela cardiomiopatia que acomete metade dos pacientes, ocorrendo concomitante a graves manifestações neurológicas, enquanto a D-2HGA1 corresponde a uma variante mais branda da doença com sinais exclusivamente neurológicos. Por outro lado, a acidúria L-2-hidroxiglutárica (L-2-HGA) tem como causa mutações patogênicas no gene que codifica a enzima mitocondrial FAD-dependente L-2-hidroxiglutarato desidrogenase (L-2-HGDH). Os pacientes afetados pela L-2-HGA apresentam um fenótipo clínico mais brando, homogêneo e progressivo, apresentando exclusivamente sinais neurológicos, como atraso no desenvolvimento motor e cognitivo, epilepsia, ataxia cerebelar, macrocefalia e sintomas extrapiramidais, tais como tremor e distonia, sendo também considerada uma acidúria orgânica cerebral. A neuropatologia da D-2HGA é caracterizada por atraso na maturação cerebral e anormalidades na substância branca cerebral, com alargamento dos ventrículos laterais e alterações anatômicas nos gânglios da base, enquanto a L-2HGA apresenta alterações na substância branca (leucodistrofia) e anormalidades no córtex cerebral, nos núcleos da base (núcleo denteado, globo pálido, putamen e no núcleo caudado) e no cerebelo. Tendo em vista que a patogênese do dano cerebral nos pacientes afetados por essas doenças ainda é pouco conhecida, bem como da cardiomiopatia da D-2HGA2, a presente investigação teve por objetivo inicial avaliar os efeitos ex vivo da administração intracerebroventricular (icv) do L-2HG a ratos neonatos sobre a homeostase redox no cerebelo, bem como parâmetros imunohistoquimicos de viabilidade neuronal, reatividade astrocitária, ativação microglial e mielinização no córtex cerebral e estriado dos animais. Também foram avaliados os efeitos da administração icv de L-2-HG sobre o desenvolvimento neurocomportamental, motor e cognitivo. Em alguns experimentos, os animais foram pré-tratados intraperitonealmente com o antioxidante melatonina uma hora antes da administração icv de L-2HG. Por fim, avaliamos os efeitos in vitro do D-2-HG sobre a homeostase energética em coração de ratos adolescentes e em culturas de cardiomioblastos (H9c2). Inicialmente, avaliamos os efeitos do L-2-HG 6 horas após a administração icv sobre os parâmetros de homeostase redox no cerebelo. Os resultados mostraram que a administração de L-2-HG aumentou a oxidação da 2',7' - diclorofluoresceína (DCFH), refletindo uma maior produção de espécies reativas de oxigênio (EROs), acompanhada de uma maior lipoperoxidação, determinada pelo aumento significativo nos níveis de malondialdeído (MDA). A injeção icv do metabólito provocou alterações do sistema antioxidante cerebelar, diminuindo as concentrações de glutationa reduzida (GSH) e aumentando as atividades das enzimas antioxidantes glutationa peroxidase (GPx) e superóxido dismutase (SOD), indicando um provável mecanismo compensatório com aumento da transcrição gênica dessas enzimas secundário a elevação das espécies reativas no cerebelo dos animais neonatos. Demonstramos também que o pré-tratamento com melatonina preveniu totalmente o aumento na produção de EROs, a lipoperoxidação e a diminuição do GSH, sem alterar as atividades

das enzimas antioxidantes. Na sequência, observamos nos dias pós-natais (DPN) 15 e 75, que a administração neonatal do metabólito aumentou significativamente o conteúdo da proteína glial fibrilar ácida (GFAP) e da proteína ligante de cálcio S100B, indicando aumento da reatividade astrocitária, bem como induziu a diminuição do número de células NeuN-positivas (perda neuronal), aumentou o conteúdo de Iba1 (ativação microglial) e redução das proteínas de mielina MBP e CNPase (distúrbio na mielinização) no córtex cerebral e no estriado. Além disso, a melatonina preveniu esses efeitos, sugerindo que o estresse oxidativo pode estar relacionado a esses efeitos deletérios do L-2-HG. Por fim, observou-se que uma única injeção icv de L-2-HG no período neonatal causou atraso no neurodesenvolvimento de ratos jovens e déficit cognitivo e motor nestes animais em idade adulta. Mais uma vez, a melatonina preveniu o comprometimento do desenvolvimento neuromotor e o déficit cognitivo provocado pelo L-2-HG. Em conjunto, nossos dados fornecem pela primeira vez evidências de vários mecanismos patológicos de dano cerebral causados pelo principal metabólito acumulado na L-2-HGA administrado a ratos neonatos e, mais importante, que a melatonina foi capaz de prevenir a maioria das alterações neuroquímicas, histológicas e comportamentais provocadas por este metabólito, indicando que o estresse oxidativo pode ser central na patogênese da L-2-HGA. Nesse particular, o uso de antioxidantes poderia representar uma nova estratégia terapêutica para a doença.

O presente trabalho também investigou a toxicidade do D-2-HG sobre o coração, estudando seus efeitos *in vitro* sobre um amplo espectro de parâmetros do metabolismo energético em coração de ratos jovens e em cardiomioblastos cultivados (H9c2). O D-2-HG inibiu a respiração celular em preparações mitocondriais purificadas e homogeneizados brutos de coração de ratos jovens, bem como em células H9c2. A produção de ATP e as atividades das enzimas citocromo c oxidase (complexo IV), alfa-cetoglutarato desidrogenase, citrato sintase e creatina quinase também foram inibidas pelo D-2-HG, enquanto as atividades dos complexos I, II e II-III da cadeia respiratória, glutamato, succinato e malato desidrogenases não foram alterados. Também verificamos que este ácido orgânico comprometeu a capacidade de retenção de Ca^{2+} mitocondrial em preparações mitocondriais de coração. Finalmente, o D-2-HG reduziu a viabilidade dos cardiomioblastos H9c2 cultivados, como determinado por uma diminuição do MTT e aumento da incorporação de iodeto de propídio. Enfatize-se que o L-2-HG não alterou alguns desses parâmetros (atividades do complexo IV e da creatina quinase) em preparações mitocondriais do coração, indicando um efeito inibitório seletivo do enantiômero D. Em conclusão, presume-se que o D-2-HG compromete a bioenergética mitocondrial e a capacidade de retenção de Ca^{2+}, o que pode contribuir potencialmente para a cardiomiopatia comumente observada na D2HGA2. Assim, drogas estimuladoras da respiração celular, tais como o bezafibrato, e a triheptanoína que é uma droga anaplerótica poderiam beneficiar os pacientes com essa doença.

ABSTRACT

D-2-hydroxyglutaric aciduria (D-2-HGA) and L-2-hydroxyglutaric aciduria (L-2-HGA) are neurometabolic disorders biochemically characterized by tissue accumulation and high urinary excretion of D-2-hydroxyglutaric acid (D -2-HG) and L-2-hydroxyglutaric acid (L-2-HG), respectively. D-2HGA type 1 (D-2-HGA1) is caused by pathogenic mutations in the gene encoding the mitochondrial enzyme D-2-hydroxyglutarate dehydrogenase (D-2-HGDH), while mutations with gain of function of the enzyme isocitrate dehydrogenase 2 (IDH2) causes D-2HGA2. The clinical manifestations of D-2HGA1 and D-2-HGA2 are predominantly neurological, including seizures, hypotonia and delayed psychomotor development, hence they are considered cerebral organic acidurias. However, D-2HGA2 is more severe, manifesting in the neonatal period with high risk of life caused by the cardiomyopathy that affects one third of patients, occurring concomitantly with severe neurological manifestations, while D-2HGA1 corresponds to a milder variant of the disease with exclusively neurological signs. On the other hand, L-2-hydroxyglutaric aciduria (L-2-HGA) is caused by pathogenic mutations in the gene encoding the mitochondrial FAD-dependent enzyme L-2-hydroxyglutarate dehydrogenase (L-2-HGDH). Patients affected by L-2-HGA have a milder, homogeneous and progressive clinical phenotype, presenting exclusively neurological signs, such as delayed motor and cognitive development, epilepsy, cerebellar ataxia, macrocephaly and extrapyramidal symptoms, such as tremor and dystonia, being also considered a cerebral organic aciduria. The neuropathology of D-2HGA is characterized by delayed brain maturation and abnormalities in the cerebral white matter, with enlargement of the lateral ventricles and anatomical changes in the basal ganglia, while L-2HGA has white matter changes (leukodystrophy) and abnormalities in the cerebral cortex, the basal ganglia (dentate nucleus, globus pallidus, putamen, and caudate nucleus), and the cerebellum. Considering that the pathogenesis of brain damage in patients affected by these diseases is still poorly understood, as well as of D-2HGA2 cardiomyopathy, the present investigation initially aimed to evaluate the *ex vivo* effects of intracerebroventricular (icv) administration of L-2HG to neonatal rats on redox homeostasis in the cerebellum, as well as immunohistochemical parameters of neuronal viability, astrocyte reactivity, microglial activation, and myelination in the cerebral cortex and striatum of the animals. The effects of icv administration of L-2-HG on neurobehavioral, motor and cognitive development were also evaluated. In some experiments, animals were intraperitoneally pretreated with the antioxidant melatonin one hour before icv administration of L-2HG. Finally, we evaluated the in vitro effects of D-2-HG on energy homeostasis in adolescent rat hearts and in cardiomyoblast (H9c2) cultures. Initially, we evaluated the effects of L-2-HG 6 hours after icv administration on redox homeostasis parameters in the cerebellum. The results showed that L-2-HG administration increased the oxidation of 2',7' -dichlorofluorescein (DCFH), reflecting an increased production of reactive oxygen species (ROS), accompanied by an increased lipoperoxidation, determined by a significant increase in malondialdehyde (MDA) levels. The icv injection of the metabolite also altered the brain antioxidant system, decreasing the concentrations of reduced glutathione (GSH) and increasing the activities of the antioxidant enzymes glutathione peroxidase (GPx) and superoxide dismutase (SOD), indicating a likely compensatory mechanism with increased gene transcription of these enzymes secondary to the elevation of reactive species in the cerebellum of neonatal animals. We also demonstrated that pretreatment with melatonin totally prevented the increase in ROS production, lipid peroxidation and decrease in GSH, without altering the activities of the antioxidant enzymes. Subsequently, we observed at postnatal days (PND) 15 and 75, that neonatal administration of the metabolite significantly increased the content of glial fibrillary

acidic protein (GFAP) and calcium-binding protein S100B, indicating increased astrocyte reactivity, as well as induced a decrease in the number of NeuN-positive cells (neuronal loss), increased Iba1 content (microglial activation) and reduced myelin proteins MBP and CNPase (disturbance in myelination) in the cerebral cortex and striatum. Furthermore, melatonin prevented these effects, suggesting that oxidative stress may be involved in these deleterious effects. Finally, it was observed that a single icv injection of L-2-HG in the neonatal period caused delayed neurodevelopment in young rats and cognitive and motor deficits in these animals at adulthood. Once again, melatonin prevented the impairment of neuromotor development and cognitive deficit caused by L-2-HG. Taken together, our data provide for the first time evidence for several pathological mechanisms of brain damage caused by the major metabolite accumulated in L-2-HGA administered to neonatal rats and, more importantly, that melatonin was able to prevent most of the neurochemical, histological and behavioral changes caused by this metabolite, indicating that oxidative stress may be central to the pathogenesis of L-2-HGA. We propose that antioxidants may serve in the future as adjunctive therapy for patients with L-2-HGA.

The present work also investigated the toxicity of D-2-HG on the heart, studying its in vitro effects on a wide spectrum of energy metabolism parameters in young rat hearts and in cultured cardiomyocytes (H9c2). D-2-HG inhibited cellular respiration in purified mitochondrial preparations and crude homogenates from young rat hearts, as well as in H9c2 cells. ATP production and the activities of cytochrome c oxidase (complex IV) of the respiratory chain, as well as of alpha-ketoglutarate dehydrogenase, citrate synthase and creatine kinase were also inhibited by D-2-HG, while the activities of complexes I, II and II- II, glutamate, succinate and malate dehydrogenases were not altered. We also verified that this organic acid compromised the mitochondrial Ca^{2+} retention capacity in mitochondrial preparations from the heart and in H9c2 myoblasts. Finally, D-2-HG reduced the viability of cultured H9c2 cells, as determined by a decrease in MTT and by an increase in propidium iodide incorporation. It should be emphasized that L-2-HG did not change some of these parameters (complex IV and creatine kinase activities) in heart mitochondrial preparations, indicating a selective inhibitory effect of the D-enantiomer. In conclusion, it is assumed that D-2-HG compromises mitochondrial bioenergetics and Ca^{2+} retention capacity, which could potentially contribute to the cardiomyopathy commonly seen in D2HGA2. Thus, drugs that stimulate cellular respiration, such as bezafibrate, and triheptanoin, which is an anaplerotic drug, could benefit patients with this disease.

LISTA DE ABREVIATURAS

2-HG – ácido 2-hidróxiglutárico

2-KG – α-cetoglutarato

CAC – ciclo do ácido cítrico

CE-MS/MS – eletroforese capilar hifenizada com espectrometria de massa em tandem

CNPase – 2',3'-nucleotídeo cíclico 3'-fosfodiesterase

CRM – cadeia respiratória mitocondrial

D-2-HG – ácido D-2-hidroxiglutárico

D-2-HGA – acidúria D-2-hidroxiglutárica

D-2-HGA1 – acidúria D-2-hidroxiglutárica tipo 1

D-2-HGA2 – acidúria D-2-hidroxiglutárica tipo 2

D-2-HGDH – D-2-hidroxiglutarato desidrogenase

DCFH – 2',7'- diclorofluoresceína

DPN – dia pós-natal

ERN – espécie reativa de nitrogênio

ERO – espécie reativa de oxigênio

FAD – flavina adenina dinucleotídeo de sódio

GC-MS – cromatografia gasosa acoplada à espectrometria de massa

GFAP – proteína glial fibrilar ácida

GPx – glutationa peroxidase

GSH – glutationa reduzida

H_2O_2 – peróxido de hidrogênio

HOT – hidróxiácido-oxoácido transidrogenase

Iba1 – molécula adaptadora ligante de cálcio ionizado-1

ICV – intracerebroventricular

IDH2 – isocitrato desidrogenase 2

L-2-HG – ácido L-2-hidróxiglutárico

L-2-HGA – acidúria L-2-hidroxiglutárica

L-2-HGDH – L-2-hidroxiglutarato desidrogenase

L-malDH – L-malato desidrogenase

MBP – proteína básica da mielina

MDA – malondialdeído

NADH - nicotinamida adenina dinucleotídeo reduzido

NADPH – nicotinamida adenina dinucleótido fosfato reduzido

NeuN - proteína nuclear neuronal

NMDA - N-metil-D-aspartato

$NO^{\bullet}$ – óxido nítrico

O_2 – oxigênio molecular

$O2^{\bullet -}$ – ânion superóxido

OH• – radical hidroxila

$ONOO^-$ – peroxinitrito

OPCs – células precursoras de oligodendrócitos

PTP - Poro de transição de permeabilidade mitocondrial

S100B – Proteína ligante de cálcio S100B

SNC – sistema nervoso central

SOD – superóxido dismustase

YKL040 – glicoproteína cartilaginosa 40

PARTE I: INTRODUÇÃO E OBJETIVOS

1. INTRODUÇÃO

1.1. Acidúrias orgânicas

As acidemias ou acidúrias orgânicas formam um grupo de doenças hereditárias metabólicas caracterizadas pelo acúmulo de um ou mais ácidos orgânicos nos líquidos biológicos e tecidos dos pacientes afetados, sendo causadas pela deficiência da atividade de enzimas do metabolismo de aminoácidos, lipídeos ou carboidratos (Chalmers e Lawson, 1983). A frequência destas doenças na população em geral é pouco conhecida, o que pode ser creditado à falta de laboratórios especializados para o seu diagnóstico e ao desconhecimento médico sobre essas enfermidades. Na Holanda, país considerado referência para o diagnóstico de erros inatos do metabolismo, a incidência destas doenças é estimada em 1: 2.200 recém-nascidos, enquanto que, na Alemanha, Israel e Inglaterra é de aproximadamente 1: 6.000 - 1: 9.000 recém-nascidos (Hoffmann et al., 2004). Na Arábia Saudita, onde a taxa de consanguinidade é elevada, a frequência é de 1: 740 nascidos vivos (Rashed et al., 1994). Chalmers e colaboradores (Chalmers et al., 1980) demonstraram que as acidúrias orgânicas eram os erros inatos do metabolismo mais frequentes em crianças hospitalizadas, motivando diversos estudos clínicos, laboratoriais e epidemiológicos a partir de então.

Clinicamente os pacientes afetados por acidúrias orgânicas apresentam predominantemente disfunção neurológica em suas mais diversas formas de expressão: convulsões, coma, ataxia, hipotonia, hipertonia, irritabilidade, tremores, movimentos coreatetóticos, tetraparesia espástica, atraso no desenvolvimento psicomotor e outras manifestações (Wajner, 2019). As mais frequentes manifestações laboratoriais são cetonemia, cetonúria, neutropenia, trombocitopenia, acidose metabólica, baixos níveis de bicarbonato, hiperglicinemia, hiperamonemia, hipo/hiperglicemia, acidose lática, aumento dos níveis séricos de ácidos graxos livres e outros (Beaudet et al., 2014). A tomografia computadorizada e a ressonância magnética nuclear cerebrais revelaram alterações de substância branca (hipomielização e / ou desmielização), atrofia cerebral generalizada ou dos gânglios da base (necrose ou calcificação), megaencefalia, atrofia frontotemporal e atrofia cerebelar na maioria dos pacientes afetados por essas doenças (Mayatepek et al., 1996).

1.2. Acidúrias 2-hidroxiglutáricas

O ácido 2-hidroxiglutárico (2-HG) é um ácido dicarboxílico de 5 carbonos com uma hidroxila no carbono 2, o que confere a esta molécula um centro quiral que permite que este composto exista em duas conformações enantioméricas, ou seja, pode ser encontrado como ácido D-2-hidroxiglutárico ou ácido L-2-hidroxiglutárico (Figura 1).

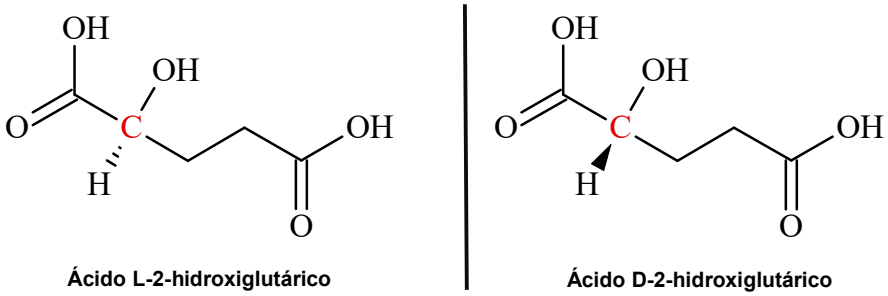

Figura 1. Estrutura química dos ácidos L-2-hidróxiglutárico e D-2-hidróxiglutárico destacando o carbono quiral em vermelho.

As duas formas enantioméricas do ácido 2-hidroxiglutárico foram identificadas pela primeira vez como constituintes normais da urina humana em baixas concentrações (Gregersen et al., 1977). Em 1980, dois novos distúrbios hereditários do metabolismo caracterizados bioquimicamente por aumento desses enantiômeros foram descritos. Chalmers e colaboradores (Chalmers et al., 1980) identificaram um paciente com acidúria D-2-hidroxiglutárica (D-2-HGA, OMIM # 600721 e OMIM # 613657), enquanto Duran e colaboradores (Duran et al., 1980) descreveram um caso de acidúria L-2-hidroxiglutárica (L-2-HGA, OMIM # 236792), publicações estas que estabeleceram os marcadores bioquímicos (D-2-HG e L-2-HG) nessas duas doenças metabólicas distintas.

1.3. Acidúria D-2-hidroxiglutárica

A acidúria D-2-hidroxiglutárica (D-2-HGA) é uma doença neurometabólica autossômica recessiva, caracterizada bioquimicamente pelo acúmulo tecidual e excreção aumentada do ácido D-2-hidróxiglutárico (D-2-HG). Dois fenótipos distintos da D-2-HGA foram descritos: uma forma neonatal severa (tipo 1) (Kranendijk et al., 2010b) e uma variante infantil menos grave (tipo 2) (Kranendijk et al., 2010a).

Na década passada, estudos de biologia molecular foram capazes de estabelecer as bases moleculares que levam ao acúmulo do D-2-HG e assim começar a elucidar os fundamentos bioquímicos para a existência de dois fenótipos distintos de D-2-HGA. A

enzima mitocondrial hidróxiácido-oxoácido transidrogenase (HOT) catalisa a conversão do α-cetoglutarato (2-KG) em D-2-HG (figura 2). Este metabólito, cuja função fisiológica ainda é desconhecida, é novamente convertido a 2-KG por ação da D-2-hidroxiglutarato desidrogenase (D-2-HGDH) (figura 2). Uma mutação no gene que codifica a D-2-HGDH, provocando a diminuição ou perda total da atividade desta enzima, está associada ao aumento do D-2-HG, caracterizando bioquimicamente a acidúria D-2-hidroxiglutárica tipo 1 (D-2-HGA1) (Kranendijk et al., 2010a).

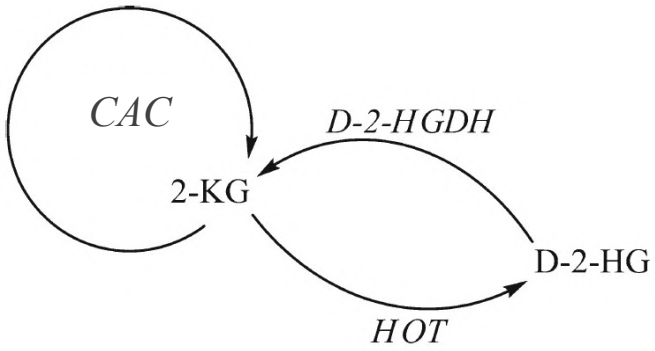

Figura 2. D-2-HG é formado a partir de 2-KG por ação da HOT. D-2-HGDH catalisa a conversão de D-2-HG a 2-KG. O acumulo de D-2-HG em pacientes com D-2-HGA1 ocorre quando há deficiência da D-2-HGDH (Adaptado de *Kranendjik et al., 2012*).

Já a acidúria D-2-hidroxiglutárica tipo 2 é causada por mutações no gene da isocitrato desidrogenase II (IDH2) (figura 3), que levam a um aumento de 8 vezes na atividade desta enzima e conferem a esta a capacidade de converter o alfa-cetoglutarato em D-2-HG (Kranendijk et al., 2010b), sem alterar a atividade da HOT ou mesmo da D-2-HGDH.

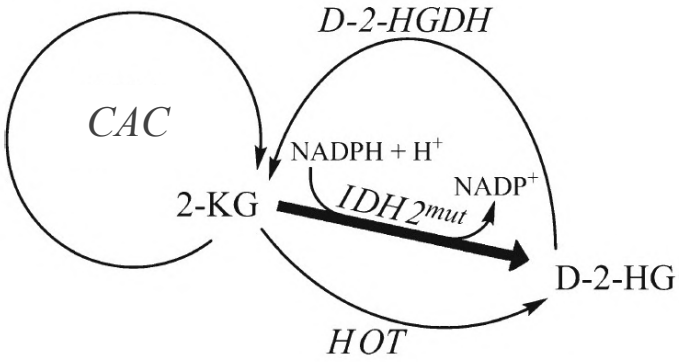

Figura 3. A IDH2 mutada ganha função de converter o 2-KG em D-2-HG. O D-2-HG também é formado pela HOT. A D-2-HGDH não consegue metabolizar completamente todo o D-2-HG gerado, resultando em acúmulo de D-2-HG em pacientes com D-2-HGA2 (Adaptado de *Kranendjik et al., 2012*).

1.3.1. Aspectos clínicos e neuropatológicos

As manifestações clínicas de ambos os fenótipos da D-2-HGA incluem retardo no desenvolvimento, hipotonia e convulsões. Contudo, alguns estudos demonstram que os pacientes acometidos pela D-2-HGA2 apresentam convulsões mais frequentes e o atraso no desenvolvimento é mais severo do que o observado em pacientes com D-2-HGA1. Além disso, cerca de metade dos pacientes com o tipo 2 apresenta cardiomiopatia (Kranendijk et al., 2012), achado este que pode ser potencialmente fatal. Por outro lado, a D-2-HGA1 é muito mais variável quanto à sintomatologia clínica do que a D-2-HGA2. Em determinados casos os pacientes não apresentam alterações neurológicas graves (D-2-HGA1). Já o fenótipo severo (D-2-HGA2) caracteriza-se principalmente por encefalopatia epilética de início neonatal ou infantil, além de movimentos distônicos ou coreoatetóticos e deficiência visual. Um terço dos pacientes morre durante a infância (Kranendijk et al., 2012).

Os achados neuropatológicos dos pacientes afetados são principalmente alargamento dos ventrículos laterais e alterações anatômicas nos gânglios da base. Além disso, um aumento dos espaços subaracnóideos frontais, pseudocistos subependimais, sinais de atraso na maturação cerebral e anormalidades na substância branca cerebral com múltiplos focos são observadas por estudos de neuroimagem em ambos os fenótipos da D-2-HGA (van der Knaap et al., 1999a, 1999b; Wajner et al., 2002). Neste contexto, devido à disfunção neurológica severa e atrofia e outras anormalidades cerebrais apresentadas pelos pacientes, ambas as formas da D-2-HGA são classificadas como doenças neurometabólicas.

1.4. Acidúria L-2-hidroxiglutárica

A acidúria L-2-hidroxiglutárica (L-2-HGA), descrita primeiramente por Duran e colaboradores em 1980 e posteriormente caracterizada por Barth e colaboradores em 1983, é uma doença autossômica recessiva rara, considerada como uma acidemia orgânica cerebral, por afetar exclusivamente o sistema nervoso central (SNC). A única enzima conhecida por gerar L-2- HG em humanos é L-malato desidrogenase (L-malDH), cuja função catalítica primária é a conversão de L-malato em oxalacetato, mas que em

condições fisiológicas também catalisa a conversão do α-cetoglutarato em L-2-HG (Fig. 4). O bloqueio metabólico presente nos pacientes afetados pela L-2-HGA deve-se à deficiência na atividade da enzima mitocondrial FAD-dependente L-2-hidroxiglutarato desidrogenase (L-2-HGDH, EC 1.1.99.2), como consequência de mutações patogênicas no gene *L2HGDH* localizado no cromossomo 14q21.3 (Rzem et al., 2004; Samuraki et al., 2008; Steenweg et al., 2010; Topçu et al., 2004). Essas mutações comprometem a atividade da L-2-HGDH, levando ao acúmulo do ácido L-2-hidroxiglutarato (L-2-HGH) no cérebro e nos líquidos biológicos dos pacientes, caracterizando-se como o principal achado bioquímico da L-2-HGA.

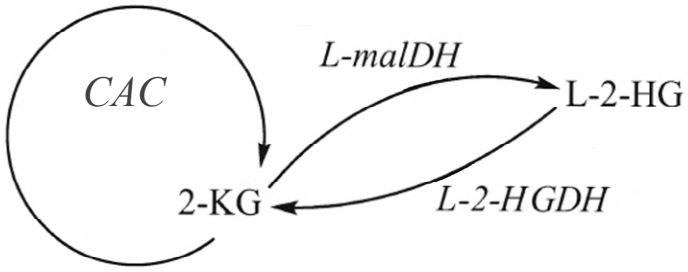

Figura 4. O L-2-HG é formado a partir de 2-KG por ação da L-malDH. O L-2-HGDH catalisa a conversão de L-2-HG a 2-KG. O acumulo de L-2-HG em pacientes com L-2-HGA ocorre quando há deficiência da L-2-HGDH (Adaptado de *Kranendjik et al., 2012*).

1.4.1. Aspectos clínicos e neuropatológicos

Diferentemente dos pacientes com D-2-HGA, os pacientes acometidos pela L-2-HGA apresentam um fenótipo clínico homogêneo. As manifestações clínicas da doença podem começar a ser percebidas já na infância. Dentre eles podemos citar como principais o atraso no desenvolvimento motor e cognitivo, epilepsia e ataxia cerebelar (Steenweg et al., 2010). Geralmente a doença progride de forma lenta e progressiva, sendo que alguns pacientes com L-2-HGA com a forma mais branda podem permanecer sem diagnóstico até a adolescência, podendo ser diagnosticados apenas em idade adulta.

A maior parte dos pacientes acometidos pela L-2-HGA apresentam algum grau de déficit no desenvolvimento psicomotor e cerca de dois terços desenvolvem epilepsia e disfunção cerebelar. Além disso, aproximadamente metade dos pacientes possuem macrocefalia e sintomas extrapiramidais, incluindo tremor e distonia. Finalmente, um quarto dos pacientes acometidos pela L-2-HGA possuem problemas na fala (Kranendijk et al., 2012).

Os achados neuropatológicos dessa doença são principalmente anormalidades a nível cortical e subcorticais no núcleo denteado, globo pálido, putamen e no núcleo caudado, além de alterações cerebelares (Barbot et al., 1997; Barth et al., 1998; Gunduz et al., 2022; Kranendijk et al., 2012; Topçu et al., 2005). Conforme a doença progride, a intensidade das alterações na substância branca e nos gânglios da base começa a ficar mais difusa, seguida de atrofia da substância branca cerebral e ataxia cerebelar (Barbot et al., 1997; Steenweg et al., 2009).

1.5. Diagnóstico das acidúrias 2-hidroxiglutáricas

O diagnóstico diferencial das acidúrias 2-hidroxiglutáricas inicia com a avaliação clínica do paciente que possui um atraso no desenvolvimento não esclarecido e/ou que seja portador de disfunção neurológica de etiologia desconhecida, elevando o nível de suspeita para uma desordem metabólica. O diagnóstico para estas doenças inicia pela triagem urinária de ácidos orgânicos por cromatografia gasosa acoplada à espectrometria de massa (GC-MS) que revela um aumento nos níveis de 2-HG, sem revelar a forma do enantiômero e, portanto, do diagnóstico de D-2-HGA ou L-2-HGA. Contudo, a determinação da configuração quiral ainda precisa ser determinada e é feita por eletroforese capilar hifenizada com espectrometria de massa em tandem (CE-MS/MS) que permite a separação dos enantiômeros sem a etapa de derivatização (Švidrnoch et al., 2016). Embora as manifestações clínicas possam sugerir tanto D-2-HGA como L-2-HGA, a diferenciação quiral realizada através de CE-MS/MS é obrigatória para o correto diagnóstico diferencial e consequente confirmação de D-2-HGA ou L-2-HGA (Kranendijk et al., 2012). Subsequentemente, a caracterização genética e enzimática possibilita tanto confirmação de qual acidemia 2-hidróxiglutárica o paciente é portador, bem como a diferenciação entre os 2 subtipos da D-2-HGA, representando uma importante informação para diagnóstico pré-natal futuro (Gibson et al., 1993b; Struys et al., 2004).

1.6. Tratamento das acidúrias 2-hidroxiglutáricas

Até o momento não há tratamento disponível efetivo para a L-2-HGA e a D-2-HGA, embora riboflavina, carnitina e flavina adenina dinucleotídeo de sódio (FAD) são opções de tratamento que foram relatadas como benéficas e proporcionaram melhora parcial em dados limitados em L-2HGA (Samuraki et al., 2008; Yilmaz, 2009). No que se refere à D-2-HGA, não há qualquer tratamento disponível. Tendo em vista a falta de

tratamento eficaz para essas doenças, tornou-se importante esclarecer a patogênese das mesmas que certamente facilitaria o desenvolvimento de novas estratégias terapêuticas.

1.7. Patogênese das acidúrias D- e L-2-hidroxiglutáricas

Tendo em vista que as D-2-HGA tipo 1 e tipo 2 possuem como característica comum o acúmulo de D-2-HG nos fluidos corporais e principalmente no cérebro, é possível que o D-2-HG potencialmente contribui para a fisiopatologia das manifestações clínicas, tais como do atraso no desenvolvimento, hipotonia e epilepsia presentes em ambos os tipos da D-2-HGA. A superprodução de D-2-HG ocorre na mitocôndria, já que a D-2-HGDH e a IDH2 são enzimas mitocondriais. As concentrações de D-2-HG intracelular e mitocondriais são desconhecidas, já no plasma se sabe que, nos pacientes afetados, as concentrações do metabólito estão aumentadas de 30 a 840 vezes (26-757 μM) (Gibson et al., 1993a; Kranendijk et al., 2011, 2010a, 2010b). Os níveis de D-2HG no plasma de pacientes com o D-2-HGA2 são cerca de 5 vezes mais elevados do que nos pacientes com D-2-HGA1. Sabendo que os pacientes com o tipo 2 da doença apresentam sintomas mais severos do que os acometidos pelo tipo 1, sugere-se que possa existir uma correlação entre as concentrações de D-2-HG e a severidade da doença.

Por outro lado, há na literatura trabalhos demonstrando efeitos deletérios do D-2-HG sobre a bioenergética mitocondrial e a homeostase redox em tecidos de roedores e humanos com essa doença. Estudos *in vitro* demonstraram que a exposição de cérebro ao D-2-HG provocou diminuição da atividade da enzima creatina quinase e das atividades dos complexos IV e V da cadeia respiratória (da Silva et al., 2004, 2002; Kölker et al., 2002), além de induzir estresse oxidativo (Kölker et al., 2002; Latini et al., 2005, 2003b). Também foi demonstrado que a administração intraestriatal de D-2-HG a ratos Wistar de 30 dias induziu estresse oxidativo e algumas alterações histopatológicas (da Rosa et al., 2014) nesta estrutura cerebral. Além disso, o D-2-HG apresentou efeito excitotóxico em culturas primárias de neurônios de pintos através da ativação de receptores NMDA (Kölker et al., 2002). Recentemente, também foi demonstrado que a administração intracerebroventricular deste metabólito foi capaz de provocar estresse oxidativo, alterações bioenergéticas, morte neuronal e reatividade glial em ratos neonatos (Ribeiro et al., 2021). Por outro lado, a cardiotoxicidade exercida pelo D-2-HG já foi investigada em 2 estudos envolvendo modelos genéticos de D-2-HGA tipo 2 em roedores (Akbay et al., 2014; Wang et al., 2016), os quais demonstraram que o acumulo do metabólito está diretamente relacionado a disfunção cardíaca em seus modelos animais e que o bloqueio

na produção deste metabólito foi capaz de melhorar a função cardíaca. No entanto, os mecanismos de cardiotoxicidade deste metabólito não foram investigados e permanecem desconhecidos.

No que se refere à L-2-HGA, ações neurotóxicas foram demonstradas para o L-2-HG. Assim, a exposição *in vitro* de tecidos cerebrais a concentrações elevadas de L-2-HG inibiu significativamente a atividade da creatina cinase em homogeneizado de cerebelo de ratos (da Silva et al., 2003), induziu estresse oxidativo (Latini et al., 2003a) e alterou a captação de glutamato em sinaptossomas e vesículas sinápticas (Junqueira et al., 2003), indicando disfunção bioenergética, bem como da homeostase redox e do sistema glutamatérgico como possíveis mecanismos fisiopatológicos para a L-2-HGA. Também foram demonstrados *in vivo* efeitos pró-oxidantes do L-2-HG em ratos adolescentes submetidos a injeção intraestriatal deste metabólito, bem como no córtex cerebral e estriado de ratos neonatos injetados intracerebroventricularmente (da Rosa et al., 2015; Ribeiro et al., 2018). No entanto, os efeitos de uma exposição a altas concentrações de L-2-HG no período neonatal sobre o cerebelo, estrutura cerebral muito afetada nessa condição patológica, bem como sobre estudos imunohistoquímicos com marcadores para astrogliose e neuroinflamação e morte neuronal, e também sobre o desenvolvimento motor e a cognição permanecem totalmente desconhecidos.

1.8. Mitocôndria, Ciclo do Ácido Cítrico, Fosforilação Oxidativa, Cadeia Transportadora de Elétrons e Parâmetros Respiratórios

As mitocôndrias são organelas recobertas por uma membrana externa, altamente permeável a pequenas moléculas e íons, e que possuem uma membrana interna impermeável à maioria das moléculas e íons (Nelson e Cox, 2017). Estas complexas estruturas subcelulares desempenham papel central no metabolismo energético por meio da fosforilação oxidativa (OXPHOS), respostas adaptativas ao estresse e de processos de biossíntese. Também desempenham papeis fundamentais em processos celulares, incluindo inflamação, homeostase redox e do cálcio, e morte celular (Bock e Tait, 2020; Faas e de Vos, 2020; Javadov et al., 2020; Nunnari e Suomalainen, 2012; Onishi et al., 2021; Popov, 2020).

Acetilcoenzima A ou outros intermediários oriundos do metabolismo da glicose, aminoácidos e ácidos graxos podem ser completamente oxidados a CO_2 no ciclo do ácido cítrico (CAC), produzindo as coenzimas reduzidas NADH (nicotinamida adenina

dinucleotídeo reduzido) e $FADH_2$ (flavina adenina dinucleotídeo reduzido), que irão suprir a cadeia respiratória mitocondria (CRM) (Nicholls e Ferguson, 2013).

A CRM é composta por vários complexos enzimáticos (complexos I, II, III, IV e V), os quais possuem grupamentos prostéticos especializados em exercer o papel de aceptores e doadores de elétrons, tendo a participação do citocromo c e uma coenzima lipossolúvel (coenzima Q). NADH e $FADH_2$ abastecem com elétrons os complexos I e II, respectivamente, sendo estas as vias convencionais de entrada de elétrons na CRM. O fluxo de elétrons através dos complexos da CRM é acompanhado ao bombeamento de prótons da matriz mitocondrial para o espaço intermembranas, através dos complexos I, III e IV, gerando um gradiente eletroquímico que é utilizado pela ATP sintase (complexo V) para a síntese de ATP, e tendo o O_2 como aceptor final dos elétrons provenientes do complexo IV. Deste modo, a oxidação de substratos energéticos ligados ao CAC está acoplada ao processo de fosforilação do ADP (difosfato de adenosina), ou seja, quando a energia do gradiente eletroquímico é dissipada pelo fluxo de prótons de volta para a matriz mitocondrial, a energia liberada é utilizada pela ATP sintase para sintetizar moléculas de ATP (Nicholls e Ferguson 2013; Nelson e Cox 2021).

A existência de uma inter-relação de acoplamento entre os processos de transferência de elétrons, bombardeio de prótons, formação de gradiente eletroquímico e síntese de ATP com o consumo mitocondrial de oxigênio, faz com que a medida da quantidade de O_2 consumido seja um ótimo sensor da atividade do CRM. Experimentalmente, a respiração mitocondrial pode ser dividida em cinco estados respiratórios, sendo os estados 3 e 4 os mais amplamente utilizados. O estado 3 (estado fosforilante) é dado pelo consumo de oxigênio associado a oxidação de substratos capazes de fornecer elétrons à CRM em um meio suplementado com ADP, estimulando assim a produção de ATP. O estado 4 geralmente é estimulado por oligomicina, um inibidor da ATP sintase, refletindo o consumo de O_2 necessário para a formação e manutenção do gradiente eletroquímico, reduzindo a taxa da respiração (estado não-fosforilante). Ainda, é possível utilizar compostos desacopladores da fosforilação oxidativa que provocam um vazamento de prótons do espaço intermebrana para a matriz mitocondrial, estimulando a atividade da cadeia respiratória mitocondrial e o consumo de O_2 sem produção de ATP (estado desacoplado) (Nicholls e Ferguson, 2013).

1.9. Papel da Mitocôndria sobre a Homeostase de Cálcio

A manutenção da homeostase do cálcio celular, responsável pela sinalização e gerenciamento de uma série de atividades intracelulares, é uma das tarefas mais importantes desempenhadas pelas mitocôndrias. Quando íntegra e funcional, essa organela tem a capacidade de absorver cálcio do citosol ou liberá-lo, mantendo a concentração intracelular desse cátion em níveis ideais ao pleno funcionamento celular (Figueira et al., 2013; Rizzuto et al., 2012). A proteína transportadora mitocondrial responsável pela captação de cálcio foi recentemente elucidada, sendo um sistema uniporte de captação de cálcio (Baughman et al., 2011; de Stefani et al., 2011; Pan et al., 2013; Pendin et al., 2014). Por outro lado, a liberação de cálcio para a matriz é realizada pelos trocadores Na^+/Ca^{2+} (mNCX) e H^+/Ca^{2+} (mHCX) (Bernardi e von Stockum, 2012; Rizzuto et al., 2012).

A capacidade das mitocôndrias de absorver e reter cálcio é essencial para o tamponamento das concentrações citosólicas deste cátion, evitando flutuações que podem ser muito prejudiciais ao funcionamento celular (Figueira et al., 2013; Rizzuto et al., 2012). Contudo, uma alta taxa de absorção mitocondrial de cálcio, para além de sua capacidade de retenção, pode resultar em um estado chamado transição de permeabilidade, que é provocado pela abertura de um poro na membrana mitocondrial interna (Adam-Vizi e Starkov, 2010; Starkov, 2010; Zoratti e Szabò, 1995). Embora a identidade das proteínas que compõem o poro de transição de permeabilidade mitocondrial (PTP) permaneça desconhecida (Starkov, 2010), já se sabe que a ciclofilina D desempenha um papel crucial na abertura do PTP (Baines et al., 2005; Basso et al., 2005; Bernardi, 2013; Tanveer et al., 1996).

A célula pode sofrer graves consequências quando a abertura do PTP ocorre de forma permanente, incluindo a liberação de cálcio no citosol, inchamento mitocondrial, liberação de fatores apoptogênicos intramitocondriais como citocromo c (Liu et al., 1996), despolarização mitocondrial, perda de metabólitos (Ca^{2+}, Mg^{2+}, glutationa reduzida (GSH), NADH e NADPH), prejuízo na síntese de ATP que, em última instância, resultam na morte da célula (Bernardi e von Stockum, 2012; Crompton, 1999; Rasola e Bernardi, 2011; Rizzuto et al., 2012). Inúmeros trabalhos *in vitro* e *in vivo* tem associado a indução do PTP com uma disfunção mitocondrial na presença de cálcio, demonstrando alteração nos parâmetros da homeostase bioenergética mitocondrial (Cecatto et al., 2020; Maciel et al., 2004; Mirandola et al., 2010). Além disso, o ataque oxidativo por espécies

reativas de oxigênio está descrito como um importante mecanismo potencializador da abertura do PTP (Adam-Vizi e Starkov, 2010; Kowaltowski et al., 2001). Neste contexto, altas concentrações de NADH previnem a abertura do PTP, por promover a redução do $NADP^+$ catalisada pela transidrogenase mitocondrial e consequentemente melhoram a capacidade redox da mitocôndria (Hoek e Rydstrom, 1988; Lehninger et al., 1978; Zago et al., 2000).

1.10. Radicais Livres, Defesas Antioxidantes e Estresse oxidativo

Espécies reativas são moléculas ou átomos que frequentemente têm elétrons desemparelhados em seus orbitais, sendo capazes de existir independentemente, cuja instabilidade eletrônica promove uma maior propensão a reagir com outras moléculas ou átomos, levando a oxidação das mesmas (Halliwell, B., Gutteridge, 2015a; Southorn e Powis, 1988).

Sob condições fisiológicas, o O_2 é reduzido no complexo IV da CRM resultando na formação de H_2O. Todavia, centros redox presentes nos complexos da CRM, como nos complexos I e III, podem ser diretamente oxidados pelo O_2, resultando na transferência de um único elétron para essa molécula e gerando o ânion superóxido ($O2^{\bullet-}$). Por sua vez, a enzima superóxido dismutase (SOD) pode converter o $O2^{\bullet-}$ a peróxido de hidrogênio (H_2O_2), uma espécie reativa com ausência de elétrons desemparelhados. O H_2O_2 pode reagir com Fe_2^+ dando origem ao radical hidroxila (OH^-), um radical livre extremamente reativo. O $O_2^{\bullet-}$, o H_2O_2 e o OH^- fazem parte das chamadas espécies reativas de oxigênio (EROs). Além das EROs, existem ainda as espécies reativas de nitrogênio (ERNs), representadas principalmente pelo óxido nítrico ($NO^{\bullet}$) e o peroxinitrito ($ONOO^-$) (Halliwell, B., Gutteridge, 2015a).

As espécies reativas atuam como moléculas sinalizadoras em funções fisiológicas cruciais, sendo essenciais para uma resposta celular adequada. A sinalização celular da insulina, adaptação ao exercício e a defesa contra infecções através da liberação de espécies reativas pelos neutrófilos são exemplos de processos significativamente influenciados pela geração fisiológica de EROs e ERNs (Aratani et al., 2012; Delanty e Dichter, 1998; Hamann et al., 2014; Irani, 2000; Wall et al., 2012; Webb et al., 2017). EROs e ERNs são constantemente gerados e eliminados por mecanismos de defesas antioxidantes endógenos. Contudo, quando produzidas em excesso, EROs e ERNs podem

ocasionar danos às células através da oxidação de biomoléculas, tais como proteínas, lipídios, carboidratos e ácidos nucleicos (Halliwell, B., Gutteridge, 2015a).

As defesas antioxidantes enzimáticas e não enzimáticas conferem as células um arsenal altamente especializado na detoxificação dos efeitos nocivos causados pelas espécies reativas. Essas defesas estão estrategicamente distribuídas em diferentes compartimentos celulares e tecidos e compreendem agentes que removem cataliticamente os radicais livres, como as enzimas SOD, catalase (CAT), glutationa peroxidase (GPx); proteínas que minimizam a disponibilidade de pró-oxidantes (íons de ferro e cobre, por exemplo) ao se ligarem aos mesmos, como as transferrinas; agentes que aprisionam espécies reativas e que são substratos de enzimas antioxidantes, como a GSH; além de proteínas que protegem biomoléculas de danos por outros mecanismos (Halliwell, B., Gutteridge, 2015b, 2015c).

Em situações onde o aumento de espécies reativas é relativamente pequeno, a resposta antioxidante será suficiente para compensar esse aumento. Entretanto, sob certas condições patológicas, a produção de espécies reativas estará aumentada, e as defesas antioxidantes podem ser insuficientes para restabelecer a homeostase redox (Halliwell e Gutteridge, 2015). Este rompimento do equilíbrio entre eventos pró-oxidantes e a capacidade antioxidante é descrito como estresse oxidativo, e pode representar um mecanismo central na fisiopatologia de doenças humanas (Halliwell, 2006). O estresse oxidativo ser resultado de uma produção aumentada de oxidantes quanto tanto de uma diminuição das defesas antioxidantes, bem como da liberação de metais de transição ou a combinação de quaisquer desses fatores (Halliwell, B., Gutteridge, 2015a).

Um nível moderado de estresse oxidativo pode ser tolerado pela maioria das células, o que muitas vezes causa um aumento na produção de enzimas antioxidantes para ajudar a neutralizar o excesso de espécies reativas. Em contrapartida, se o dano celular adjacente ao estresse oxidativo ocorrer de forma exacerbada, a célula pode sofrer morte celular por necrose ou apoptose (Halliwell e Gutteridge, 2015).

1.11. Melatonina

A melatonina é um hormônio neuroendócrino derivado do triptofano que é produzido e liberado principalmente pela glândula pineal em resposta a diminuição da luminosidade e está envolvido na regulação de funções biológicas, como sono, ritmo circadiano, imunidade e reprodução (Cipolla-Neto e Amaral, 2018). Para além de suas

ações fisiológicas, a melatonina tem demonstrado um potencial antioxidante em um número crescente de situações fisiológicas e patológicas. A melatonina exerce sua ação antioxidante através de uma variedade de mecanismos que envolvem a desintoxicação (scavenger) de EROs e ERNs e indiretamente através do aumento na expressão de enzimas antioxidantes (Pieri et al., 1994; Reiter et al., 2016). Além dessas ações bem descritas, a melatonina também pode quelar metais de transição, que estão envolvidos nas reações de Fenton/Haber-Weiss, reduzindo a formação do radical hidroxila que é considerado o radical livre mais tóxico (Gulcin et al., 2003). A distribuição intracelular ubíqua, mas desigual, da melatonina, incluindo suas altas concentrações nas mitocôndrias, provavelmente ajuda em sua capacidade de combater o estresse oxidativo e a apoptose celular (Reiter et al., 2016, 2013). A melatonina também demonstrou efeitos neuroprotetores, especialmente no que diz respeito ao SNC, em inúmeros modelos experimentais *in vivo* e *in vitro* de distúrbios hereditários do metabolismo, frente ao estresse oxidativo induzido por metabólitos acumulados nestas doenças (da Silva et al., 2017; Moura et al., 2018; Ribeiro et al., 2021; Seminotti et al., 2019a).

1.12. Neuroinflamação

Respostas imunológicas agudas e de longo prazo são desencadeadas pelo sistema imunológico para manter a integridade e a funcionalidade dos tecidos e órgãos, mantendo assim um equilíbrio contínuo entre as agressões e as defesas teciduais. A resposta inflamatória no SNC é conhecida como neuroinflamação e é caracterizada pela ativação de células gliais, principalmente micróglia e astrócitos, sendo uma resposta de defesa do organismo contra um estímulo que induz dano (Ramos et al., 2017). A microglia é formada por células imunes inatas de origem mieloide que se instalam no SNC durante a embriogênese, tendo como função crucial a capacidade de gerar respostas imunes inatas e adaptativas significativas (Lenz e Nelson, 2018; Yang et al., 2010). A neuroinflamação geralmente tem início com o recrutamento e ativação da micróglia local em resposta a fatores de sinalização liberados pelo tecido neuronal (Hines et al., 2009; Kreutzberg, 1996).

Durante o processo de ativação microglial ocorrem alterações em termos de morfologia, tamanho, expressão de proteínas de superfície, bem como no perfil de citocinas e fatores de crescimento que são produzidos em grande quantidade (Norden et al., 2016). Dentre as alterações fisiológicas que promovem a modificação do fenótipo quiescente para a forma ativada da micróglia, destaca-se o aumento na expressão da

molécula adaptadora ligante de cálcio ionizado-1 (Iba1), fazendo com que esta proteína seja considerada um excelente marcador de ativação microglial (Hovens et al., 2014; Sasaki et al., 2001). A partir dessas alterações, a micróglia é capaz de fagocitar "restos" biológicos, incluindo corpos apoptóticos, e uma variedade de patógenos e partículas exógenas através de vias de fagocitose bem estabelecidas (Chan et al., 2003; Fu et al., 2014).

Os astrócitos são as células gliais mais abundantes no cérebro, que para além de funções de suporte aos neurônios, desempenham papéis ativos e essenciais na homeostase cerebral (Oksanen et al., 2019). Estas células regulam o fluxo sanguíneo, mantêm a barreira hematoencefálica (BHE), fornecem substratos energéticos aos neurônios, modulam a atividade sináptica, controlam a secreção de neurotrofinas, além de regular o equilíbrio extracelular de íons, fluidos e neurotransmissores (Kwon e Koh, 2020). Os astrócitos são reguladores cruciais das respostas imunes inatas e adaptativas no SNC. No entanto, a atividade exagerada dos astrócitos pode exacerbar reações inflamatórias e danos teciduais contribuindo para o estabelecimento do processo de neuroinflamação, ou promover imunossupressão e reparo tecidual (Colombo e Farina, 2016). Alterações na expressão molecular e morfologia dos astrócitos mediadas pela proteína glial fibrilar ácida (GFAP) podem indicar a gravidade da astrogliose reativa, sendo essa proteína considerada um marcador de reatividade astrocitária associado a inúmeras patologias que acometem o SNC (Sofroniew, 2009). Desta forma, na doença de Alzheimer, a proteína GFAP, bem como a proteína ligante de cálcio S100B, a glicoproteína cartilaginosa 40 (YKL040) e a D-serina são consideradas como biomarcadores de reatividade astrocitária no LCR, enquanto a GFAP e a S100B são biomarcadores séricos (Carter et al., 2019). Expressiva reatividade astrocitária durante as fases iniciais de patologias, incluindo lesão medular e encefalomielite autoimune experimental, são consistentemente correlacionados com resultados clínicos exacerbados, neuroinflamação, alteração da barreira hematoencefálica e morte neuronal (Colombo e Farina, 2016).

A neuroinflamação está presente em doenças neurodegenerativas comuns como as doenças de Parkinson e Alzheimer e esclerose lateral amiotrófica. Nessas enfermidades o processo neuroinflamatório caracteriza-se por elevação nas concentrações de citocinas pró-inflamatórias e na produção de espécies reativas que pode resultar na morte celular sob certas condições (Smith et al., 2012). Uma resposta neuroinflamatória aumentada também foi demonstrada em vários modelos experimentais de distúrbios hereditários do

metabolismo, tais como acidemia glutárica tipo I, hiperglicinermia, aciduria D-2-hidroxiglutárica e deficiência de S-adenosilhomocisteína hidrolase (Amaral et al., 2018; Guerreiro et al., 2021; Moura et al., 2016; Olivera-Bravo et al., 2015; Ribeiro et al., 2021; Seminotti et al., 2022a, 2019b)

1.13. Mielina

A bainha de mielina, estrutura formada por uma membrana lipídica rica em glicerofosfolipídios e colesterol, é gerada por longos prolongamentos da membrana plasmática que os oligodendrócitos estendem em camadas concêntricas ao redor dos axônios, facilitando a rápida comunicação entre os neurônios e assim elevando a velocidade dos potenciais de ação neuronais (Nave, 2010). A alta velocidade que ocorre a neurotransmissão saltatória em neurônios mielinizados só é possível graças a mielina, que reduz a capacitância e aumenta a resistência transversal ao longo do eixo da membrana axonal, diminuindo substancialmente a quantidade de energia necessária para restaurar as concentrações de íons em repouso após cada despolarização (Duncan et al., 2021).

Durante o neurodesenvolvimento as células precursoras de oligodendrócitos (OPCs) se multiplicam e se movem do neuroepitélio da zona ventricular/subventricular do cérebro para a substância branca em formação no sistema nervoso central (SNC). Após a identificação dos axônios-alvo, as OPCs se diferenciam em oligodendrócitos mielinizantes e dão início ao processo de crescimento da membrana e o envolvimento dos axônios ocorre logo depois(Simons and Nave, 2015). Os oligodendrócitos e neurônios têm uma relação de sinalização recíproca, na qual os oligodendrócitos recebem sinais dos axônios direcionando sua mielinização. Além disso, os oligodendrócitos também fornecem fatores tróficos para os axônios, lactato como combustível energético e têm papel fundamental na manutenção da integridade axonal (Dulamea, 2017; Duncan et al., 2021).

Nos mamíferos, o processo de mielinização no SNC é caracterizado pelo aparecimento tardio pré-natal e/ou pós-natal, crescimento e diferenciação de células precursoras de oligodendrócitos (OPCs) em oligodendrócitos maduros. Estudos recentes demonstraram que as OPCs mantêm sua capacidade proliferativa mesmo no SNC adulto, com variações regionais relacionadas à idade nas taxas de proliferação e maturação destas células, o que torna esta propriedade alvo de estratégias terapêuticas inovadoras para

doenças desmielinizantes (de Almeida et al., 2022; Fernandez-Castaneda and Gaultier, 2016; Hughes et al., 2013; Young et al., 2013).

Proteínas específicas desempenham um papel crucial em todas as etapas do processo de mielinização, desde a identificação do axônio até a compactação final e manutenção da bainha de mielina (Fulton et al., 2010). A proteína básica da mielina (MBP) é a proteína de maior prevalência na mielina. A MBP auxilia no processo de compactação e manutenção da estrutura da mielina por manter a adesão das faces citoplasmáticas da membrana celular (Fulton et al., 2010; Tzakos et al., 2005). A calmodulina é um dos ligantes de MBP mais bem estudados, quando ativada por cálcio, ela interage com a MBP, promovendo a estabilização da estrutura da mielina (Wang et al., 2011). Outra importante proteína constitutiva da mielina é a 2',3'-nucleotídeo cíclico 3'-fosfodiesterase (CNPase), compreendendo cerca de 4% do total das proteínas da mielina. A CNPase está relacionada à organização do citoesqueleto através da interação com heterodímeros de tubulina, induzindo a montagem de microtúbulos por copolimerização, auxiliando assim na regulação do crescimento de processo mielinizantes dos oligodendrócitos (Fulton et al., 2010; Lee et al., 2005).

Hipomielinização e desmielinização são alterações que têm sido relatadas em muitas doenças neurológicas, podendo ser causadas por danos aos oligodendrócitos, prejuízos na maturação de OPCs ou produção ineficiente de proteínas específicas da mielina (Han et al., 2013; Motavaf e Piao, 2021; Wang et al., 2018). Nesse particular, foi demonstrado *in vivo* que as células oligodendrociticas (OPCs e maduros) representam a subpopulação celular do SNC mais vulnerável ao estresse oxidativo, podendo sofrer oxidação do DNA, nitração de proteínas e peroxidação de lipídeos, acarretando em prejuízos na capacidade mielinizante destas células (Giacci et al., 2018).

2. OBJETIVOS

2.1. Objetivo geral

Esta tese objetivou investigar os efeitos da administração intracerebroventricular de L-2-HG a ratos neonatos (DPN1) sobre parâmetros da homeostase redox, marcadores imunohistoquímicos de dano neuronal, reatividade glial e mielinização em estruturas cerebrais de ratos jovens e adultos no intuito de esclarecer mecanismos fisiopatológicos da neurodegeneração observada em pacientes portadores da L-2-HGA. O desenvolvimento neuromotor, a motricidade e a cognição de ratos injetados no período neonatal com o L-2-HG também foram investigados. As ações neuroprotetoras da melatonina sobre as alterações neuroquímicas, histológicas e comportamentais causadas pelo L-2-HG também foram avaliadas. Finalmente foi investigada a influência do D-2-HG sobre importantes funções mitocondriais (metabolismo energético e retenção mitocondrial de cálcio) em preparações mitocondriais e homogeneizados de coração de ratos jovens, bem como em células H9c2 cultivados para avaliar se um comprometimento dessas funções mitocondriais poderia potencialmente contribuir para a cardiomiopatia apresentada pelos pacientes afetados pela D-2-HGA2.

2.2. Objetivos específicos

a) Avaliar os efeitos da administração icv do L-2-HG (0.75 μmol/g de peso corporal) a ratos neonatos (DPN1) sobre parâmetros de estrese oxidativo (oxidação de DCFH, níveis de MDA, concentrações de GSH e a atividade das enzimas antioxidantes GPx e SOD) no cerebelo 6 horas após a injeção.

b) Avaliar a influência da administração icv do L-2-HG (0.75 μmol/g de peso corporal) a ratos neonatos sobre parâmetros imunohistoquímicos de reatividade astrocitária (GFAP e S100B), dano ou morte neuronal (NeuN), neuroinflamação (Iba1) e mielinização (MBP e CNPase) em estriado e córtex cerebral dos animais nos DPN15 e 75.

c) Avaliar a influência da administração icv do L-2-HG (0.75 μmol/g de peso corporal) a ratos neonatos sobre o desenvolvimento neuromotor, motricidade e cognição nos DPN7 e 45, respectivamente.

d) Avaliar o efeito neuroprotetor da melatonina sobre as alterações neuroquímicas, imunohistoquímicas e comportamentais causadas pela injeção icv do L-2-HG a ratos neonatos.

e) Avaliar os efeitos *in vitro* do ácido D-2-HG sobre um amplo espectro de parâmetros do metabolismo energético (respiração mitocondrial, produção de ATP, atividades dos complexos da cadeia respiratória, atividade de enzimas do CAC, da glutamato desidrogenase e da creatina cinase, bem como sobre a capacidade mitocondrial de retenção de cálcio e parâmetros de viabilidade) em preparações celulares (mitocondriais purificadas e homogeneizados) de coração de ratos jovens e/ou em cardiomioblastos cultivados (células H9c2).

PARTE II: ARTIGOS CIENTÍFICOS

CAPÍTULO I

L-2-hydroxyglutaric acid administration to neonatal rats elicits marked neurochemical alterations and long-term neurobehavioral disabilities mediated by oxidative stress

Rafael Teixeira Ribeiro, Andrey Vinícios Soares Carvalho, Rafael Palavro, Luz Elena Durán-Carabali, Ângela Beatris Zemniaçak, Alexandre Umpierrez Amaral, Carlos Alexandre Netto, Moacir Wajner

Artigo científico publicado em

Neurotoxicity Research (2022)

Neurotoxicity Research (2023) 41:119–140
https://doi.org/10.1007/s12640-022-00625-0

RESEARCH ARTICLE

L-2-Hydroxyglutaric Acid Administration to Neonatal Rats Elicits Marked Neurochemical Alterations and Long-Term Neurobehavioral Disabilities Mediated by Oxidative Stress

Rafael Teixeira Ribeiro[1] · Andrey Vinícios Soares Carvalho[1] · Rafael Palavro[2] · Luz Elena Durán-Carabali[2] · Ângela Beatris Zemniaçak[1] · Alexandre Umpierrez Amaral[1,3] · Carlos Alexandre Netto[1,2] · Moacir Wajner[1,2,4]

Received: 6 November 2022 / Revised: 28 November 2022 / Accepted: 16 December 2022 / Published online: 29 December 2022

Abstract

L-2-Hydroxyglutaric aciduria (L-2-HGA) is an inherited neurometabolic disorder caused by deficient activity of L-2-hydroxyglutarate dehydrogenase. L-2-Hydroxyglutaric acid (L-2-HG) accumulation in the brain and biological fluids is the biochemical hallmark of this disease. Patients present exclusively neurological symptoms and brain abnormalities, particularly in the cerebral cortex, basal ganglia, and cerebellum. Since the pathogenesis of this disorder is still poorly established, we investigated the short-lived effects of an intracerebroventricular injection of L-2-HG to neonatal rats on redox homeostasis in the cerebellum, which is mostly affected in this disorder. We also determined immunohistochemical landmarks of neuronal viability (NeuN), astrogliosis (S100B and GFAP), microglia activation (Iba1), and myelination (MBP and CNPase) in the cerebral cortex and striatum following L-2-HG administration. Finally, the neuromotor development and cognitive abilities were examined. L-2-HG elicited oxidative stress in the cerebellum 6 h after its injection, which was verified by increased reactive oxygen species production, lipid oxidative damage, and altered antioxidant defenses (decreased concentrations of reduced glutathione and increased glutathione peroxidase and superoxide dismutase activities). L-2-HG also decreased the content of NeuN, MBP, and CNPase, and increased S100B, GFAP, and Iba1 in the cerebral cortex and striatum at postnatal days 15 and 75, implying long-standing neuronal loss, demyelination, astrocyte reactivity, and increased inflammatory response, respectively. Finally, L-2-HG administration caused a delay in neuromotor development and a deficit of cognition in adult animals. Importantly, the antioxidant melatonin prevented L-2-HG-induced deleterious neurochemical, immunohistochemical, and behavioral effects, indicating that oxidative stress may be central to the pathogenesis of brain damage in L-2-HGA.

Keywords L-2-Hydroxyglutaric aciduria · L-2-Hydroxyglutaric acid · Oxidative stress · Neuronal damage · Glial reactivity · Melatonin

Introduction

L-2-Hydroxyglutaric aciduria (L-2-HGA) is a rare autosomal recessive disease that exclusively compromises the central nervous system (CNS). It was first described in 1980 (Duran et al. 1980) and further characterized by Barth and colleagues (Barth et al. 1992). The disorder is due to pathogenic mutations in the gene encoding L-2-hydroxyglutarate dehydrogenase (LHGDH), located at chromosome 14q21.3. These mutations compromise the activity of LHGDH, leading to the accumulation of L-2-hydroxyglutaric acid (L-2-HG) in the brain and biological fluids, which is the biochemical hallmark of L-2-HGA (Topçu et al. 2004; Rzem et al. 2004). Noteworthy, LHGDH gene is mainly expressed in the brain, although its expression also occurs in multiple tissues such as skeletal muscle and testis (Topçu et al. 2004).

✉ Moacir Wajner
mwajner@ufrgs.br

1 Programa de Pós-Graduação Em Ciências Biológicas: Bioquímica, Instituto de Ciências Básicas da Saúde, Universidade Federal Do Rio Grande Do Sul, Porto Alegre, RS, Brazil

2 Departamento de Bioquímica, Instituto de Ciências Básicas da Saúde, Universidade Federal Do Rio Grande Do Sul, Rua Ramiro Barcelos, Porto Alegre, RS 260090035-003, Brazil

3 Departamento de Ciências Biológicas, Universidade Regional Integrada Do Alto Uruguai E das Missões, Av. Sete de Setembro, Erechim, RS 162199709-910, Brazil

4 Serviço de Genética Médica, Hospital de Clínicas de Porto Alegre, Rua Ramiro Barcelos, Porto Alegre, RS 235090035-007, Brazil

L-2-HGA patients usually manifest with psychomotor regression, motor alterations, and epilepsy, which appear during infancy and early childhood, gradually evolving to cerebellar ataxia, moderate to severe cognitive impairment, and pyramidal and extrapyramidal signs such as tremor, dystonia, or parkinsonism (Topçu et al. 2005; Steenweg et al. 2009, 2010; Shah et al. 2020). Cerebral magnetic resonance imaging (MRI) findings consist of subcortical and deep white matter hyperintensities also involving the dentate nucleus, putamen, caudate nucleus, globus pallidus, and cerebellum detected in early stages of the disease, and progressing to deeper layers with a centripetal extension of the white matter lesions (van der Knaap et al. 1995; Saidha et al. 2010; Weimar et al. 2013; Faiyaz-Ul-Haque et al. 2014; Fourati et al. 2016; Shah et al. 2020). Severe atrophy, loss of neurons and gliosis of the brainstem, and the cerebellum were reported in the brain of a 1-month-old baby (Chen et al. 1996).

Elevated levels of L-2-HG in urine, in cerebrospinal fluid, and, to a lesser extent, in plasma are pathognomonic of L-2-HGA (Barth et al. 1992; Shah et al. 2020). DNA analysis denoting pathogenic mutations of the LHGDH gene is also used to confirm the diagnosis and is particularly important for prenatal diagnosis purposes (Topçu et al. 2004; Rzem et al. 2004). L-2-HGA treatment is non-existent or very precarious, although some reports described positive effects of FAD in combination with L-carnitine in an adult patient (Samuraki et al. 2008) and riboflavin in an adolescent patient (Yilmaz 2009). FAD increases the oxidation of L-2-HG to α-ketoglutarate, whereas L-carnitine facilitates the formation and excretion of short-chain acylcarnitine derivatives, thus reducing the neurotoxicity caused by the accumulation of this metabolite. Finally, antioxidants have recently been proposed to decrease neurotoxicity in L-2-HGA (Cansever et al. 2019), but more investigation is still needed to evaluate this therapeutic strategy.

Although neurological symptoms and brain abnormalities are well characterized, the pathophysiology of brain damage in L-2-HGA is still poorly known. However, brain L-2-HG accumulation due to local production and dicarboxylic acid trapping is thought to be responsible for disease neurotoxicity (Schaftingen et al. 2009; Sauer et al. 2010). Further support for this hypothesis is the correlation between the clinical symptomatology and the extent of the pathologic changes on cerebral MRI (Steenweg et al. 2009) with the brain levels of L-2-HG (Anghileri et al. 2016). Furthermore, augmented levels of L-2-HG in body fluids were linked to the neurological manifestations of the disease, all these indicating that this organic acid may be potentially neurotoxic (Yilmaz 2009).

On the other hand, the observations of elevated concentrations of lactate in cerebrospinal fluid, blood, and urine, as well as of Krebs cycle, intermediates in the urine of L-2-HGA patients suggest that bioenergetics dysfunction may be involved in the pathogenesis of this disease (Chen et al. 1996; Barth et al. 1998). This hypothesis is supported by experimental evidence showing that L-2-HG inhibits mitochondrial creatine kinase activity in rat brain (da Silva et al. 2003). It is also feasible that a disturbed glutamatergic neurotransmission may contribute to the pathogenesis of L-2-HGA, since L-2-HG increases glutamate uptake into synaptosomes and synaptic vesicles (Junqueira et al. 2003). Finally, a growing number of studies performed in the cerebral cortex and striatum of developing rats indicate a relevant role of oxidative stress in the brain injury of L-2-HGA patients (Latini et al. 2003; da Rosa et al. 2015; Ribeiro et al. 2018).

Considering that L-2-HGA neurologic symptomatology and brain abnormalities can appear early in life, it is essential to evaluate the pathogenesis of brain damage at this period of life. In this particular, it was previously reported that intracerebroventricular (icv) administration of L-2-HG to neonatal rats impairs redox homeostasis in the cerebral cortex and striatum (Ribeiro et al. 2018). Therefore, in the present study, we investigated whether an icv injection of L-2-HG to neonatal rats could disturb redox homeostasis in the cerebellum, which is mostly injured in this disorder and has not yet been evaluated. We also studied whether icv L-2-HG injection would cause long-standing effects on immunohistochemical landmarks of neuronal viability, reactive astrogliosis, neuroinflammation, and myelination in cerebral cortex and striatum, as well as on neuromotor development and cognition of adult rats. Finally, we studied the role of the potent antioxidant melatonin (Mel) on the neurochemical, immunohistochemical, neuromotor development, and cognitive alterations caused by L-2-HG intracerebral administration.

Experimental Procedure

Animals and Reagents

In this study, 1-day-old male and female Wistar rats were obtained from the Center for Breeding and Experimentation of Laboratory Animals at the Federal University of Rio Grande do Sul (UFRGS), Porto Alegre, RS, Brazil. The animals were kept in standard conditions, at 22 ± 2 °C room temperature and 12-h light/dark cycle. Water and a 20% (w/w) protein commercial pellet chow (SUPRA, Porto Alegre, RS, Brazil) were provided ad libitum. Procedures were performed in accordance with the Principles of Laboratory Animal Care (NIH publication 80–23, 2011), Brazilian Federal Law No. 11.794/2008, and Normative Resolution No. 30 (CONCEA-Brazilian Practice Guidelines for the Care and Use of Animals for Scientific). The experimental protocols used in this study were approved

by the Ethics Committee on the Use of Animals (CEUA) of UFRGS (protocol #35,426) and designed to reduce the number of animals used and their suffering.

All chemicals used were acquired from Sigma-Aldrich Co., St. Louis, MO, USA. L-2-HG and Mel solutions were prepared fresh in 0.01 M phosphate-buffered saline (PBS) on the day of the experiments and the pH was adjusted to 7.4.

L-2-HG Intracerebroventricular (icv) Injection

A timeline of the experimental design is shown in Fig. 1. On postnatal day 1 (PND 1), rat pups were injected with L-2-HG (0.75 µmol/g body weight, pH 7.4) or an equivalent volume of vehicle (0.01 M PBS, pH 7.4) into the cisterna magna as previously described (Olivera-Bravo et al. 2011; Ribeiro et al. 2021). The neonatal rats were kept on a heating pad at 37 °C for 20 min after icv injection to recover and then returned to the dam in their home cage. One hour before the L-2-HG injection, a group of rats received a single intraperitoneal injection of Mel (20 mg/kg body weight) (Olivier et al. 2009). Sixty rats were randomly allocated into three groups: control (PBS), L-2-HG and L-2-HG + Mel. The animals were euthanized at different time points: at 6 h after L-2-HG injection (redox homeostasis parameters), at PND15 (immunohistochemical evaluation 1) and PND75 (immunohistochemical evaluation 2). Neurodevelopmental parameters were evaluated at PND7 and motor and cognitive behavior at PND45 (Fig. 1). It is emphasized that in the neonate period the blood–brain barrier and cell membranes are immature and highly permeable to many metabolites, making the brain more vulnerable to endogenous and exogenous toxic compounds (Zhao et al. 2015; Zhou et al. 2016; Li et al. 2022).

Brain Preparation for Oxidative Stress Parameters

For redox homeostasis assessment, eighteen rats were used. The rats were euthanized by decapitation 6 h after L-2-HG icv administration. The cerebellum was rapidly removed and homogenized in 10 volumes (w/v) of 20 mM sodium phosphate buffer, pH 7.4, containing 140 mM potassium chloride for determination of 2′,7′-dichlorofluorescein (DCFH) oxidation, malondialdehyde (MDA) values, reduced glutathione (GSH) levels and the activities of the antioxidant enzymes glutathione peroxidase (GPx), and superoxide dismutase (SOD). Homogenates were centrifuged at 750 × g for 10 min and the supernatants were utilized in the assays.

Redox Homeostasis Parameters

2′,7′-Dichlorofluorescein

Reactive oxygen species (ROS) production was assessed by a 15-min incubation of cerebellum supernatants (approximately 0.06 mg of protein) with 5 µM of 2′,7′-dichlorofluorescein diacetate (DCF-DA) at 37 °C, according to the method described by LeBel et al. (1992), with slight modifications (Parmeggiani et al. 2019). The fluorescence of DCF, the ROS-oxidized form of DCF-DA, was measured at excitation and emission wavelengths of 480 and 535 nm, respectively. Cerebellar ROS production was expressed as picomoles DCF per milligram of protein.

Malondialdehyde Levels

We used Yagi's method (1998), with some modifications (Ribeiro et al. 2018), to measure MDA levels and thus estimate oxidative damage to lipids. Cerebellum supernatants containing approximately 0.3 mg of protein were reacted with a 0.67% thiobarbituric acid solution for 1-h incubation over heating at 100 °C. The organic solvent butanol was used to extract the stained complex resulting from the reaction. The fluorescence was then measured at wavelengths of 515 (excitation) and 553 (emission) nm. The level of lipoperoxidation was expressed as nanomoles of MDA per milligram of protein.

Reduced Glutathione Concentrations

GSH concentrations were measured to estimate the non-enzymatic antioxidant ability of the cerebellum after icv

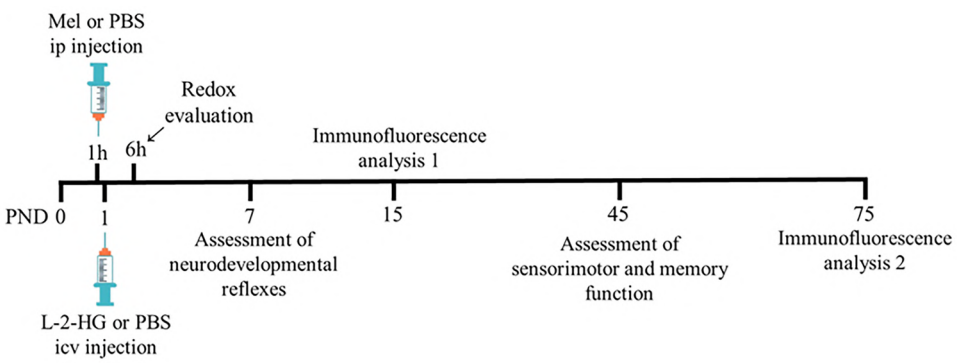

Fig. 1 Schematic representation of the experimental design showing the procedures performed on Wistar rats from neonatal (PND1) age to adulthood (PND75). icv, intracerebroventricular; ip, intraperitoneal; L-2-HG, L-2-hydroxyglutaric acid; Mel, melatonin; PND, postnatal day; PBS, phosphate-buffered saline

injection of L-2-HG using the method described by Browne and Armstrong (1998) with some modifications (Ribeiro et al. 2018). Approximately 45 µg of protein from cerebellar supernatants was deproteinized by the addition of 2% metaphosphoric acid which was followed by centrifugation at 7000 × *g* for 10 min. The deproteinized supernatant resulting from the centrifugation was reacted for 15 min with o-phthaldialdehyde. Fluorescence was then measured using excitation and emission wavelengths of 350 and 420 nm, respectively. GSH concentrations were expressed as nanomoles per milligram of protein.

Antioxidant Enzyme Activities

Cerebellum supernatants (approximately 2 µg of protein) were used to evaluate the activities of the antioxidant enzymes GPx and SOD. The method described by Wendel (1981), which uses NADPH, GSH, and tert-butyl hydroperoxide as substrates, was performed to determine GPx activity spectrophotometrically by monitoring the reduction of NADPH absorbance at a wavelength of 340 nm. SOD activity was monitored at 420 nm, based on the ability of pyrogallol to autoxidize by the action of superoxide anion described in the spectrophotometric method of Marklund (1985).

Protein Determination

Protein content was measured by the method of Lowry et al. (1951) using bovine serum albumin as a standard.

Immunohistochemical Analysis

For immunofluorescence studies, eighteen rats were used (nine rats at PND15 and nine at PND75).

At PND15 and PND75, three rats per group were anesthetized and subjected to transcardiac perfusion with 0.9% saline containing 0.16% sodium citrate followed by fixation of brain tissues with 4% paraformaldehyde. Thirty-five-micrometer-thick coronal slices were obtained from the fixed encephalic tissues using a Vibratome (VT1000S; Leica, Nussloch, Germany). For each animal and immunostaining procedure, three transverse brain slices containing the neocortex and striatum were used as previously described by Seminotti et al. (2019). All tests were carried out on free-floating slices that had been permeabilized for 20 min with 0.3% triton and incubated for 30 min in a blocking buffer (0.3% Triton prepared in PBS with 5% albumin). Subsequently, an overnight incubation at 4 °C was performed with one of the following primary antibodies: mouse anti-neuronal nuclear protein (NeuN) (1:400, Millipore #MAB377), astrocyte markers rabbit anti-glial fibrillary acidic protein (GFAP) (1:500, ThermoFisher # MA5-12,023) and rabbit anti-S100 calcium-binding protein B (S100B) (ready-to-use, Dako #IS504), microglia marker anti-ionized calcium-binding adaptor molecule 1 (Iba1) (1:1000, Wako #019–19,741), and the myelin markers mouse anti-myelin basic protein (MBP) (1:500, Sigma #AMAb91064) and rabbit anti-2′,3′-cyclic-nucleotide 3′-phosphodiesterase (CNPase) (1:500, Cell Signaling #D83E10). After incubation of the primary antibody, a secondary mouse or rabbit antibody conjugated to fluorescent probes was incubated for 90 min at room temperature with the brain Sects. (1:500, Thermo Fisher Scientific). Following that, slices were assembled using fluoroshield (Sigma-Aldrich), and images were taken using a 488- and 546-nm laser-equipped Olympus FV300 confocal microscope. Counting of NeuN-positive cells as well as measuring the fluorescence intensity of GFAP, S100B, Iba1, MPB, and CNPase was performed on three randomly selected fields per slice using Fiji software.

Neurodevelopmental Parameters

For neurodevelopmental assessment, thirty-three rats were used.

Neurodevelopmental Reflex Assessment

Neurodevelopmental reflex testing was performed at PND7 by means of negative geotaxis, righting reflex, gait, cliff avoidance, hindlimb suspension, and forelimb grasping test. Each reflex was performed in triplicate between 9:00 a.m. and 12:00 p.m. by an evaluator blinded to the experimental groups. The time (latency) to perform the task for each animal was recorded and the maximum latency was assigned when the task was not completed. In addition, the day of eye-opening was observed and a score value was assigned from the PND 10 until both eyes were opened.

Negative Geotaxis

The purpose of this test is to assess vestibular and sensorimotor competence in pups. The rats were placed on an incline board of 45° with its head down and the mean time (latency) to rotate 180° and put its face up was recorded (Ruhela et al. 2019). The maximum period for this test was 60 s.

Righting Reflex

This reflex test evaluates motor and coordination function. Each pup was kept firmly in the supine position, with all four paws upright, and the time required to reach the prone position with all four paws on the floor was recorded (Durán-Carabali et al. 2018). The maximum period to pups achieves this goal was 15 s.

Gait

The gait test allows the assessment of the locomotor function in rodents. The pups were placed in the center of a 15-cm-diameter circle, and the latency for the animals to leave the circle with both forelimbs was recorded (Nguyen et al. 2017). The maximum time allowed for the pups to leave the circle is 30 s.

Cliff Avoidance

This test assesses the development of protective responses. The pups were carefully placed with their front paws and snout on the edge of a flat acrylic platform (30 cm high). The expected result is a protective cliff aversion response, where the rat pup moves away from the edge of the cliff. The following score values were assigned for test response: 0 for falling off the platform's edge or puppy inertia, 1 for making an effort to leave the cliff but keeping limbs hanging down, 2 for effective movements that permitted the pup to move away from the cliff (Nguyen et al. 2017).

Hindlimb Suspension

This test assesses neuromuscular function by monitoring the position of the hindlimb and tail of the neonatal rats during the first 15 s of the task. The test was performed as previously described by El-Khodor and colleagues (El-Khodor et al. 2008), with minor modifications. Using a 50-ml laboratory glass beaker, the pups were gently placed face down in the beaker with the hind legs hanging over the edge of the beaker and the posture of the hindlimbs and tail was observed. The posture adopted was scored according to the following criteria: a score of 0 indicates a failure of the pup's hindlimbs to hold on to the beaker or a continuous lowering of the tail and clasping of the hindlimbs; a score of 1 shows inherent weakness and virtually constant clasping of the hindlimbs with the tail up; a score of 2 means that both hindlimbs are in close proximity to and frequently touch one other; in a score of 3, the hindlimbs are closest to each other but rarely touch; a score of 4 represents proper hindlimb separation with an extended tail.

Forelimb Grasping

The forelimb griping test is related to spinal reflexes and corticospinal inhibition of non-primary motor areas. The test involves lightly pressing a blunt rod into the palm of each pup's front paw, then watching the animal's grasping reflex, as previously described by Nguyen et al. (2017). According to the pup's reflex response, the following score values will be assigned: 0 for no grasping; 1 for grasping with just one paw; 2 for grasping with both paws.

Eye-Opening Test

To examine the maturation process of the pups, eye-opening status was monitored at PND10, 11, 12, and 13, according to the following score values: 0 for no visible eyes, 1 for one visible eye, and 2 for both visible eyes (Nguyen et al. 2017; Ruhela et al. 2019).

Body Weight

The rats had their body weight measured at PND1, before icv administration of L-2-HG or PBS injection, and weekly during the animals' development (PND7, 14, and 21).

Behavioral Analysis

Between PND45 and PND73, sensorimotor ability (ladder walking and rotarod) and cognition (Morris water maze) were assessed in adult rats, as previously described by Sanches et al. (2021). Thirty-three rats were used for behavioral analysis. The rats were filmed during the Morris water maze tests and data were analyzed using Any-Maze software (Stoelting, USA).

Rotarod Test

The Rotarod machine (Insight, 540 × 540 × 420 mm) consists of a rotating cylinder that is 20 cm above the table surface. For 2 days, the animals were habituated to the equipment through a training session consisting of 3 attempts of maximum of 300 s of walking at a constant speed of 8RPM. On the following day (test session), the motor function was evaluated by adjusting the Rotarod to increase the speed over time until it reached the maximum speed of 37 RPM. In the test session, the latency in seconds was recorded during 3 trials and the time limit to perform the task was 180 s for each trial (Sanches et al. 2021).

Ladder Walking Test

To assess forelimb and hindlimb function and gait ability, the ladder walking test was performed as previously described (Cordeiro et al. 2020). Each animal had to walk three times across an apparatus suspended at a height of 30 cm, which consists of metallic bars inserted horizontally into two transparent acrylic walls, forming a ladder. During

two consecutive days, animals were trained on the apparatus, keeping the rungs (metal bars) in a regular pattern with a 1 cm distribution between each bar. On the day of the test, the rungs were placed in an irregular pattern with a variation between 1 and 3 cm between the rungs, in order to prevent the animals from adapting to the test. The test was performed in triplicate and recorded with a digital camera positioned below the apparatus, allowing a detailed assessment of the posture and placement of the paw on the rung. The paw placement was scored from 0 to 6, in which 0 representing a total failure, when the limb misses the arrival at the rung and falls, and 6 corresponding to the correct placement of the limb on the rung, observing the perfect execution of the grasping movement. The score assignment followed the criteria described by Metz and Whishaw (2002).

Morris Water Maze

Cognitive function and learning memory were assessed using the Morris water maze. The animals' spatial reference and working memories were tested as described previously (Sanches et al. 2013). Briefly, rats were trained in a circular black acrylic tank (200-cm diameter), filled with 40 cm water (temperature 21 ± 2 °C), located in an adjustable light–dark room containing visual clues on the walls. A transparent platform (10-cm diameter) was submerged 2 cm below the water's surface. The tank was divided virtually into 4 quadrants and had 4 starting points designated as N (north), S (south), L (east), and O (west).

Reference memory protocol was carried out for five consecutive days (four trials/day) and the platform position remained in the same location throughout the training period. Animals had 60 s to locate the platform; when the task was not successful, the animal was gently guided to the platform and left on it for 15 s. An intertrial interval of 10 min was used. The Probe test for reference memory was performed without the platform for 60 s. Animals were placed at the same starting point, and the latency to cross the platform zone for the first time was registered.

In the working memory protocol, the animals were assessed during four consecutive days. The platform location was set daily at a new place and four starting positions were chosen randomly. The animal performance was determined by the difference in the mean latencies between the first and the last trial, along the 4 days.

Statistical Analysis

The data were first tested for normal distribution by the Shapiro–Wilk test and homogeneity of variances by Bartlett's test. When the data followed a normal distribution ($p > 0.05$) and variances were found to be homogeneous ($p > 0.05$), a one-way analysis of variance (ANOVA) was performed followed by the post hoc Tukey multiple range test when F was significant. However, when normality and homoscedasticity criteria were not satisfied, we used the non-parametric Kruskal–Wallis test followed by Dunn's test for multiple comparisons. All data had homogeneity of variance and followed a normal distribution, except for the neurodevelopmental tests of cliff avoidance, righting, and hindlimb suspension which did not pass the Shapiro–Wilk test for normality ($p < 0.05$). In order to analyze changes over time in longitudinal assessments, a repeated measures ANOVA was performed. The statistical test used in each of the parameters evaluated is described in the legend of the respective figure. All tests were performed in triplicate and the mean of each animal was used in the statistical calculations. Data are represented as mean ± standard deviation. All analyses were performed with GraphPad Prism 8 software and significance was reached when $P < 0.05$.

Results

Redox Homeostasis Parameters

For these measurements, we used the cerebellum of neonatal rats euthanized 6 h after L-2-HG icv injection.

L-2-HG Induces ROS Production in the Cerebellum

ROS generation was determined by measuring DCFH oxidation. Figure 2A shows that DCFH oxidation was significantly increased in the cerebellum of neonatal rats after L-2-HG administration ($F_{2, 15} = 11.82$; $P < 0.001$) and that Mel pretreatment was not able to prevent this increase.

L-2-HG Increases Lipid Oxidation in the Cerebellum

Thereafter, we tested whether L-2-HG icv injection to neonatal rats could induce lipid peroxidation evaluated by MDA levels in the cerebellum. We observed that MDA levels were significantly increased by L-2-HG (Fig. 2B) and that Mel totally prevented this effect ($F_{2, 15} = 13.61$; $P < 0.001$).

L-2-HG Disrupts Antioxidant Defenses in the Cerebellum

The levels of GSH, the major antioxidant defense in the CNS, and the activities of the antioxidant enzymes GPx and SOD were next measured in the cerebellum. L-2-HG markedly decreased GSH concentrations (Fig. 2C) ($F_{2, 15} = 24.12$; $P < 0.001$) and increased the activities of GPx (Fig. 2D) ($F_{2, 15} = 32.66$; $P < 0.001$) and SOD (Fig. 2E) ($F_{2, 15} = 23.97$; $P < 0.001$). Noteworthy, Mel normalized GSH levels, but did not influence the augmented GPx and SOD activities elicited by L-2-HG.

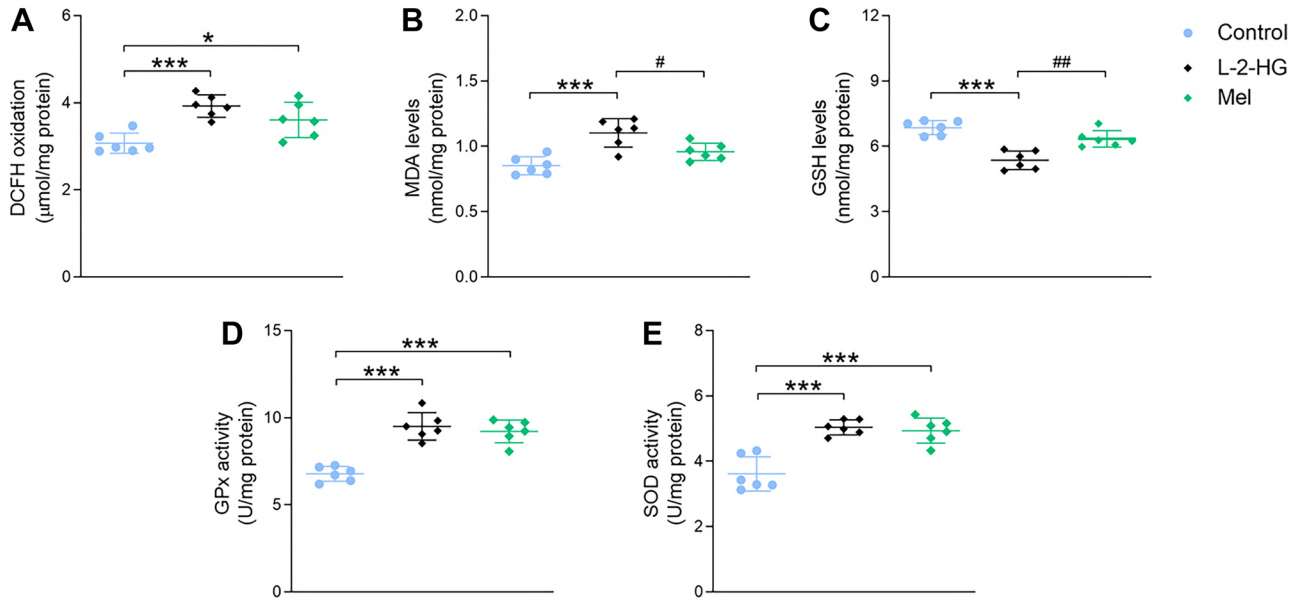

Fig. 2 Effects of intracerebroventricular (icv) injection of L-2-hydroxyglutaric acid (L-2-HG; 0.750 µmol/g) on redox homeostasis parameters in the cerebellum of neonate rats. 2′,7′-Dichlorofluorescein (DCFH) oxidation **A**, malondialdehyde (MDA) levels **B**, reduced glutathione (GSH) concentrations **C**, and the activities of the antioxidant enzymes glutathione peroxidase (GPx) **D** and superoxide dismutase (SOD) **E** were evaluated 6 h after icv injection of the metabolite. Experiments were performed in triplicate and data are represented as the mean ± SD of six animals per group. $^{*}P < 0.05$, $^{***}P < 0.001$, compared to control; $^{\#}P < 0.05$, $^{\#\#}P < 0.01$ compared to L-2-HG (one-way ANOVA, followed by the Tukey's multiple range test)

Immunofluorescence Analysis

We evaluated the immunofluorescence staining of NeuN, S100B, GFAP, and Iba1, indicating neuronal quantity, reactive astrogliosis, and microglia activation, respectively, in cerebral cortex and striatum of rats at PND15 and 75. MBP and CNPase contents were also determined at PND75 in order to evaluate myelination.

L-2-HG Decreases NeuN-Positive Cells in the Cerebral Cortex and Striatum

Figure 3 shows that L-2-HG icv injection to neonatal rats significantly decreased the number of NeuN-positive cells in the cerebral cortex (Fig. 3A, C) and striatum (Fig. 3B, D) of rats at PND15 (cerebral cortex: $[F_{2,6} = 33.80; P < 0.001]$; striatum: $[F_{2,6} = 16.97; P < 0.01]$) and PND75 (cerebral cortex: $[F_{2,6} = 11.04; P < 0.01]$; striatum: $[F_{2,6} = 21.14; P < 0.01]$), reflecting therefore long-standing neuronal loss. More importantly, Mel was able to totally prevent the reduction of the neuronal amount caused by L-2-HG.

L-2-HG Increases the Immunofluorescence Staining of GFAP and S100B in the Cerebral Cortex and Striatum

Next, we quantified the immunofluorescence staining of the astrocytic proteins GFAP and S100B. Figure 4 shows that icv injection of L-2-HG in neonatal rats increased GFAP content in the cerebral cortex (Fig. 4A $[F_{2,6} = 236.4; P < 0.001]$) and striatum (Fig. 4B striatum: $[F_{2,6} = 321.\ 4; P < 0.001]$) at PND15. The increase of the content of this protein persisted until PND75 in both brain structures (cerebral cortex: Fig. 4C $[F_{2,6} = 55.73; P < 0.001]$; striatum: Fig. 4D $[F_{2,6} = 38.10; P < 0.001]$). We also observed that L-2-HG injection was also able to increase S100B staining in the cerebral cortex (Fig. 5A $[F_{2,6} = 15.17; P < 0.01]$; Fig. 5C $[F_{2,6} = 36.74; P < 0.001]$) and in the striatum (Fig. 5B $[F_{2,6} = 18.39; P < 0.01]$; Fig. 5D $[F_{2,6} = 15.62; P < 0.01]$) both at the two PND analyzed. These results indicate a long-standing astrocyte activation caused by L-2-HG. It can also be seen in the figure that animals injected with L-2-HG and pretreated with Mel had an important reduction on reactive astrogliosis (decrease of GFAP and S100B immunofluorescence).

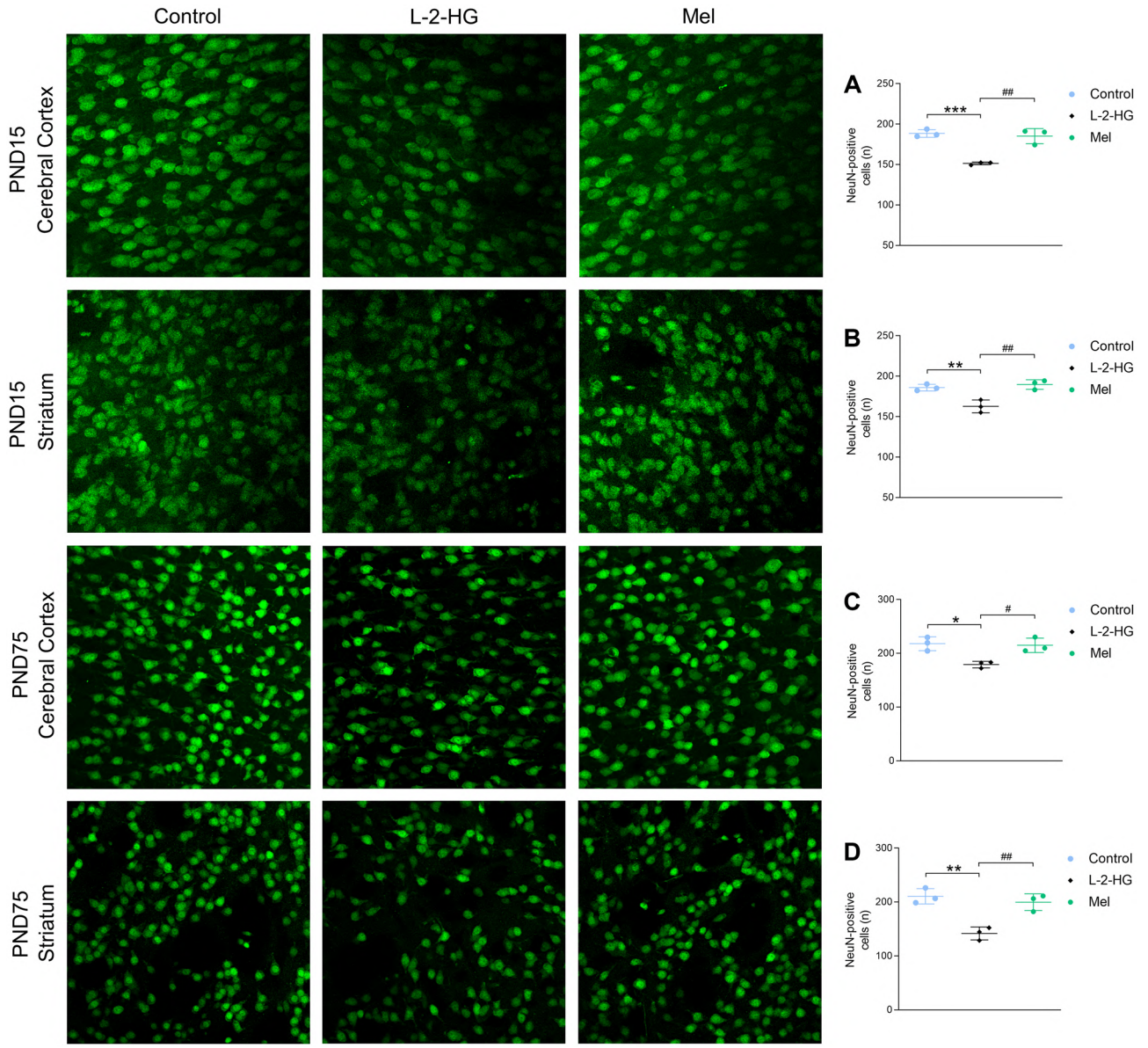

Fig. 3 NeuN immunofluorescence staining showing representative images of cerebral cortex and striatum at PND15 (**A**, **B**) and PND75 (**C**, **D**) following neonatal L-2-HG icv administration. Quantitation of NeuN-positive cells was performed on 400 × magnification images using the mean of three randomly selected fields of each brain structure per slice. Data were obtained using three slices (containing cerebral cortex and striatum) per rat brain from three animals in each experimental group and are expressed as mean ± SD. $^{*}P<0.05$, $^{**}P<0.01$, $^{***}P<0.001$ compared to control; $^{\#}P<0.05$, $^{\#\#}P<0.01$ compared to L-2-HG (One-way ANOVA, followed by the Tukey's multiple range test)

L-2-HG Increases Iba1 Immunofluorescence Staining in the Cerebral Cortex and Striatum

Cerebral cortex and striatum sections of animals injected with L-2-HG revealed a marked increase of Iba1 staining in the cerebral cortex (Fig. 6A, C) and striatum (Fig. 6B, D) of rats at PND15 (cerebral cortex: $[F_{2,6}=37.58; P<0.001]$; striatum: $[F_{2,6}=11.54; P<0.01]$) and PND75 (cerebral cortex: $[F_{2,6}=121.0; P<0.001]$; striatum: $[F_{2,6}=110.8; P<0.001]$), suggesting microglia activation. Of note, Mel was able to reduce the inflammatory process associated with activated microglia caused by L-2-HG.

L-2-HG Decreases the Expression of Myelin-Associated Proteins in Cerebral Cortex and Striatum

In order to assess whether L-2-HG icv injection in the neonatal period could impair myelination in adulthood, we

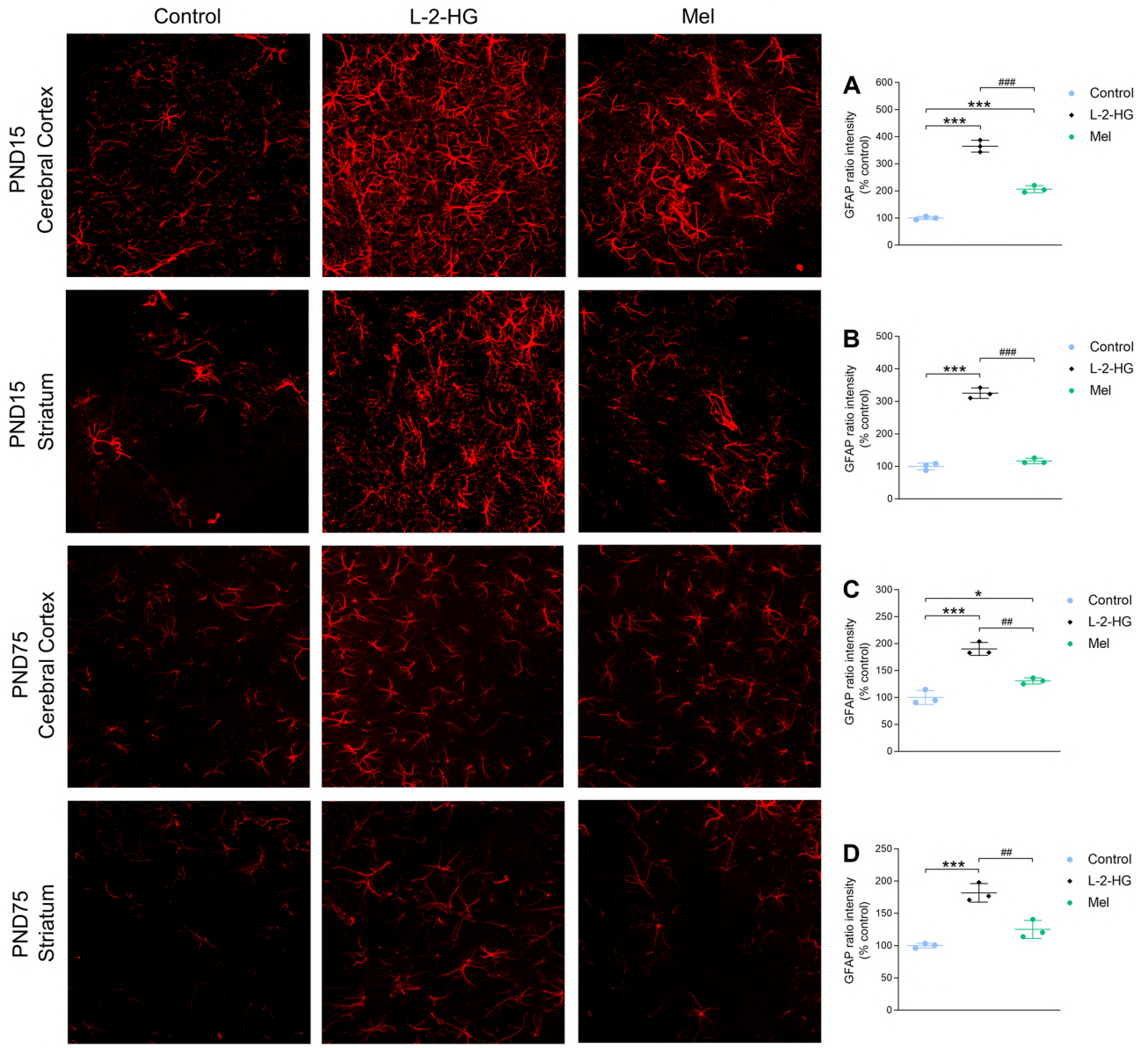

Fig. 4 GFAP immunofluorescence staining showing representative images of cerebral cortex and striatum at PND15 (**A**, **B**) and PND75 (**C**, **D**) following neonatal L-2-HG icv administration. Quantitation of GFAP fluorescence intensity was performed on 400 × magnification images using the mean of three randomly selected fields of each brain structure per slice. Data were obtained using three slices (containing cerebral cortex and striatum) per rat brain from three animals in each experimental group and are expressed as mean ± SD. $^{*}P < 0.05$, $^{***}P < 0.001$ compared to control; $^{\#\#}P < 0.01$, $^{\#\#\#}P < 0.001$, compared to L-2-HG (One-way ANOVA, followed by the Tukey's multiple range test)

evaluated MBP and CNPase myelin-associated proteins at PND75. Sections of cerebral cortex and striatum displayed a striking decrease in MBP (Fig. 7A, B) (cerebral cortex: $[F_{2,6} = 367.8; P < 0.001]$; striatum: $[F_{2,6} = 166.8; P < 0.001]$) and CNPase (Fig. 7D, E) (cerebral cortex: $[F_{2,6} = 62.39; P < 0.001]$; striatum: $[F_{2,6} = 13.16; P < 0.01]$) in both brain structures. Noteworthy, the animals pretreated with Mel had a reduction in myelin loss when compared to the L-2-HG animals, and this preventive effect was more evident in the striatum.

Neurodevelopmental Parameters

We next determined whether the neurochemical alterations found in the brain of L-2-HG-injected animals may impair their neurodevelopment over time.

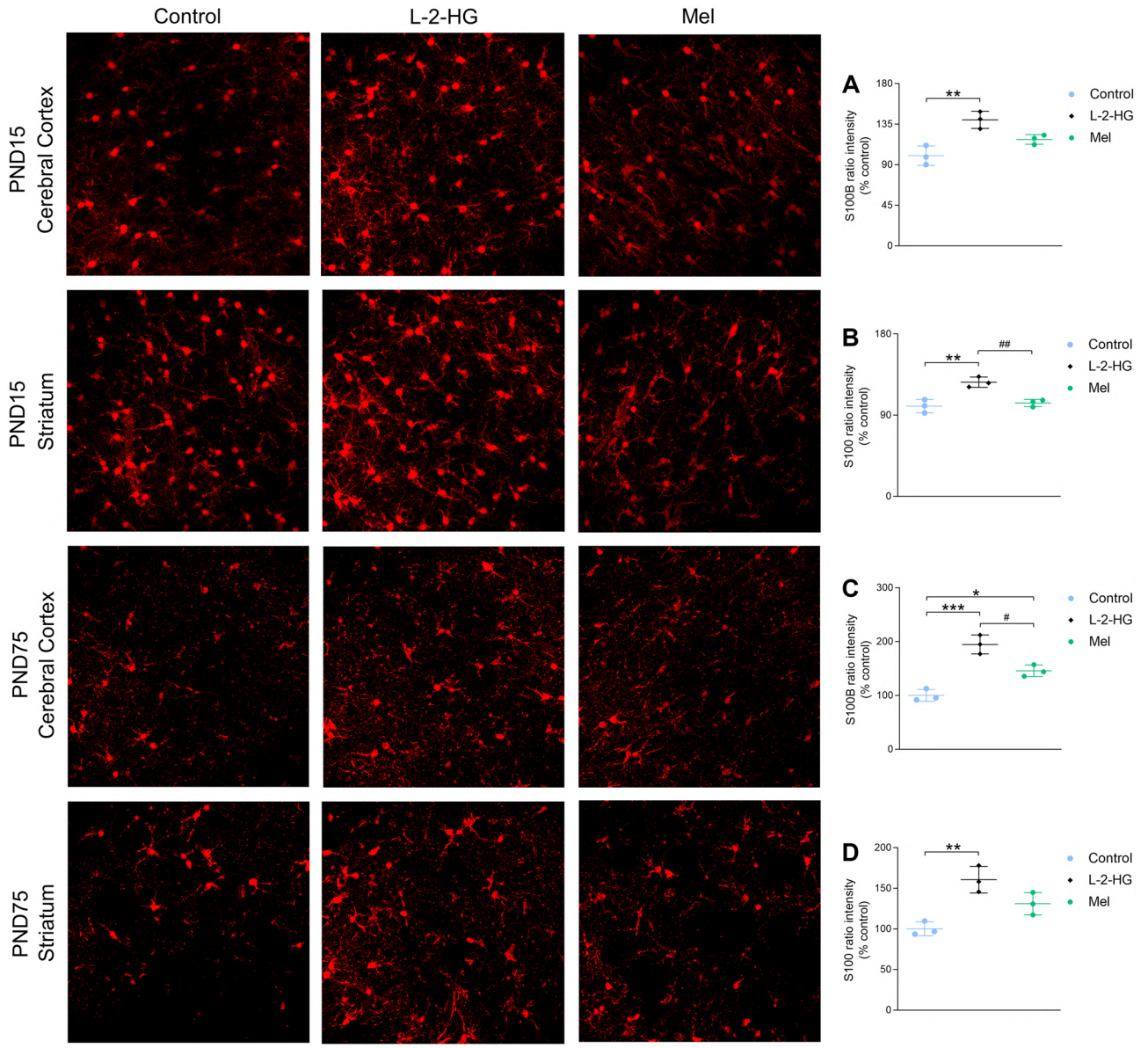

Fig. 5 S100B immunofluorescence staining showing representative images of cerebral cortex and striatum at PND15 (**A**, **B**) and PND75 (**C**, **D**) following neonatal L-2-HG icv administration. Quantitation of S100B fluorescence intensity was performed on 400 × magnification images using the mean of three randomly selected fields of each brain structure per slice. Data were obtained using three slices (containing cerebral cortex and striatum) per rat brain from three animals in each experimental group and are expressed as mean ± SD. $^{*}P<0.05$, $^{**}P<0.01$, $^{***}P<0.001$ compared to control; $^{\#}P<0.05$, $^{\#\#}P<0.01$ compared to L-2-HG (One-way ANOVA, followed by the Tukey's multiple range test)

Mel Prevents L-2-HG-Induced Delayed Neurodevelopment

We assessed whether neonatal L-2-HG icv administration could disturb rat neurodevelopment by monitoring body growth, eye-opening, and neonatal sensorimotor landmarks. The administration of L-2-HG provoked a reduction in animals' weight gain at PND7 ($F_{2,30}=8.758$; $P<0.01$), PND14 ($F_{2,30}=7.194$; $P<0.01$), and PND21 ($F_{2,30}=5.895$; $P<0.01$) (Fig. 8A). L-2-HG animals also showed delayed eye-opening at PND11 ($F_{2,30}=4.560$; $P<0.05$) and 12 ($F_{2,30}=28.64$; $P<0.001$) (Fig. 8B), verified by low score values. Interestingly, pretreatment of L-2-HG-injected animals with Mel improved the delay in eye-opening, although it was not able to prevent the L-2-HG-induced decrease in growth. Furthermore, the difference in the body weight persisted only during the lactation of the pups, whereas no difference was observed in this parameter between the experimental groups after PND21 (weaning).

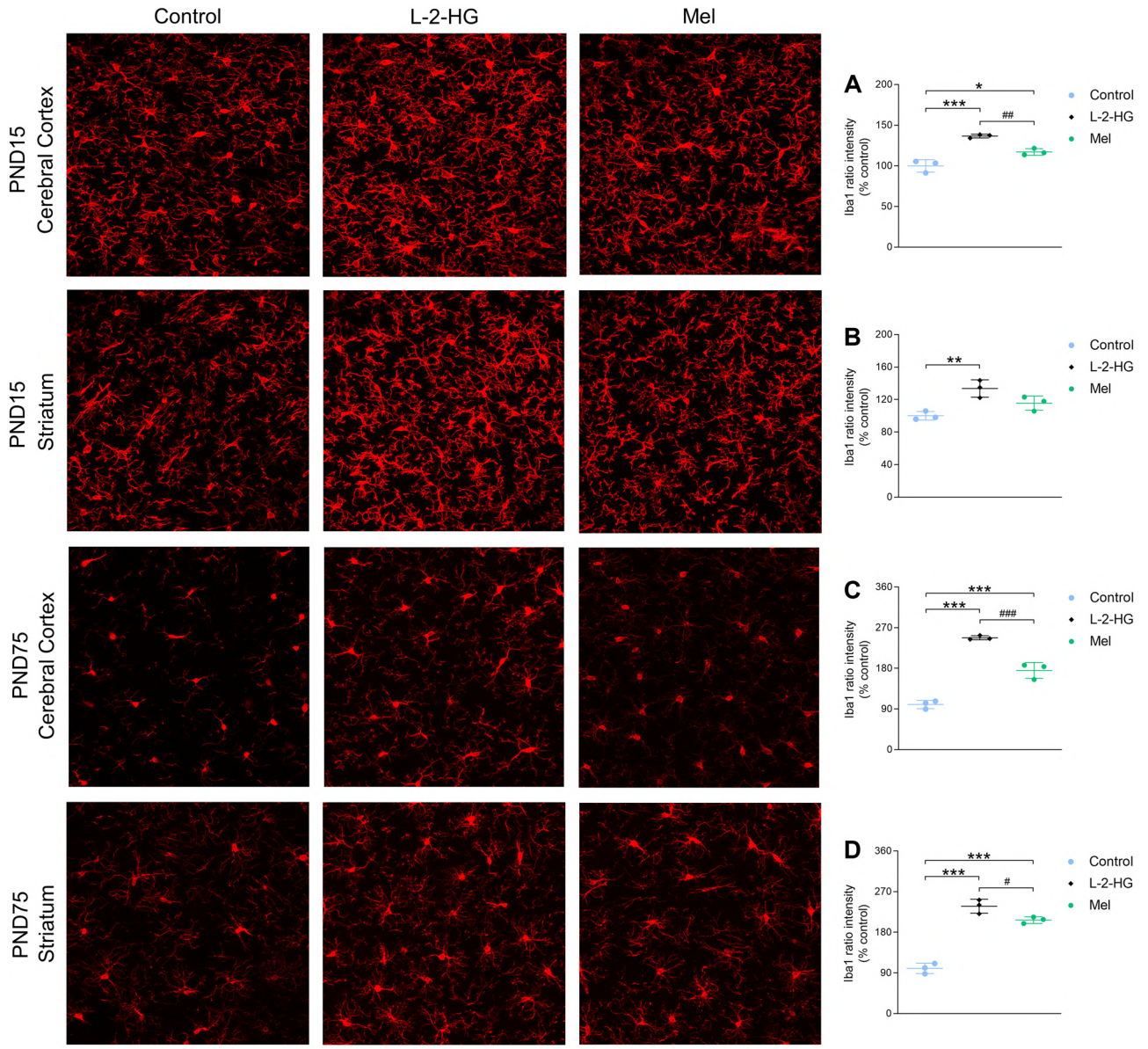

Fig. 6 Iba1 immunofluorescence staining showing representative images of cerebral cortex and striatum at PND15 (**A**, **B**) and PND75 (**C**, **D**) following neonatal L-2-HG icv administration. Quantitation of Iba1 fluorescence intensity was performed on 400×magnification images using the mean of three randomly selected fields of each brain structure per slice. Data were obtained using three slices (containing cerebral cortex and striatum) per rat brain from three animals in each experimental group and are expressed as mean ± SD. $^{*}P<0.05$, $^{**}P<0.01$, $^{***}P<0.001$ compared to control; $^{\#}P<0.05$, $^{\#\#}P<0.01$, $^{\#\#\#}P<0.001$ compared to L-2-HG (One-way ANOVA, followed by the Tukey's multiple range test)

We also evaluated the effects of L-2-HG administration on sensorimotor landmarks at PND7 (Fig. 9). It was observed that L-2-HG-treated rats spent more time to perform a vestibular response compared to controls in the negative geotaxis test ($F_{2,30}=15.96$; $P<0.001$) (Fig. 9A). The metabolite also caused an increased latency on the righting reflex ($F_{2,30}=55.67$; $P<0.001$) (Fig. 9B) and a poor performance in the cliff avoidance test ($F_{2,30}=13.63$; $P<0.001$) (Fig. 9E), as demonstrated by the low score values of the L-2-HG-injected animals. Additionally, the L-2-HG pups showed reduced mobility in the gait test ($F_{2,30}=15.17$; $P<0.001$) (Fig. 9C), followed by a loss of muscle tone in the hindlimbs (hindlimb suspension test) ($F_{2,30}=27.45$; $P<0.001$) (Fig. 8D), with no alterations in the forelimbs grasping reflex (Fig. 9F). Importantly, Mel improved most of the L-2HG deleterious effects on the sensorimotor responses, as demonstrated by an improvement in developmental parameters on negative geotaxis, righting, and

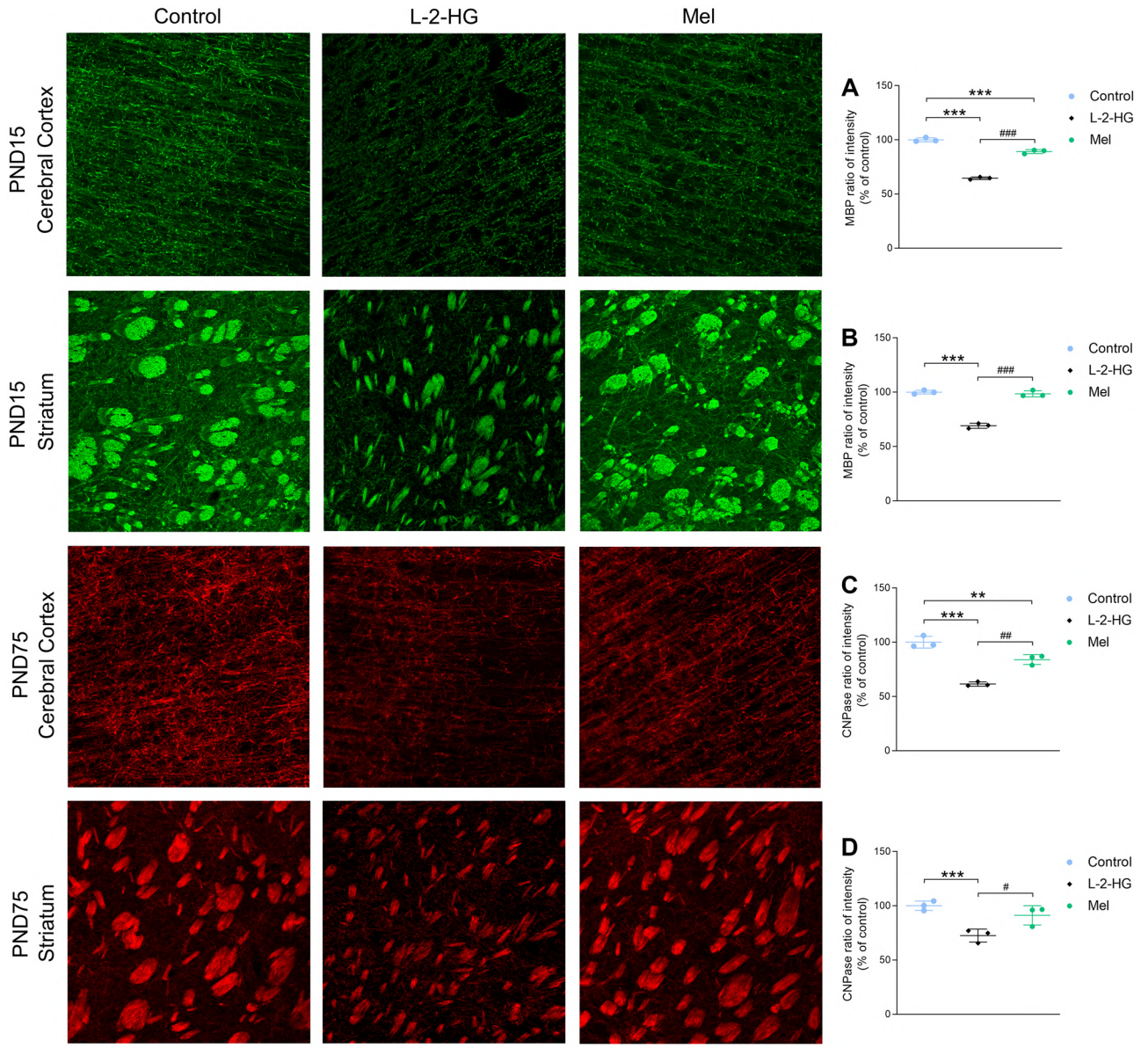

Fig. 7 Representative immunofluorescence images showing staining of the myelin-associated proteins MBP (**A**, **B**) and CNPase (**C**, **D**) in the cerebral cortex and striatum at PND75 following neonatal L-2-HG icv administration. Quantitation of MBP and CNPase fluorescence intensities was performed on 400×magnification (cerebral cortex) or 200×(striatum) images using the mean of three randomly selected fields of each brain structure per slice. Data were obtained using three slices (containing cerebral cortex and striatum) per rat brain from three animals in each experimental group and are expressed as mean ± SD. $^{**}P<0.01$, $^{***}P<0.001$ compared to control; $^{\#}P<0.05$, $^{\#\#}P<0.01$, $^{\#\#\#}P<0.001$ compared to L-2-HG (One-way ANOVA, followed by the Tukey's multiple range test)

cliff avoidance. However, Mel did not prevent the effects of L-2-HG on gait and hindlimb suspension tests.

Mel Improves L-2-HG-Induced Motor Impairment

In order to assess motor coordination in adulthood (PND45), the animals were tested on the rotarod and ladder-walking task. Motor skills evaluation is shown in Fig. 10. The L-2-HG-treated animals showed impaired gross and fine motor function, as evidenced by the decreased latencies to fall off the cylinder during the rotarod test ($F_{2,30}=10.93$; $P<0.001$) (Fig. 10A), and by a lower paw placement score of both hindlimbs ($F_{2,30}=39.51$; $P<0.001$) (Fig. 10B) and forelimbs ($F_{2,30}=59.88$; $P<0.001$) (Fig. 10C) in the ladder walking task, respectively. Furthermore, it was observed that the L-2-HG animals receiving Mel took longer to fall out of the cylinder, and improved the quality of steps in both limbs, denoting a significant improvement in fine and gross motor activity in adulthood.

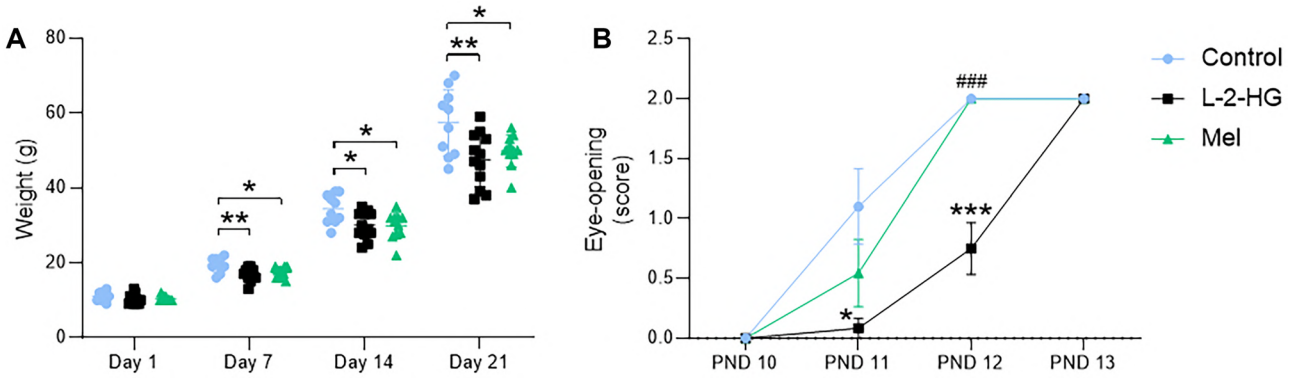

Fig. 8 Effects of icv injection of L-2-hydroxyglutaric acid (L-2-HG; 0.750 µmol/g) to rat pups on body weight (from PND1 to PND21) and eye-opening (PND10-13). Rats were weighed weekly and the eye-opening process was observed daily from PND10 onwards. Data are represented as the mean ± SD of ten to twelve animals per group. $^{*}P<0.05$, $^{**}P<0.01$, $^{***}P<0.001$ compared to control; $^{\#\#\#}P<0.001$ compared to L-2-HG (one-way ANOVA, followed by the Tukey's multiple range test)

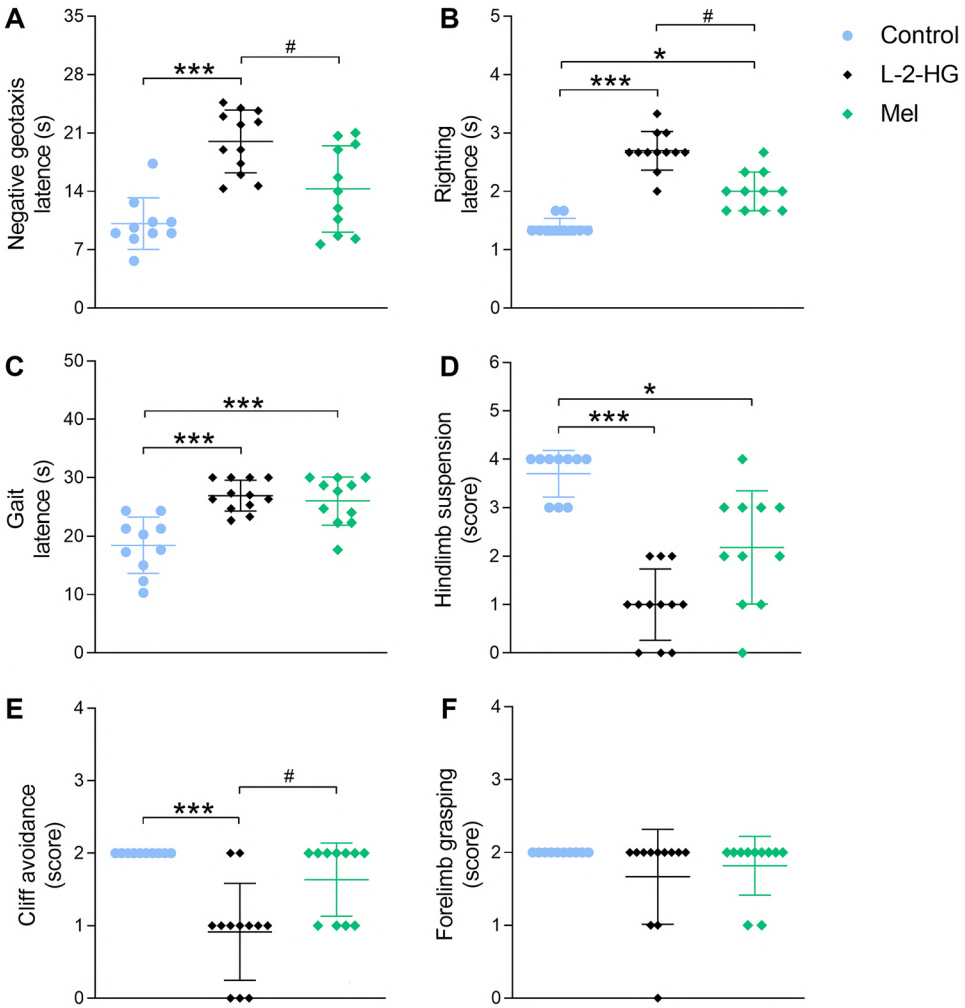

Fig. 9 Effects of icv injection of L-2-hydroxyglutaric acid (L-2-HG; 0.750 µmol/g) to neonate rats on a battery of neurodevelopmental tests. Negative geotaxis **A**, righting **B**, gait **C**, hindlimb suspension **D**, cliff avoidance **E**, and forelimb grasping **F** were evaluated 7 days after icv injection of the metabolite. The tests were performed in triplicate on each of the animals, and data are represented as the mean ± SD of ten to twelve animals per group. $^{*}P<0.05$, $^{***}P<0.001$ compared to control; $^{\#}P<0.05$ compared to L-2-HG (one-way ANOVA, Tukey's multiple range test or Kruskal–Wallis, followed by the Dunn test)

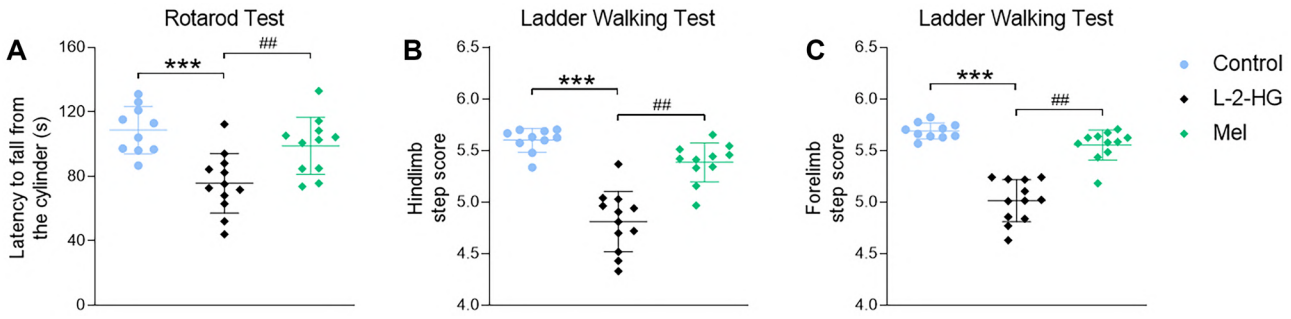

Fig. 10 Effects of icv injection of L-2-hydroxyglutaric acid (L-2-HG; 0.750 µmol/g) to neonatal rats on sensorimotor function. Gross motor coordination was assessed by means of the rotarod test **A** and gait skills of the hindlimbs **B** and forelimbs **C** through the ladder-walking test, both assessed 45 days after the icv injection of the metabolite. The tests were performed in triplicate in each of the animals, and data are represented as mean ± SD of ten to twelve animals per group. $^{***}P < 0.001$ compared to control; $^{\#\#}P < 0.01$ compared to L-2-HG (One-way ANOVA, followed by the Tukey's multiple range test)

L-2-HG Causes Impairment of Working Memory

The Morris Water Maze was performed to assess reference and working memory. The learning capability of animals is plotted in Fig. 11. Repeated ANOVA showed an effect of time, demonstrating that animals learned to find the platform over the days ($F_{2,30} = 22.79$; $P < 0.001$). Therefore, no effects of L-2-HG were observed in the learning curve (Fig. 11A). Furthermore, probe-test trial did not show differences on the time L-2-HG-treated and control animals reached the place where the platform was located during the training days (Fig. 11B). Although the reference memory was not affected, L-2-HG-injected animals had difficulties in performing the task when we evaluated working memory (Fig. 11C, D). The impairment in working memory became evident at PND4 ($F_{2,30} = 3.458$; $P < 0.05$) (Fig. 11A) and also by the difference of the mean latencies between the first and the last trial along the 4 days ($F_{2,30} = 9.846$; $P < 0.001$) (Fig. 11B).

Discussion

Neurological symptoms, including epilepsy, psychomotor delay, tremors, and ataxia, accompanied by abnormalities in the cerebral cortex, basal ganglia, and cerebellum are characteristically observed in patients affected by L-2-HGA (Gunduz et al. 2022; Shah et al. 2020; Steenweg et al. 2009, 2010; Topçu et al. 2005). The lack of effective treatment for this disorder is presumably attributed to the still poorly known pathomechanisms of brain damage. However, it is conceivable that L-2-HG is neurotoxic because this organic acid accumulates within the brain due to its low efflux, similar to what occurs with other dicarboxylic acids (Sauer et al. 2010). The observations of an L-2-HG cerebrospinal fluid/plasma ratio higher than one support this hypothesis, indicating the production and accumulation of this compound within the brain (Kranendijk et al. 2012). In this respect, L-2-HG induces oxidative stress in vitro and in vivo in the cerebral cortex and striatum of young adult rodents (Latini et al. 2003; da Rosa et al. 2015), a finding that was also found in plasma and urine of patients with L-2-HGA (Jellouli et al. 2014; Rodrigues et al. 2017). Furthermore, a study from our group revealed that early icv administration of L-2-HG impairs redox homeostasis in the cerebral cortex and striatum of neonatal rats (Ribeiro et al. 2018). L-2-HG increased the generation of ROS, caused lipid peroxidation and protein oxidation, and decreased the non-enzymatic antioxidant defenses in the cerebral cortex. Changes in the activities of several antioxidant enzymes were also observed in the cerebral cortex and striatum after L-2-HG administration. In addition, melatonin and the NMDA glutamate receptor antagonist MK-801 were able to avoid lipid oxidation and the decrease in GSH concentrations caused by L-2-HG in the cerebral cortex, implying that reactive species generation and overstimulation of NMDA receptors were involved in the deleterious effects of L-2-HG (Ribeiro et al. 2018).

However, to the best of our knowledge, nothing has been reported on the effects of high concentrations of this organic acid during the neonatal period in the cerebellum, which is mainly affected in this disease, resulting in movement disorders. Therefore, in this work, we administered an icv injection of L-2-HG to neonatal rats and evaluated its influence on redox homeostasis in the cerebellum, as well as on the neuromotor abilities along development and on the cognition of adult rats. Immunohistochemical studies aiming to determine the amount of neurons, reactive astrogliosis, and microglial reactivity in the cerebral cortex and striatum were also carried out at different postnatal ages to clarify the brain damage following a L-2-HG cerebral overload in the neonatal stage. Since previous works observed that L-2-HG elicits oxidative stress, we pre-treated a group of animals with the potent antioxidant Mel to test whether disturbance of redox homeostasis could underlie the deleterious effects

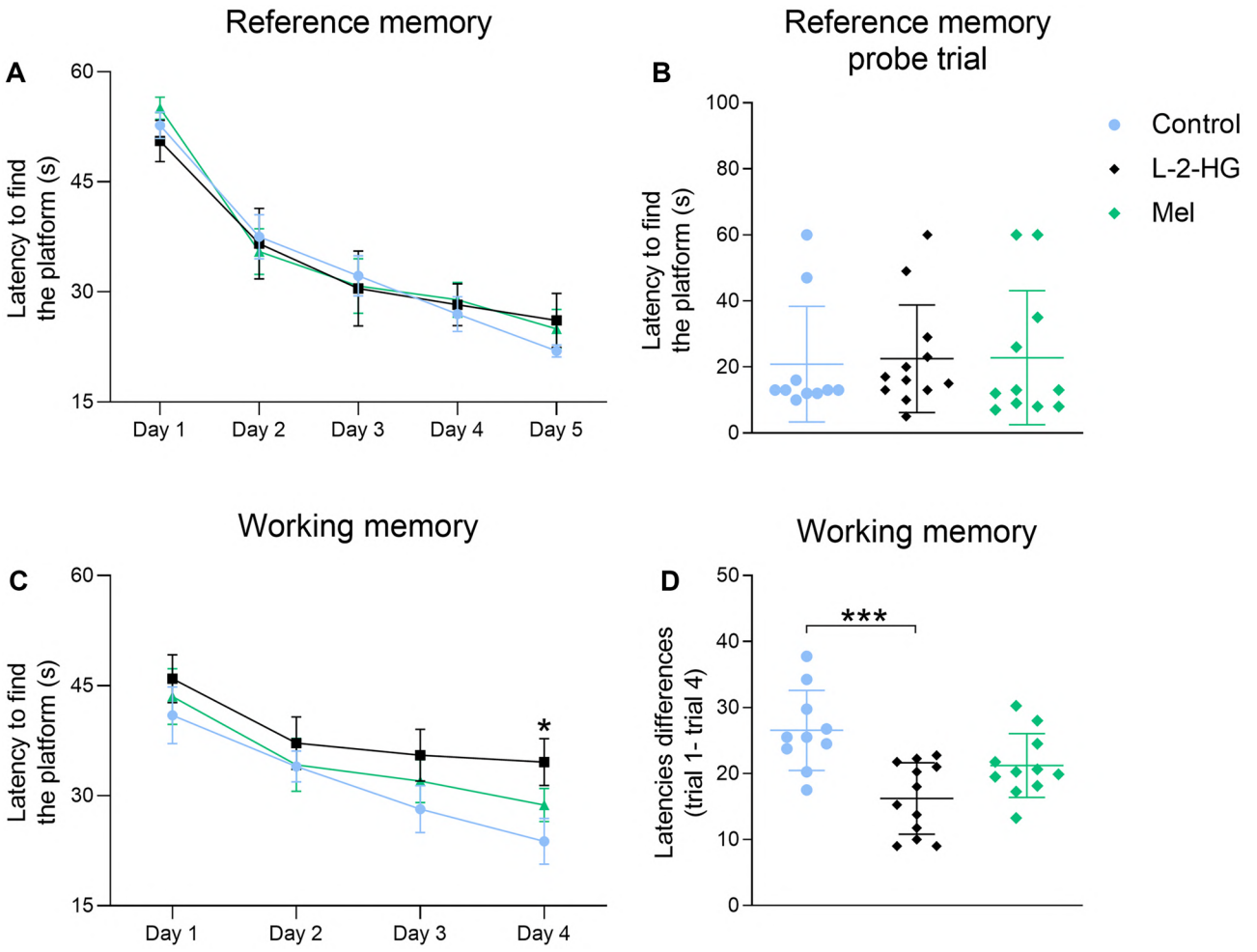

Fig. 11 Effects of icv injection of L-2-hydroxyglutaric acid (L-2-HG; 0.750 µmol/g) to neonatal rats on cognitive abilities. Reference and working memory performance in the Morris Water Maze were assessed at adult age (PND55), following L-2-HG administration. Mean latencies to reach the platform during five consecutive days of training **A** and the latency to cross the platform location in the probe test **B** for reference memory protocol. Mean latencies to reach the platform during four consecutive days of training **C** and the latency differences from day 1 to day 4 **D** for working memory protocol. Data are expressed as mean ± SD of ten to twelve animals per group. $^{*}P < 0.05$, $^{***}P < 0.001$ compared to control (One-way ANOVA, followed by the Tukey's multiple range test)

of L-2-HG in the cerebellum and whether this class of drugs could possibly serve as a potential treatment for this disease. In this particular, Mel has been previously shown to prevent oxidative stress elicited by various compounds accumulating in inborn errors of intermediary metabolism, including D-2-hydroxyglutaric aciduria, hyperglycinemia, and 3-hydroxy-3-methylglutaryl-coenzyme A lyase deficiency (Moura et al. 2016; da Rosa et al. 2016; Ribeiro et al. 2021), as well as in common neurodegenerative diseases, such as Alzheimer's and Parkinson's diseases (Morén et al. 2022).

At this point, it should be stressed that although the primary accumulation of L-2-HG is intramitochondrial, it is conceivable that this metabolite can cross through cell membranes since it is detected at very high concentrations in the biological fluids of patients affected by L-2-HGA. Furthermore, considering that at physiological pH (i.e., 7.4) L-2-HG predominates in its ionized form, one or more still unidentified carrier proteins seem necessary to facilitate the membrane transport of this organic acid. Recent studies showing that bone-marrow-derived macrophages and human monocyte-derived dendritic cells are permeable to L-2-HG provide indirect evidence of a possible transport carrier for this organic acid in these cells (Ugele et al. 2019; Williams et al. 2022).

We initially observed that neonatal icv L-2-HG administration provokes short-lived effects in the cerebellum, increasing ROS production (increased DCFH oxidation) and lipid oxidative damage (increased MDA values) and disturbing the antioxidant system (decreased GSH concentrations and increased activities of the antioxidant enzymes GPx and SOD). The later effects were probably through a compensatory effect at the transcription level augmenting

the synthesis of these antioxidant enzymes due to the high production of ROS, which are scavenged by these antioxidant activities (Halliwell and Gutteridge 2015). Regarding the elevated lipoperoxidation levels verified in the cerebellum, it is emphasized that phospholipid peroxidation of membranes leads to cell damage, which is one of the most important effects of oxidative damage (Catalá 2009; Ayala et al. 2014). L-2HG-injected animals were more susceptible to lipid damage possibly due to the increased production of ROS (DCFH oxidation). In this particular, it is possible that the reduction of the concentrations of GSH, the most potent antioxidant in the brain that effectively scavenges ROS (Kwon et al. 2019), could make lipids more susceptible to oxidative damage. Taken together, these findings provide a strong indication that oxidative stress was induced in the cerebellum by in vivo administration of L-2-HG at the neonatal age, given that this condition usually occurs when the capacity of the antioxidant defenses is overwhelmed by reactive species production. It is important to mention that similar findings were previously described in the cerebral cortex and striatum using this model (Ribeiro et al. 2018), indicating that various cerebral structures are affected by L-2HG brain overload following an icv injection of this compound at the neonatal stage.

We also stress that increased generation of ROS facilitates the oxidation of molecules essential to the maintenance of the cellular environment, such as lipids, proteins, carbohydrates, and DNA, and may represent an important pathogenic event in the cascade of cellular necrosis and apoptosis (Ryter et al. 2007; Chan et al. 2009; Circu and Aw 2010). Another important finding of the present study was that Mel totally avoided L-2-HG-induced lipoperoxidation and the decreased GSH concentrations, but had no effect on the increased antioxidant enzymatic defenses in the cerebellum. Since Mel is able to scavenge hydroxyl and peroxyl radicals (Reiter et al. 2010; Morén et al. 2022), which are also involved in DCFH oxidation, it is presumed that these reactive radicals may underlie at least in part the L-2-HG-induced oxidative stress observed in the cerebellum.

Interestingly, oxidative stress was previously observed in tissues and biological fluids of patients with L-2HGA (Jellouli et al. 2014; Rodrigues et al. 2017; Cansever et al. 2019). In this particular, significant increases of oxidized guanine species (DNA oxidative damage) and di-tyrosine (protein oxidation) were found in the urine of 11 L-2-HGA patients (Rodrigues et al. 2017). Furthermore, Jellouli et al. (2014) observed increased lipid peroxidation (increased MDA levels) and decrease of GSH and of the antioxidant enzymes SOD and GPx in plasma of 14 L-2-HGA patients. Finally, increased levels of disulfide, as well as of the ratios disulfide/native thiol and disulfide/total thiol, were detected in the plasma of two nontreated patients with this disorder (Cansever et al. 2019). Taken together the human and animal studies showing pro-oxidant effects of L-2-HG, it may be presumed that disruption of redox homeostasis induced by the major metabolite accumulating in L-2-HGA is involved in the brain damage of this disease.

Since the present work demonstrated oxidative stress induction in the cerebellum of neonatal rats 6 h after icv injection of L-2-HG, which was similarly demonstrated in the cerebral cortex and striatum using this model (Ribeiro et al. 2018), we next investigated whether the L-2-HG-induced redox homeostasis disturbance might lead to injury to striatal and cortical neural cells. The immunohistochemical studies revealed that L-2-HG neonatal administration caused long-standing (PND 15 and 75) neuronal loss (decreased NeuN positive cells), demyelination (decreased MBP and CNPase), reactive astrogliosis (increased GFAP and S100B), and microglial reactivity (increased Iba1) in the striatum and cerebral cortex following icv injection of L-2-HG to neonatal rats, which were fully prevented (NeuN, MBP, and CNPase) or attenuated (S100B, GFAP, and Iba1) by Mel pretreatment.

It is stressed that GFAP is an excellent astrocyte marker, being the main constituent protein of astrocyte intermediate filaments, while S100B is a calcium-binding protein mainly concentrated in astrocytes (Michetti et al. 2019; Escartin et al. 2021). Noteworthy, the expression of these proteins is increased by reactive astrocytes (Janigro et al. 2022). Although a slight increase in GFAP and S100B indicates a moderate activation of astrocytes and is thought to be linked to mechanisms of protection to surrounding neurons, excessive glial reactivity (astrogliosis) is usually associated with brain damage, as evidenced in various neurodegenerative conditions (Hol and Pekny 2015; Michetti et al. 2019; Sreejit et al. 2020). In this particular, we also verified in our present study that L-2-HG-treated rats showed a decrease of NeuN staining, indicating neuronal damage or/and loss, in parallel with glial reactivity. In line with our data, neuronal loss associated with astrogliosis was previously observed in the brainstem and the cerebellum of a 1-month-old infant with L-2-HGA (Chen et al. 1996).

Another important finding of the present study was that icv injection of L-2-HG increased the immunofluorescence of Iba1, a constitutively expressed protein in microglia. Iba1 plays an essential role in the morphological changes from quiescent to activated microglia, being therefore a suitable marker of microglia activation (Sasaki et al. 2001; Hovens et al. 2014). Once activated, microglia can lead to exacerbated increases in proinflammatory cytokines and ROS production, contributing to neuroinflammation (Wirths et al. 2010; Norden et al. 2016; Seminotti et al. 2019).

Myelin is formed by modified extensions of the oligodendrocyte cell membrane that, in addition to a diversity of lipids, contain several proteins, which are crucial to maintain the structure and stability of the myelin sheath (Fulton

et al. 2010). We evaluated the content of two of these proteins, MBP (myelin basic protein), the main constituent of the myelin membrane, and CNPase (2′,3′-cyclic nucleotide 3′-phosphodiesterase), which constitutes 4% of CNS myelin, being sensitive markers of myelination status. MBP is found within the myelin sheath and assists in the compaction process that generates the mature multilevel myelin structure, while CNPase, in addition to its structural role, acts in the regulation of oligodendrocyte process outgrowth (Lee et al. 2005; Fulton et al. 2010). In our study, the animals submitted to a single icv administration of L-2-HG in the neonatal period developed long-lasting white matter damage, verified by the decrease in immunofluorescence staining of MBP and CNPase proteins at PND75 in the cerebral cortex and striatal, that may explain the hypomyelination seen in patients and in the L-2-HGA genetic mouse model (Rzem et al. 2015).

Taken together, the mechanisms of L-2-HG-induced neurotoxicity seem to involve a complex cellular interaction, initiated by an early redox imbalance elicited by toxic levels of this metabolite that may lead to astrocyte and microglia reactivity over time, ultimately leading to progressive neurodegeneration and demyelination.

The early stages of brain maturation are crucial for the healthy and complete development of the newborn brain. Homeostasis disorders or injuries in the postnatal period can contribute to brain abnormalities, leading to functional impairments. Furthermore, it has already been shown in the literature that neonatal injuries in animal models associated with motor deficit can also result in feeding difficulties, which may lead to decreased weight gain, especially in early periods after injury (Buratti et al. 2019; Tassinari et al. 2020; Sanches et al. 2021). In addition, neonatal injuries can induce alterations in neonatal rat vocalization, affecting maternal-pup interaction and reducing effective maternal care (Saucier et al. 2008). In this particular, we found that the body weight of L-2-HG-injected animals was lower than the control group over time for about 3 weeks (from PND7 to PND21).

On the other hand, assessment of developmental milestones is highly relevant for estimating CNS maturation and the impact of perinatal damage in experimental animal models (Horvath et al. 2015), being an essential tool for tracking development due to administration of metabolites such as L-2-HG. The neurodevelopment of the L-2-HG-treated pups was evaluated using the righting reflex, cliff avoidance, and negative geotaxis at PND7. Our data show that L-2-HG-treated animals exhibit a worse sensorimotor response when compared to the control group. Sensorimotor tests require adequate coordination between sensory input and motor output involving the integration of the vestibular system, spinal cord, and muscles (Arakawa and Erzurumlu 2015; Nguyen et al. 2017). Therefore, the damage caused by L-2-HG on these parameters may reflect a delayed maturation of the CNS. We also investigated whether L-2-HG administration could cause neurodevelopmental disturbances associated with locomotion (gait test) and muscle tone strength (hindlimb suspension) at PND7. The injection of L-2-HG promoted a marked decrease in gait ability and muscle strength in the pups, which is consistent with the motor symptoms observed in L-2-HGA patients, which are classic manifestations of neurological dysfunction, even at early stages of the disease (Kranendijk et al. 2012).

To assess whether L-2-HG injection could affect the maturation of the visual system, we determined the day of eye-opening. Control animals exhibited eye-opening as widely described in the literature (Heyser 2004), with this process beginning at PND11. Furthermore, both eyes opened at PND12 in all control rats, whereas L-2-HG-treated animals had 1 day delay in the total opening of both eyes (PND13). It is emphasized that during neocortical development and maturation, neural connectivity and synaptic transmission are influenced by afferent visual activity (Katz and Shatz 1996; Pecka et al. 2014; Guan et al. 2017). Thus, delays in eye-opening such as that caused by L-2-HG may suggest an impairment on visual system maturation and of muscle tone strength (hindlimb suspension) at PND7. The injection of L-2-HG promoted a marked decrease in gait ability and muscle strength in the pups, which is consistent with the motor symptoms observed in L-2-HGA patients, which are classic manifestations of neurological dysfunction, even at early stages of the disease (Kranendijk et al. 2012). The deleterious effects on neurodevelopment induced by L-2-HG may be linked to oxidative stress, neuronal loss, and neuroinflammation observed both short and long time after metabolite injection. In this sense, there are many evidences that perinatal brain injury leading to disruption of redox homeostasis, glial reactivity, neuronal death, and white matter injury may compromise neurodevelopmental outcome (Rains et al. 2021; Yeh et al. 2021; Xiao et al. 2021; Herrera et al. 2022).

Importantly, pre-treatment of L-2-HG-injected animals with Mel improved the neurodevelopmental deficits in most of the tests evaluated here, denoting a neuroprotective effect of this hormone on our experimental model of L-2-HGA. Accordingly, Mel has been used as a neuroprotective agent ameliorating oxidative stress, neuroinflammation, and pro-apoptotic signaling pathways in various neuropathologies (Wakatsuki et al. 2001; Chitimus et al. 2020; Elsayed et al. 2021; Victor et al. 2021). Moreover, the neonatal age has been considered a critical period of intervention in previous works using Mel as a therapeutic strategy (Victor et al. 2021), acting as a mediator of synaptic plasticity and neuroglial development, with apparent benefits to the neurodevelopment (Aridas et al. 2018; Ramírez-Rodríguez et al. 2018).

Motor and cognitive deficits are predominant clinical features in patients with L-2-HGA, and as the disease progresses, cerebellar ataxia and other motor disorders become

more evident (Steenweg et al. 2010; Kranendijk et al. 2012; Gunduz et al. 2022). Neurological diseases linked to the deterioration of brain regions associated with motor control usually show reduced motor activity (Gowen and Miall 2007; Guo et al. 2012; Ryan et al. 2014; Sebastianutto et al. 2017; Ermine et al. 2019), which can easily be verified in animal models performing behavioral tests of motor function (Brooks and Dunnett 2009). In this study, L-2-HG caused motor impairment that persisted until adulthood, as verified by the assessment of gross motor function (Rotarod) and gait skills (ladder walking test) at PND45. In this context, morphological alterations in brain structures related to input and output projections from and to the striatum affecting movement quality and motor feedback control mediated by sensorimotor information have been previously described (Smith et al. 2000). Moreover, insults at early postnatal period coincide with the formation and maturation of thalamocortical, cortico-cortical, and corticospinal tracts, which could lead to aberrant connectivity and subsequent sensorimotor deficits (Clowry et al. 2014).

Clinical studies associated with neuroimaging in a cohort of 56 L-2-HGA patients showed marked white matter abnormalities in subcortical regions, especially in the basal ganglia (Steenweg et al. 2009). Furthermore, irregular movements and impaired somatosensory responses have been recently correlated with cerebellar atrophy in L-2-HGA patients (Gunduz et al. 2022). The marked loss of neurons, chronic glial reactivity, and especially the demyelination observed in the cerebral cortex and striatum concomitant with the motor deficits mediated by intracerebral injection of L-2-HG demonstrate the enormous potential of our model to mimic the neuropathological findings of L-2-HGA.

Rzem et al. (2015) developed a L-2-hydroxyglutarate dehydrogenase-deficient mice (l2hgdh$^{-/-}$) that exhibited extensive white matter spongiform lesions, most markedly in subcortical regions and basal ganglia, and milder in the cerebral cortex, cerebellum, and hippocampus. Despite extensive leukodystrophy in several encephalic structures, this genetic model of L-2-HGA showed no changes in rotarod test performance, denoting the absence of motor dysfunction in this model. On the other hand, Rzem demonstrated that L-2-HGA animals showed cognitive impairments related to working and reference memory evocation assessed by the Y-maze and water-maze tests, respectively. In consonance with the data from the genetic model, we also found an impairment in working memory in the water-maze test, but without altering spatial reference memory. Different from hippocampus-dependent memory, recent studies have evidenced that cerebellar-cortical structures contribute to working memory performance (Stein 2021). Thus, cellular disruptions induced by L-2-HGA in subcortical and frontoparietal brain regions could be possibly responsible for the working memory deficits observed here.

Finally, positive effects of Mel treatment against cognitive deficits after brain insults at different periods of neurodevelopment have been recently reported. This hormone was shown to exert neuroprotection by modulating inflammatory responses, increasing neurotrophic factor levels, promoting synaptic plasticity, decreasing lipid peroxidation and nitric oxide, and increasing SOD and catalase activities in important cerebral structures related to memory function such as the hippocampus and cerebral cortex (Lamtai et al. 2022; Thangwong et al. 2022; Mansouri et al. 2022). The data presented in this study suggest that Mel possesses beneficial effects in our neonatal model of L-2-HGA, improving neurochemical, histopathological, and behavioral alterations. It could be therefore presumed that oxidative stress mediates the abovementioned deleterious effects caused by L-2-HG.

Conclusions

Our present work shows for the first time that L-2-HG administered during the neonatal period causes oxidative stress in the cerebellum of neonatal rats. Other novel findings of this study were that this treatment induced long-standing neuronal loss, microglia activation, increased inflammatory response, and disturbances of myelination in the cerebral cortex and striatum of adolescent (PND15) and adult (PND75) rats. It is hypothesized that these multiple alterations may represent deleterious mechanisms of brain damage that may underlie the neurodevelopmental delay and motor/cognitive deficits observed in adult rats after neonatal administration of this organic acid, and be possibly involved in the onset and progression of neurological symptoms and brain abnormalities commonly found in L-2-HGA patients. Another important novel finding of this work was that an antioxidant (Mel) restored the altered neurochemical and immunohistochemical landmarks, as well as the neurodevelopmental delay and cognitive deficit caused by L-2-HG early administration. Therefore, we presume that disturbances of redox homeostasis are involved in L-2-HGA neurotoxicity and that future research on effective antioxidants to the brain may represent a new therapeutic strategy to improve the prognosis of patients with this disorder.

Author Contribution RTR, MW, and CAN contributed to the conception and design of the study; RTR, AVSC, LEDC, RP, and ABZ contributed to the acquisition and analysis of data; RTR, MW, and AUA contributed to drafting the text.

Funding This work was supported by grants from Conselho Nacional de Desenvolvimento Científico e Tecnológico (grant number #402440/2021–8), Fundação de Amparo à Pesquisa do Estado do Rio Grande do Sul (PRONEX II) (grant number #16/0465–0), and Instituto Nacional de Ciência e Tecnologia em Excitotoxicidade e Neuroproteção (INCT-EN) (grant number #465671/2014–4).

Data Availability Data will be made available on request.

Declarations

Conflict of Interest The authors declare no competing interests.

References

Anghileri E, Bertolino N, Salsano E et al (2016) In-vivo brain H1-MR-spectroscopy identification and quantification of 2-hydroxyglutarate in L-2-Hydroxyglutaric aciduria. Brain Res 1648:506–511. https://doi.org/10.1016/j.brainres.2016.08.013

Arakawa H, Erzurumlu RS (2015) Role of whiskers in sensorimotor development of C57BL/6 mice. Behav Brain Res 287:146–155. https://doi.org/10.1016/J.BBR.2015.03.040

Aridas JDS, Yawno T, Sutherland AE et al (2018) Systemic and transdermal melatonin administration prevents neuropathology in response to perinatal asphyxia in newborn lambs. J Pineal Res 64:e12479. https://doi.org/10.1111/JPI.12479

Ayala A, Muñoz MF, Argüelles S (2014) Lipid peroxidation: production, metabolism, and signaling mechanisms of malondialdehyde and 4-hydroxy-2-nonenal. Oxid Med Cell Longev. https://doi.org/10.1155/2014/360438

Barth PG, Hoffmann GF, Jaeken J et al (1992) L-2-hydroxyglutaric acidemia: a novel inherited neurometabolic disease. Ann Neurol 32:66–71. https://doi.org/10.1002/ANA.410320111

Barth PG, Wanders RJA, Scholte HR et al (1998) L-2-hydroxyglutaric aciduria and lactic acidosis. J Inherit Metab Dis 21:251–254. https://doi.org/10.1023/A:1005316121584

Brooks SP, Dunnett SB (2009) Tests to assess motor phenotype in mice: a user's guide. Nat Rev Neurosci 10:519–529. https://doi.org/10.1038/NRN2652

Browne RW, Armstrong D (1998) Reduced glutathione and glutathione disulfide. Free Radical and Antioxidant Protocols 108:347–352. https://doi.org/10.1385/0-89603-472-0:347

Buratti P, Covatti C, Centenaro LA et al (2019) Morphofunctional characteristics of skeletal muscle in rats with cerebral palsy. Int J Exp Pathol 100:49–59. https://doi.org/10.1111/IEP.12304

Cansever MS, Zubarioglu T, Oruc C et al (2019) Oxidative stress among L-2-hydroxyglutaric aciduria disease patients: evaluation of dynamic thiol/disulfide homeostasis. Metab Brain Dis 34:283–288. https://doi.org/10.1007/S11011-018-0354-8/TABLES/3

Catalá A (2009) Lipid peroxidation of membrane phospholipids generates hydroxy-alkenals and oxidized phospholipids active in physiological and/or pathological conditions. Chem Phys Lipids 157:1–11. https://doi.org/10.1016/J.CHEMPHYSLIP.2008.09.004

Chan PH, Niizuma K, Endo H (2009) Oxidative stress and mitochondrial dysfunction as determinants of ischemic neuronal death and survival. J Neurochem 109:133–138. https://doi.org/10.1111/J.1471-4159.2009.05897.X

Chen E, Nyhan WL, Jakobs C et al (1996) L-2-Hydroxyglutaric aciduria: neuropathological correlations and first report of severe neurodegenerative disease and neonatal death. J Inherit Metab Dis 19:335–343. https://doi.org/10.1007/BF01799264

Chitimus DM, Popescu MR, Voiculescu SE et al (2020) Melatonin's impact on antioxidative and anti-inflammatory reprogramming in homeostasis and disease. Biomolecules 10:1211. https://doi.org/10.3390/BIOM10091211

Circu ML, Aw TY (2010) Reactive oxygen species, cellular redox systems, and apoptosis. Free Radic Biol Med 48:749–762. https://doi.org/10.1016/j.freeradbiomed.2009.12.022

Clowry GJ, Basuodan R, Chan F (2014) What are the best animal models for testing early intervention in cerebral palsy? Front Neurol 5. https://doi.org/10.3389/FNEUR.2014.00258

Cordeiro JL, Neves JD, Nicola F et al (2020) Arundic acid (ONO-2506) attenuates neuroinflammation and prevents motor impairment in rats with intracerebral hemorrhage. Cell Mol Neurobiol. https://doi.org/10.1007/S10571-020-00964-6

da Rosa MS, João Ribeiro CA, Seminotti B et al (2015) In vivo intracerebral administration of L-2-hydroxyglutaric acid provokes oxidative stress and histopathological alterations in striatum and cerebellum of adolescent rats. Free Radic Biol Med 83:201–213. https://doi.org/10.1016/j.freeradbiomed.2015.02.008

da Rosa MS, Seminotti B, Ribeiro CAJ et al (2016) 3-Hydroxy-3-methylglutaric and 3-methylglutaric acids impair redox status and energy production and transfer in rat heart: relevance for the pathophysiology of cardiac dysfunction in 3-hydroxy-3-methylglutaryl-coenzyme A lyase deficiency. Free Radic Res 50:997–1010. https://doi.org/10.1080/10715762.2016.1214952

da Silva CG, Bueno ARF, Schuck PF et al (2003) L-2-Hydroxyglutaric acid inhibits mitochondrial creatine kinase activity from cerebellum of developing rats. Int J Dev Neurosci 21:217–224. https://doi.org/10.1016/S0736-5748(03)00035-2

Duran M, Kamerling JP, Bakker HD et al (1980) L-2-Hydroxyglutaric aciduria: an inborn error of metabolism? J Inherit Metab Dis 3:109–112

Durán-Carabali LE, Arcego DM, Odorcyk FK et al (2018) Prenatal and early postnatal environmental enrichment reduce acute cell death and prevent neurodevelopment and memory impairments in rats submitted to neonatal hypoxia ischemia. Mol Neurobiol 55:3627–3641. https://doi.org/10.1007/s12035-017-0604-5

El-Khodor BF, Edgar N, Chen A et al (2008) Identification of a battery of tests for drug candidate evaluation in the SMNDelta7 neonate model of spinal muscular atrophy. Exp Neurol 212:29–43. https://doi.org/10.1016/j.expneurol.2008.02.025

Elsayed NA, Boyer TM, Burd I (2021) Fetal neuroprotective strategies: therapeutic agents and their underlying synaptic pathways. Front Synaptic Neurosci 13:33. https://doi.org/10.3389/FNSYN.2021.680899/BIBTEX

Ermine CM, Somaa F, Wang TY et al (2019) Long-term motor deficit and diffuse cortical atrophy following focal cortical ischemia in athymic rats. Front Cell Neurosci 13:552. https://doi.org/10.3389/FNCEL.2019.00552/BIBTEX

Escartin C, Galea E, Lakatos A et al (2021) Reactive astrocyte nomenclature, definitions, and future directions. Nat Neurosci 24:312–325. https://doi.org/10.1038/S41593-020-00783-4

Faiyaz-Ul-Haque M, Al-Sayed MD, Faqeih E et al (2014) Clinical, neuroimaging, and genetic features of L-2-hydroxyglutaric aciduria in Arab kindreds. Ann Saudi Med 34:107. https://doi.org/10.5144/0256-4947.2014.107

Fourati H, Ellouze E, Ahmadi M et al (2016) MRI features in 17 patients with L2 hydroxyglutaric aciduria. Eur J Radiol Open 3:245–250. https://doi.org/10.1016/j.ejro.2016.09.001

Fulton D, Paez PM, Campagnoni AT (2010) The multiple roles of myelin protein genes during the development of the oligodendrocyte. ASN Neuro 2:25–37. https://doi.org/10.1042/AN20090051

Gowen E, Miall RC (2007) The cerebellum and motor dysfunction in neuropsychiatric disorders. Cerebellum 6:268. https://doi.org/10.1080/14734220601184821

Guan W, Cao J-W, Liu L-Y et al (2017) Eye opening differentially modulates inhibitory synaptic transmission in the developing visual cortex. Elife 6. https://doi.org/10.7554/ELIFE.32337

Gunduz A, Aktuglu-Zeybek AC, Tezer D et al (2022) Postural tremor in L-2-hydroxyglutaric aciduria is associated with cerebellar atrophy. Neurol Sci 43:2051–2058. https://doi.org/10.1007/S10072-021-05555-X

Guo Z, Rudow G, Pletnikova O et al (2012) Striatal neuronal loss correlates with clinical motor impairment in Huntington's disease. Mov Disord 27:1379. https://doi.org/10.1002/MDS.25159

Halliwell B, Gutteridge JMC (2015) Oxidative stress and redox regulation: adaptation, damage, repair, senescence, and death. Free Radicals in Biology and Medicine. Oxford University Press, New York, NY, pp 199–2083

Herrera MI, Udovin LD, Kobiec T et al (2022) Palmitoylethanolamide attenuates neurodevelopmental delay and early hippocampal damage following perinatal asphyxia in rats. Front Behav Neurosci 16:327. https://doi.org/10.3389/FNBEH.2022.953157/BIBTEX

Heyser CJ (2004) Assessment of developmental milestones in rodents. Curr Protoc Neurosci 25(1):8–18. https://doi.org/10.1002/0471142301.ns0818s25

Hol EM, Pekny M (2015) Glial fibrillary acidic protein (GFAP) and the astrocyte intermediate filament system in diseases of the central nervous system. Curr Opin Cell Biol 32:121–130. https://doi.org/10.1016/J.CEB.2015.02.004

Horvath G, Reglődi D, Farkas J et al (2015) Perinatal positive and negative influences on the early neurobehavioral reflex and motor development. Adv Neurobiol 10:149–167. https://doi.org/10.1007/978-1-4939-1372-5_8

Hovens IB, Nyakas C, Schoemaker RG (2014) A novel method for evaluating microglial activation using ionized calcium-binding adaptor protein-1 staining: cell body to cell size ratio. Neuroimmunol Neuroinflamm 1:82–88. https://doi.org/10.4103/2347-8659.139719

Janigro D, Mondello S, Posti JP, Unden J (2022) GFAP and S100B: what you always wanted to know and never dared to ask. Front Neurol 13:835597. https://doi.org/10.3389/FNEUR.2022.835597

Jellouli NK, Salem IH, Ellouz E et al (2014) Founder effect confirmation of c.241A>G mutation in the L2HGDH gene and characterization of oxidative stress parameters in six Tunisian families with L-2-hydroxyglutaric aciduria. J Human Gene 59(4):216-222. https://doi.org/10.1038/jhg.2014.4

Junqueira D, Brusque AM, Porciúncula LO et al (2003) Effects of L-2-hydroxyglutaric acid on various parameters of the glutamatergic system in cerebral cortex of rats. Metab Brain Dis 18:233–243. https://doi.org/10.1023/A:1025559200816

Katz LC, Shatz CJ (1996) Synaptic activity and the construction of cortical circuits. Science 274:1133–1138. https://doi.org/10.1126/SCIENCE.274.5290.1133

Kranendijk M, Struys EA, Salomons GS et al (2012) Progress in understanding 2-hydroxyglutaric acidurias. J Inherit Metab Dis 35:571–587. https://doi.org/10.1007/s10545-012-9462-5

Kwon DH, Cha HJ, Lee H et al (2019) Protective effect of glutathione against oxidative stress-induced cytotoxicity in RAW 264.7 Macrophages through Activating the Nuclear Factor Erythroid 2-Related Factor-2/Heme Oxygenase-1 Pathway. Antioxidants 8:82. https://doi.org/10.3390/ANTIOX8040082

Lamtai M, Zghari O, Azirar S et al (2022) Melatonin modulates copper-induced anxiety-like, depression-like and memory impairments by acting on hippocampal oxidative stress in rat. Drug Chem Toxicol 45:1707–1715. https://doi.org/10.1080/01480545.2020.1858853

Latini A, Scussiato K, Borba Rosa R et al (2003) Induction of oxidative stress by L-2-hydroxyglutaric acid in rat brain. J Neurosci Res 74:103–110. https://doi.org/10.1002/jnr.10735

LeBel CP, Ischiropoulos H, Bondy SC (1992) Evaluation of the probe 2′,7′-dichlorofluorescin as an indicator of reactive oxygen species formation and oxidative stress. Chem Res Toxicol 5:227–231. https://doi.org/10.1021/tx00026a012

Lee J, Gravel M, Zhang R et al (2005) Process outgrowth in oligodendrocytes is mediated by CNP, a novel microtubule assembly myelin protein. J Cell Biol 170:661–673. https://doi.org/10.1083/JCB.200411047

Li W, Zou J, Shang J et al (2022) Both the complexity of tight junctions and endothelial transcytosis are increased during BBB postnatal development in rats. Front Neurosci 16:452. https://doi.org/10.3389/FNINS.2022.850857/BIBTEX

Lowry OH, Rosebrough NJ, Farr AL, Randall RJ (1951) Protein measurement with the Folin phenol reagent. J Biol Chem 193:265–275

Mansouri S, Salari AA, Abedi A et al (2022) Melatonin treatment improves cognitive deficits by altering inflammatory and neurotrophic factors in the hippocampus of obese mice. Physiol Behav 254. https://doi.org/10.1016/J.PHYSBEH.2022.113919

Marklund SL (1985) Product of extracellular-superoxide dismutase catalysis. FEBS Lett 184:237–239. https://doi.org/10.1016/0014-5793(85)80613-X

Metz GA, Whishaw IQ (2002) Cortical and subcortical lesions impair skilled walking in the ladder rung walking test: a new task to evaluate fore- and hindlimb stepping, placing, and co-ordination. J Neurosci Methods 115:169–179. https://doi.org/10.1016/S0165-0270(02)00012-2

Michetti F, D'Ambrosi N, Toesca A et al (2019) The S100B story: from biomarker to active factor in neural injury. J Neurochem 148:168–187. https://doi.org/10.1111/JNC.14574

Morén C, deSouza RM, Giraldo DM, Uff C (2022) Antioxidant therapeutic strategies in neurodegenerative diseases. Int J Mol Sci 23. https://doi.org/10.3390/IJMS23169328

Moura AP, Parmeggiani B, Grings M et al (2016) Intracerebral glycine administration impairs energy and redox homeostasis and induces glial reactivity in cerebral cortex of newborn rats. Mol Neurobiol 53:5864–5875. https://doi.org/10.1007/s12035-015-9493-7

Nguyen AT, Armstrong EA, Yager JY (2017) Neurodevelopmental reflex testing in neonatal rat pups. J Vis Exp 2017. https://doi.org/10.3791/55261

Norden DM, Trojanowski PJ, Villanueva E et al (2016) Sequential activation of microglia and astrocyte cytokine expression precedes increased iba-1 or GFAP immunoreactivity following systemic immune challenge. Glia 64:300–316. https://doi.org/10.1002/GLIA.22930

Olivera-Bravo S, Fernández A, Sarlabós MN et al (2011) Neonatal astrocyte damage is sufficient to trigger progressive striatal degeneration in a rat model of glutaric acidemia-I. PLoS ONE 6:e20831. https://doi.org/10.1371/journal.pone.0020831

Olivier P, Fontaine RH, Loron G et al (2009) Melatonin promotes oligodendroglial maturation of injured white matter in neonatal rats. PLoS ONE 4:e7128. https://doi.org/10.1371/journal.pone.0007128

Parmeggiani B, Grings M, da Rosa-Junior NT et al (2019) Bezafibrate prevents glycine-induced increase of antioxidant enzyme activities in rat striatum. Mol Neurobiol 56:29–38. https://doi.org/10.1007/s12035-018-1074-0

Pecka M, Han Y, Sader E, Mrsic-Flogel TD (2014) Experience-dependent specialization of receptive field surround for selective coding of natural scenes. Neuron 84:457–469. https://doi.org/10.1016/j.neuron.2014.09.010

Rains ME, Muncie CB, Pang Y et al (2021) Oxidative stress and neurodevelopmental outcomes in rat offspring with intrauterine growth restriction induced by reduced uterine perfusion. Brain Sciences 11(1):78. https://doi.org/10.3390/BRAINSCI11010078

Ramírez-Rodríguez GB, Olvera-Hernández S, Vega-Rivera NM, Ortiz-López L (2018) Melatonin influences structural plasticity in the axons of granule cells in the dentate gyrus of Balb/C mice. Int J Mol Sci (2019) 20:73. https://doi.org/10.3390/IJMS20010073

Reiter RJ, Manchester LC, Tan D-X (2010) Neurotoxins: free radical mechanisms and melatonin protection. Curr Neuropharmacol 8:194. https://doi.org/10.2174/157015910792246236

Ribeiro RT, Zanatta Â, Amaral AU et al (2018) Experimental evidence that in vivo intracerebral administration of l-2-hydroxyglutaric acid to neonatal rats provokes disruption of redox status and histopathological abnormalities in the brain. Neurotox Res 33:681–692. https://doi.org/10.1007/s12640-018-9874-6

Ribeiro RT, Seminotti B, Zanatta Â et al (2021) Neuronal death, glial reactivity, microglia activation, oxidative stress and bioenergetics impairment caused by intracerebroventricular administration of D-2-hydroxyglutaric acid to neonatal rats. Neuroscience 471:115–132. https://doi.org/10.1016/J.NEUROSCIENCE.2021.07.024

Rodrigues DGB, de Moura CD, Sitta Â et al (2017) Experimental evidence of oxidative stress in patients with L-2-hydroxyglutaric aciduria and that L-carnitine attenuates in vitro DNA damage caused by D-2-hydroxyglutaric and L-2-hydroxyglutaric acids. Toxicol in Vitro 42:47–53. https://doi.org/10.1016/j.tiv.2017.04.006

Ruhela RK, Soni S, Sarma P et al (2019) Negative geotaxis: an early age behavioral hallmark to VPA rat model of autism. Ann Neurosci 26:25–31. https://doi.org/10.5214/ans.0972.7531.260106

Ryan NS, Shakespeare TJ, Lehmann M et al (2014) Motor features in posterior cortical atrophy and their imaging correlates. Neurobiol Aging 35:2845. https://doi.org/10.1016/J.NEUROBIOLAGING.2014.05.028

Ryter SW, Hong PK, Hoetzel A et al (2007) Mechanisms of cell death in oxidative stress. Antioxid Redox Signal 9:49–89. https://doi.org/10.1089/ARS.2007.9.49

Rzem R, Veiga-Da-Cunha M, Noël G et al (2004) A gene encoding a putative FAD-dependent L-2-hydroxyglutarate dehydrogenase is mutated in L-2-hydroxyglutaric aciduria. Proc Natl Acad Sci U S A 101:16849–16854. https://doi.org/10.1073/PNAS.0404840101

Rzem R, Achouri Y, Marbaix E et al (2015) A mouse model of L-2-hydroxyglutaric aciduria, a disorder of metabolite repair. PLoS One 10. https://doi.org/10.1371/journal.pone.0119540

Saidha S, Murphy S, McCarthy P et al (2010) L-2-hydroxyglutaric aciduria diagnosed in an adult presenting with acute deterioration. J Neurol 257:146–148. https://doi.org/10.1007/S00415-009-5319-8

Samuraki M, Komai K, Hasegawa Y et al (2008) A successfully treated adult patient with L-2-hydroxyglutaric aciduria. Neurology 70:1051–1052. https://doi.org/10.1212/01.WNL.0000287141.90944.95

Sanches EF, Arteni NS, Nicola F et al (2013) Early hypoxia–ischemia causes hemisphere and sex-dependent cognitive impairment and histological damage. Neuroscience 237:208–215. https://doi.org/10.1016/J.NEUROSCIENCE.2013.01.066

Sanches EF, Carvalho AS, van de Looij Y et al (2021) Experimental cerebral palsy causes microstructural brain damage in areas associated to motor deficits but no spatial memory impairments in the developing rat. Brain Res 1761:147389. https://doi.org/10.1016/j.brainres.2021.147389

Sasaki Y, Ohsawa K, Kanazawa H et al (2001) Iba1 is an actin-cross-linking protein in macrophages/microglia. Biochem Biophys Res Commun 286:292–297. https://doi.org/10.1006/BBRC.2001.5388

Saucier DM, Ehresman CA, Keller AJ et al (2008) Hypoxia ischemia affects ultrasonic vocalization in the neonatal rat. Behav Brain Res 190:243–247. https://doi.org/10.1016/J.BBR.2008.02.025

Sauer SW, Opp S, Mahringer A et al (2010) Glutaric aciduria type I and methylmalonic aciduria: Simulation of cerebral import and export of accumulating neurotoxic dicarboxylic acids in in vitro models of the blood–brain barrier and the choroid plexus. Biochimica et Biophysica Acta (BBA) - Molecular Basis of Disease 1802:552–560. https://doi.org/10.1016/j.bbadis.2010.03.003

Schaftingen E, Rzem R, Veiga-da-Cunha M (2009) l-2-Hydroxyglutaric aciduria, a disorder of metabolite repair. J Inherit Metab Dis 32:135–142. https://doi.org/10.1007/S10545-008-1042-3

Sebastianutto I, Cenci MA, Fieblinger T (2017) Alterations of striatal indirect pathway neurons precede motor deficits in two mouse models of Huntington's disease. Neurobiol Dis 105:117–131. https://doi.org/10.1016/J.NBD.2017.05.011

Seminotti B, Zanatta Â, Ribeiro RT et al (2019) Disruption of brain redox homeostasis, microglia activation and neuronal damage induced by intracerebroventricular administration of S-adenosylmethionine to developing rats. Mol Neurobiol 56:2760–2773. https://doi.org/10.1007/s12035-018-1275-6

Shah H, Chandarana M, Sheth J, Shah S (2020) A case report of chronic progressive pancerebellar syndrome with leukoencephalopathy:L-2 hydroxyglutaric aciduria. Mov Disord Clin Pract 7:560–563. https://doi.org/10.1002/MDC3.12967

Smith MA, Brandt J, Shadmehr R (2000) Motor disorder in Huntington's disease begins as a dysfunction in error feedback control. Nature 403:544–549. https://doi.org/10.1038/35000576

Sreejit G, Flynn MC, Patil M et al (2020) S100 family proteins in inflammation and beyond. Adv Clin Chem 98:173–231. https://doi.org/10.1016/BS.ACC.2020.02.006

Steenweg ME, Jakobs C, Errami A et al (2010) An overview of L-2-hydroxyglutarate dehydrogenase gene (L2HGDH) variants: a genotype-phenotype study. Hum Mutat 31:380–390. https://doi.org/10.1002/humu.21197

Steenweg ME, Salomons GS, Yapici Z et al (2009) l-2-Hydroxyglutaric aciduria: pattern of MR imaging abnormalities in 56 patients. 251:856–865. https://doi.org/10.1148/RADIOL.2513080647

Stein H (2021) Why does the neocortex need the cerebellum for working memory? J Neurosci 41:6368. https://doi.org/10.1523/JNEUROSCI.0701-21.2021

Tassinari IDÁ, Andrade MKG, da Rosa LA et al (2020) Lactate administration reduces brain injury and ameliorates behavioral outcomes following neonatal hypoxia-ischemia. Neuroscience 448:191–205. https://doi.org/10.1016/J.NEUROSCIENCE.2020.09.006

Thangwong P, Jearjaroen P, Govitrapong P et al (2022) Melatonin improves cognitive function by suppressing endoplasmic reticulum stress and promoting synaptic plasticity during chronic cerebral hypoperfusion in rats. Biochem Pharmacol 198. https://doi.org/10.1016/J.BCP.2022.114980

Topçu M, Jobard F, Halliez S et al (2004) L-2-Hydroxyglutaric aciduria: identification of a mutant gene C14orf160, localized on chromosome 14q22.1. Hum Mol Genet 13:2803–2811. https://doi.org/10.1093/HMG/DDH300

Topçu M, Aydin ÖF, Yalçinkaya C et al (2005) L-2-hydroxyglutaric aciduria: a report of 29 patients. Turk J Pediatr 47:1–7

Ugele I, Conejo ZEC, Hammon K et al (2019) D-2-hydroxyglutarate and L-2-hydroxyglutarate inhibit IL-12 secretion by human monocyte-derived dendritic cells. International Journal of Molecular Sciences 2019, Vol 20, Page 742 20:742. https://doi.org/10.3390/IJMS20030742

van der Knaap MS, Valk J, Barth PG et al (1995) Leukoencephalopathy with swelling in children and adolescents: MRI patterns and differential diagnosis. Neuroradiology 37:679–686. https://doi.org/10.1007/BF00593394

Victor S, Rocha-Ferreira E, Rahim A et al (2021) New possibilities for neuroprotection in neonatal hypoxic-ischemic encephalopathy. European Journal of Pediatrics 2021 181:3 181:875–887. https://doi.org/10.1007/S00431-021-04320-8

Wakatsuki A, Okatani Y, Shinohara K et al (2001) Melatonin protects against ischemia/reperfusion-induced oxidative damage to mitochondria in fetal rat brain. J Pineal Res 31:167–172. https://doi.org/10.1034/J.1600-079X.2001.310211.X

Weimar C, Schlamann M, Krägeloh-Mann I, Schöls L (2013) L-2 hydroxyglutaric aciduria as a rare cause of leukencephalopathy in adults. Clin Neurol Neurosurg 115:765–766. https://doi.org/10.1016/j.clineuro.2012.06.040

Wendel A (1981) Glutathione peroxidase. Methods Enzymol 77:325–333. https://doi.org/10.1016/s0076-6879(81)77046-0

Williams NC, Ryan DG, Costa ASH et al (2022) Signaling metabolite L-2-hydroxyglutarate activates the transcription factor HIF-1α in lipopolysaccharide-activated macrophages. J Biol Chem 298:101501. https://doi.org/10.1016/J.JBC.2021.101501

Wirths O, Breyhan H, Marcello A et al (2010) Inflammatory changes are tightly associated with neurodegeneration in the brain and spinal cord of the APP/PS1KI mouse model of Alzheimer's disease. Neurobiol Aging 31:747–757. https://doi.org/10.1016/J.NEUROBIOLAGING.2008.06.011

Xiao J, Cai T, Fang Y et al (2021) Activation of GPR40 attenuates neuroinflammation and improves neurological function via PAK4/CREB/KDM6B pathway in an experimental GMH rat model. J Neuroinflammation 18. https://doi.org/10.1186/S12974-021-02209-9

Yagi K (1998) Simple procedure for specific assay of lipid hydroperoxides in serum or plasma. Methods Mol Biol 108:107–110. https://doi.org/10.1385/0-89603-472-0:107

Yeh JH, Wang KC, Kaizaki A et al (2021) Pioglitazone ameliorates lipopolysaccharide-induced behavioral impairment, brain inflammation, white matter injury and mitochondrial dysfunction in neonatal rats. Int J Mol Sci 22. https://doi.org/10.3390/IJMS22126306

Yilmaz K (2009) Riboflavin treatment in a case with l-2-hydroxyglutaric aciduria. Eur J Paediatr Neurol 13:57–60. https://doi.org/10.1016/j.ejpn.2008.01.003

Zhao Z, Nelson AR, Betsholtz C, Zlokovic BV (2015) Establishment and dysfunction of the blood-brain barrier. Cell 163:1064–1078. https://doi.org/10.1016/J.CELL.2015.10.067

Zhou W, Zhang J, Wang G et al (2016) Permeability and distribution of nerve growth factor in the brain of neonatal rats by periphery venous injection in hypoxic-ischemic state. Springerplus 5:1–9. https://doi.org/10.1186/S40064-016-3594-2

CAPÍTULO II

Disruption of mitochondrial bioenergetics, calcium retention capacity and cell viability caused by D-2- hydroxyglutaric acid in the heart

Rafael Teixeira Ribeiro, Ana Cristina Roginski, Rafael Aguiar Marschner, Simone Magagnin Wajner, Roger Frigério Castilho, Alexandre Umpierrez Amaral, Moacir Wajner,

Artigo científico publicado em

BIOCHIMIE (2022)

Biochimie 207 (2023) 153–164

Contents lists available at ScienceDirect

Biochimie

journal homepage: www.elsevier.com/locate/biochi

Disruption of mitochondrial bioenergetics, calcium retention capacity and cell viability caused by D-2-hydroxyglutaric acid in the heart

Rafael Teixeira Ribeiro [a], Ana Cristina Roginski [a], Rafael Aguiar Marschner [b], Simone Magagnin Wajner [b], Roger Frigério Castilho [c], Alexandre Umpierrez Amaral [a, d], Moacir Wajner [a, e, f, *]

[a] Programa de Pós-Graduação Em Ciências Biológicas: Bioquímica, Instituto de Ciências Básicas da Saúde, Universidade Federal Do Rio Grande Do Sul, Porto Alegre, RS, Brazil
[b] Departamento de Medicina Interna, Faculdade de Medicina, Universidade Federal Do Rio Grande Do Sul, Porto Alegre, RS, Brazil
[c] Departamento de Patologia, Faculdade de Ciências Médicas, Universidade Estadual de Campinas, Campinas, SP, Brazil
[d] Departamento de Ciências Biológicas, Universidade Regional Integrada Do Alto Uruguai e Das Missões, Erechim, RS, Brazil
[e] Departamento de Bioquímica, Instituto de Ciências Básicas da Saúde, Universidade Federal Do Rio Grande Do Sul, Porto Alegre, RS, Brazil
[f] Serviço de Genética Médica, Hospital de Clínicas de Porto Alegre, Porto Alegre, RS, Brazil

ARTICLE INFO

Article history:
Received 2 July 2022
Received in revised form
3 November 2022
Accepted 7 November 2022
Available online 11 November 2022

Keywords:
D-2-Hydroxyglutaric aciduria
D-2-Hydroxyglutaric acid
Bioenergetics dysfunction
Mitochondria
Cardiomyopathy

ABSTRACT

Accumulation of D-2-hydroxyglutaric acid (D-2-HG) is the biochemical hallmark of D-2-hydroxyglutaric aciduria type I and, particularly, of D-2-hydroxyglutaric aciduria type II (D2HGA2). D2HGA2 is a metabolic inherited disease caused by gain-of-function mutations in the gene isocitrate dehydrogenase 2. It is clinically characterized by neurological abnormalities and a severe cardiomyopathy whose pathogenesis is still poorly established. The present work investigated the potential cardiotoxicity D-2-HG, by studying its *in vitro* effects on a large spectrum of bioenergetics parameters in heart of young rats and in cultivated H9c2 cardiac myoblasts. D-2-HG impaired cellular respiration in purified mitochondrial preparations and crude homogenates from heart of young rats, as well as in digitonin-permeabilized H9c2 cells. ATP production and the activities of cytochrome *c* oxidase (complex IV), alpha-ketoglutarate dehydrogenase, citrate synthase and creatine kinase were also inhibited by D-2-HG, whereas the activities of complexes I, II and II-III of the respiratory chain, glutamate, succinate and malate dehydrogenases were not altered. We also found that this organic acid compromised mitochondrial Ca^{2+} retention capacity in heart mitochondrial preparations and H9c2 myoblasts. Finally, D-2-HG reduced the viability of H9c2 cardiac myoblasts, as determined by the MTT test and by propidium iodide incorporation. Noteworthy, L-2-hydroxyglutaric acid did not change some of these measurements (complex IV and creatine kinase activities) in heart preparations, indicating a selective inhibitory effect of the enantiomer D. In conclusion, it is presumed that D-2-HG-disrupts mitochondrial bioenergetics and Ca^{2+} retention capacity, which may be involved in the cardiomyopathy commonly observed in D2HGA2.

1. Introduction

The inherited autosomal recessive metabolic disease D-2-hydroxyglutaric aciduria (D2HGA) was first described by Chalmers et al. [1] as a single disorder. More recently two forms of D2HGA were reported, D2HGA type I (D2HGA1) (OMIM #600721) and type II (D2HGA2) (OMIM #613657) [2,3]. Loss-of-function mutations in the gene encoding D-2-hydroxyglutarate dehydrogenase and gain-of-function mutations in the isocitrate dehydrogenase 2 (IDH2) gene are the genetic defects responsible for D2HGA1 and D2HGA2, respectively. These diseases, particularly D2HGA2, are biochemically characterized by very high concentrations of D-2-hydroxyglutaric acid (D-2-HG) in various tissues, especially in the brain, as well as in urine (11,305 mmol/mol creat), plasma (757 μmol/L) and cerebrospinal fluid (172 μmol/L) [4].

* Corresponding author. Departamento de Bioquímica, Instituto de Ciências Básicas da Saúde, Universidade Federal de Rio Grande do Sul, Rua Ramiro Barcelos, 2600, Prédio 21111, Porto Alegre, RS, 90035, Brazil.
E-mail address: mwajner@ufrgs.br (M. Wajner).

https://doi.org/10.1016/j.biochi.2022.11.004

Abbreviations

ANOVA	one-way analysis of variance
CAC	citric acid cycle
CCCP	carbonyl cyanide *m*-chloro phenyl hydrazone
CK	creatine kinase
CS	citrate synthase
D-2-HG	D-2-Hydroxyglutaric acid
D2HGA	D-2-Hydroxyglutaric aciduria
D2HGA1	D-2-hydroxyglutaric aciduria type I
D2HGA2	D-2-hydroxyglutaric aciduria type II
DMEM	Dulbecco's modified Eagle's medium
DTNB	5,5′-dithio-bis(2-nitrobenzoic acid)
GDH	glutamate dehydrogenase
IDH2	isocitrate dehydrogenase 2
MDH	malate dehydrogenase
MPT	mitochondrial permeability transition
MTT	3-[4,5-dimethylthiazol-2-yl]-2,5-diphenyltetrazoliumbromide
PI	propidium iodide
RCR	respiratory control ratio
SDH	succinate dehydrogenase
SUIT	substrate-uncoupler inhibitor titration
α-KGDH	α-Ketoglutarate dehydrogenase

Approximately one hundred D2HGA patients have been reported so far, but the prevalence of this inborn error of metabolism in the general population is still unknown [5,6].

Epilepsy, developmental delay and hypotonia are common clinical findings in both forms of the disease [4]. D2HGA1 illness progresses slowly with mild to moderate clinical signs, whereas patients affected by D2HGA2 have a more severe and early-onset characterized by generalized convulsions, severe psychomotor delay, and a potentially fatal cardiomyopathy that develops in approximately 50% of them [4]. Interestingly, D2HGA2 patients present higher levels of D-2-HG compared to those affected by D2HGA1, suggesting that the severe symptomatology including cardiac alterations may be related to a higher accumulation of this organic acid.

So far, the literature has mainly focused on the mechanisms that underlie the neurological damage and very little attention has been given on the pathogenesis of the cardiomyopathy in D2HGA2 [7–12]. In this particular, the hypothesis that accumulation of D-2-HG may represent a determinant factor in the cardiomyopathy that affects D2HGA2 patients is supported by studies demonstrating that the use of selective inhibitors of IDH2 were able to reduce D-2-HG production and in parallel improved cardiac functions and prevented cardiomyopathy in mouse models of D2HGA2 [13,14]. However, the underlying cellular mechanisms leading to cardiac damage in D2HGA2 remain poorly understood.

Mitochondria are particularly abundant in cardiac tissue, accounting for about 30% of cardiomyocyte mass [15] and being responsible for over 95% of ATP production required by the heart [16]. This is in line with the observations that disturbances of mitochondrial bioenergetics are consistently associated with the pathophysiology of several cardiac diseases [17]. Thus, the present work investigated the role of D-2-HG on a wide range of important parameters of mitochondrial bioenergetics using isolated mitochondria, crude homogenates from heart of developing rats and cultivated H9c2 cardiac myoblasts. The respiratory parameters state 3 (ADP-stimulated), state 4 (non-phosphorylating), and uncoupled (CCCP-stimulated) respiration, ATP production, the activities of the respiratory chain complexes I to IV, of various citric acid cycle enzymes, creatine kinase and glutamate dehydrogenase were evaluated in heart preparations exposed to D-2-HG. We also determined whether D-2-HG could alter mitochondrial Ca^{2+} retention capacity and cell viability of cardiac cells. Finally, we tested the effects of L-2-hydroxyglutaric acid (L-2-HG) on some of these parameters.

2. Material and methods

2.1. Animals and reagents

Male Wistar rats (30-day-old) were obtained from the breeding colony of Animal |House of Federal University of Rio Grande do Sul (UFRGS), Porto Alegre, RS, Brazil. The animals had free access to water and a 20% (w/w) protein commercial chow (Nuvilab CR-1® - Canguiri, PR, Brazil), and were maintained in a constant temperature (22 ± 1 °C) room. This work had the approval of the Committee on the Ethical Use of Animals of UFRGS (no 35426) and followed the national animal rights regulation (Law 11.794/2008) and the experimental protocol defined in the "Guide for the Care and Use of Laboratory Animals" (National Institutes of Health, publication no. 80–23, revised 2011). All procedures used in this investigation aimed to reduce the number of animals used in the experiments to a minimum, as well as to minimize animal suffering.

Analytical grade chemicals reagents were obtained from Sigma-Aldrich (St. Louis, MO, USA), except Calcium green-5N from Thermo Fisher Scientific (USA). All assays were performed with D-2-HG disodium salt.

2.2. Mitochondrial and crude homogenate preparation from heart of developing rats

Heart mitochondrial fractions used to measure bioenergetics parameters were prepared following the method described by Ferranti et al. [18], with some modifications [19]. The pellet containing the mitochondria was resuspended in a buffer without EGTA (10 mM HEPES buffer, with 225 mM mannitol, 75 mM sucrose, 0.1% bovine serum albumin, pH 7.2) at approximately 18 mg mL^{-1} protein concentration. For the assessment of respiratory parameters heart crude homogenates were prepared in a medium (0.3 M sucrose, 5 mM KH_2PO_4, 1 mM EGTA, 0.1 mg•mL^{-1} BSA, 5 mM MOPS, pH 7.4) containing approximate 3 mg mL^{-1} of protein [20].

2.3. Cardiac cell cultures

Heart-derived H9c2 cell lines (ventricular myoblasts) were acquired from Banco de Células do Rio do Janeiro (BCRJ, Rio de Janeiro, Brazil) and used to measure bioenergetics parameters and cell viability. Cells were cultivated in DMEM supplemented with 10% fetal bovine serum [21]. Experiments were carried out on cells with a confluence of 50–60% and between passages 10 and 14.

2.4. Mitochondrial respiratory parameters determined through oxygen consumption

The amount of oxygen consumption was measured in a thermostatically controlled (37 °C) and magnetically stirred incubation chamber of [22,23]. D-2-HG (0.5–5 mM) was supplemented at the beginning of the assays to a medium containing 0.3 M sucrose, 5 mM KH_2PO_4, 1 mM EGTA, 0.1 mg mL^{-1} BSA, 5 mM MOPS, pH 7.4, and the mitochondrial preparations (0.1 mg protein·mL^{-1}) supported by 5 mM glutamate. State 3 (ADP-stimulated) and state 4 (resting) respiration were evaluated after addition of 1 mM ADP and 1 μg mL^{-1} oligomycin A, respectively. One μM CCCP (two pulses of 0.5 μM) was added to the medium to measure the uncoupled respiration, and the respiratory control ratio (RCR - state 3/state 4) was then calculated.

The respiratory parameters were also performed in permeabilized H9c2 cells (1.5 million cells·mL^{-1}) and in heart homogenates from young rats (1 mg tissue·mL^{-1}). Before the assay, the cells were trypsinized, centrifuged, and resuspended in an appropriate respiring medium (20 mM of HEPES buffer, pH 7.4, containing 0.11 M of sucrose, 10 mM of KH_2PO_4, 0.5 mM of EGTA, 0.1 mg/mL of BSA, 60 mM of lactobionate, 20 mM of taurine, and 3 mM of $MgCl_2$). H9c2 were then permeabilized with digitonin (8 μM) [21]. The substrate-uncoupler inhibitor titration (SUIT) protocol was used in both crude heart homogenates and H9c2 cells in the presence of D-2-HG. Pyruvate (5 mM), malate (0.5 mM) and glutamate (10 mM), consisting of the NADH-linked substrates, were supplemented to the medium, followed by 500 μM ADP (state 3 respiration), 10 mM succinate and 1 μg mL^{-1} oligomycin (state 4 respiration). Three pulses of CCCP 0.5 μM (total 1.5 μM) were then added to induce the uncoupled respiration. Finally, succinate-induced uncoupled respiration was determined by adding 2 μM of the complex I inhibitor rotenone. Data were calculated and expressed as pmol O_2 flux·s^{-1} mg $protein^{-1}$ or pmol O_2 flux·s^{-1}·million $cells^{-1}$.

2.5. ATP production

The firefly luciferin–luciferase assay system [24,25] was used to measure ATP levels, with some modifications [23]. Heart mitochondrial fractions (0.1 mg protein·mL^{-1}) were incubated in respiring medium using 5 mM glutamate as substrate in the presence of D-2-HG (0.5–5 mM). ADP (1 mM) was then added to stimulate ATP production and the reaction was stopped 2 min afterwards by supplementing the medium with 1 μg mL^{-1} oligomycin and 130 mM $HClO_4$. The luminescence was quantified in a SpectraMax I3 spectrophotometer.

2.6. Respiratory chain complex activities

Mitochondrial respiratory chain complexes I, II, II–III, IV and succinate dehydrogenase (SDH) activities were determined in H9c2 cells (approximately 30 μg of protein) pre-incubated with D-2-HG (0.5–5 mM) or L-2-HG (5 mM, complex IV) for 30 min at 37 °C. Complex I (NADH: ubiquinone oxidoreductase) activity was measured in H9c2 cells by monitoring the absorbance of NADH at 340 nm for 6 min, as previously described [26]. SDH and complexes II (DCIP-oxidoreductase), II-III (succinate: cytochrome *c* oxidoreductase) activities were measured by the method reported by Fischer et al. [27]Complex IV (cytochrome *c* oxidase) activity was evaluated according to Rustin et al. [28] with some modifications [9]. All activities were calculated as nmol·min^{-1}·mg $protein^{-1}$.

2.7. α-Ketoglutarate dehydrogenase (α-KGDH), citrate synthase (CS), malate dehydrogenase (MDH), glutamate dehydrogenase (GDH) and creatine kinase (CK) activities

Glutamate dehydrogenase (GDH), citrate synthase (CS) and malate dehydrogenase (MDH) activities were estimated in heart mitochondria (CS: 0.01 mg protein·mL^{-1}; MDH: 0.0025 mg protein·mL^{-1}; GDH: 0.15 mg protein mL^{-1}), creatine kinase in H9c2 cells (CK: 1 μg mg protein mL^{-1}) and that of α-ketoglutarate dehydrogenase using a commercially purified enzyme from porcine heart (α-KGDH: 0.012 U mL^{-1}, K1502, Sigma-Aldrich). Kinetic analysis of α-KGDH activity was performed using concentrations of α-ketoglutarate ranging from 0.1 to 1.0 mM and D-2-HG concentrations from 1 to 5 mM. K_m, V_{max}, K_i (dissociation constant of the enzyme-inhibitor complex) and K_i' (dissociation constant of the enzyme-inhibitor-substrate complex) values were determined using a nonlinear fitting (GraphPad Prism 8.0).

The activity of MDH [29] was determined by following NADH oxidation and expressed as nmol NAD^+ · min^{-1} mg $protein^{-1}$, whereas GDH [30] and α-KGDH [31] activities were measured by measuring NAD^+ reduction and expressed as nmol NADH · min^{-1} mg $protein^{-1}$. CS activity was evaluated according to Srere [32] by monitoring DTNB reduction and expressed as μmol · min^{-1} mg $protein^{-1}$. CK activity was measured according to the colorimetric method of Hughes [33] with some modifications [34]. Pre-incubation occurred for 30 min at 37 °C in the presence of D-2-HG (0.5–5 mM) or L-2-HG (5 mM, CK), and the activities measured afterwards.

2.8. Ca^{2+} retention capacity

Measurements of mitochondrial Ca^{2+} retention capacity were carried out in a fluorescence spectrophotometer (Hitachi F-2500), as previously described [21]. The analyses were executed in state 4 (resting) respiring heart mitochondria (0.35 mg protein·mL^{-1}) supported by 5 mM glutamate in a medium containing 0.5 mM $MgCl_2$, 2 mM KH_2PO_4, 150 mM KCl, 5 mM HEPES, 30 μM EGTA, 0.1 mg mL^{-1} BSA and 1 μg L^{-1} oligomycin A, pH 7.2. D-2-HG (5 mM), $CaCl_2$ (10 μM single or 5 μM successive additions), CCCP (3 μM) were added as indicated by the arrows in the figures. To determine mitochondrial Ca^{2+} retention capacity, the fluorescent probe Calcium green-5N (0.2 μM) was used to measure extramitochondrial calcium levels by monitoring the excitation and emission wavelengths of 506 and 532 nm, respectively [35].

2.9. Cell viability

Cell viability was determined in H9c2 cells exposed for 6 h with D-2-HG by the propidium iodide (PI) incorporation assay and by the tetrazolium salt 3-[4,5-dimethylthiazol-2-yl]-2,5-diphenyltetrazoliumbromide (MTT) method.

For the PI incorporation test, 100,000 cells were seeded into a 24-well plate and stained with PI (7.5 μM) for 10 min in dark at 37 °C [36]. PI is a red-fluorescent dye that is permeable only to cells with damaged plasma membrane, binding to DNA and making the nucleus highly fluorescent. Cells were imaged with a Nikon inverted microscope with a TE-FM Epi-Fluorescence accessory. The Fiji software was used to count the number of PI-positive cells from three randomly selected fields per well.

For the MTT assay, 25,000 H9c2 cells were seeded in 96-well plates. MTT was added to the medium at a concentration of 45 μg/mL and cells were incubated for 2 h at 37 °C [36]. The purple MTT formazan crystals resulting from the action of mitochondrial dehydrogenases from living cells were dissolved in dimethyl sulfoxide. Absorbance values were estimated spectrophotometrically

at wavelengths of 570 nm and 630 nm and the net $\Delta A_{(570-630)}$ was taken as an index of cell viability. The results were compared to the mean of control samples to which 100% viability was attributed.

2.10. Protein determination

The Lowry method [37] was used to measure protein content.

2.11. Statistical analysis

The experiments were performed in triplicate and the mean was used for statistical analysis. Results were reported as means ± standard deviation. The normality of data distribution was evaluated by the Shapiro-Wilk test and the homoscedasticity by the Bartlett's and by the F test. All data followed a normal distribution and variances were found to be homogeneous. Statistical analyses were performed using the GraphPad Prism 8 software. Student's *t*-test for unpaired samples (two groups) or one-way analysis of variance (ANOVA) (three or more groups), followed by the post-hoc Tukey multiple range test when F was significant were utilized. Vales with $P < 0.05$ were considered significant.

3. Results

3.1. D-2-HG impairs mitochondrial respiration in heart mitochondria of developing rats

D-2-HG (0.5–5 mM) effects on mitochondrial respiration supported by glutamate were first evaluated in fully coupled heart mitochondria (respiratory control ratio, RCR >9), as demonstrated by higher respiratory rates in the presence of ADP (state 3) than in the presence of the ATP synthase inhibitor oligomycin A (state 4), at control conditions (Fig. 1). Furthermore, D-2-HG markedly decreased ADP-stimulated (state 3) (41%) [Fig. 1A = $F_{(4, 15)} = 32.71$, $P < 0.001$], CCCP-induced (uncoupled) (23%) [Fig. 1C = $F_{(4, 15)} = 5.20$, $P < 0.01$] respiration, and the RCR (34%) [Fig. 1D = $F_{(4, 15)} = 32.13$, $P < 0.001$]. In contrast D-2-HG did not change state 4 respiration (Fig. 1B). These results indicate that D-2-HG acts as a metabolic inhibitor, decreasing mitochondrial respiration capacity.

3.2. D-2-HG decreases ATP production in heart mitochondria of developing rats

It was then verified that D-2-HG markedly reduced ATP production (23%) [Fig. 2 = $F_{(4,20)} = 226.5$, $P < 0.001$], supporting a marked impairment of mitochondrial energy production.

3.3. D-2-HG significantly decreases mitochondrial respiration in heart crude homogenates and permeabilized H9c2 cells

In order to investigate the cardiotoxicity of D-2-HG in a cell environment that more closely resembles the *in vivo* condition, we utilized heart crude homogenates (Fig. 3) and digitonin-permeabilized H9c2 cells using the SUIT protocol (Fig. 4), measuring mitochondrial respiration. D-2-HG significantly inhibited ADP-stimulated respiration (state 3) in heart homogenates using a combination of NADH-linked substrates (pyruvate, malate and glutamate - PMG) (33%) [Fig. 3A = $t_{(8)} = 4.841$, $P < 0.01$] and NADH plus $FADH_2$-linked (succinate − S) substrates (PMG + S) (24%) [Fig. 3B = $t_{(8)} = 4.387$, $P < 0.01$]. In addition, D-2-HG significantly inhibited uncoupled respiration using NADH plus $FADH_2$-linked substrates (22%) and also succinate-supported respiration (25%) [Fig. 3D = $t_{(8)} = 3.546$, $P < 0.01$; Fig. 3E = $t_{(8)} = 3.780$, $P < 0.01$]. Similarly to the data obtained with purified mitochondria, D-2-HG did not change resting (state 4) respiration (Fig. 3C) in crude heart homogenates.

It was also verified that D-2-HG significantly decreased ADP-stimulated (19%–21%) [Fig. 4A = $t_{(6)} = 3.476$, $P < 0.05$; Fig. 4B = $t_{(6)} = 4.266$, $P < 0.01$] and uncoupled (15%–18%) [Fig. 4D = $t_{(6)} = 4.911$, $P < 0.01$; Fig. 4E = $t_{(6)} = 3.801$, $P < 0.01$] respiration in permeabilized cardiac cells (H9c2) using PMG and succinate as substrates, with no change of state 4 respiration (Fig. 4C).

3.4. D-2-HG markedly inhibits cytochrome c oxidase activity in cardiac cells

The effects of D-2-HG on the activities of SDH and of the respiratory chain complexes were also evaluated in H9c2 cells in order to better elucidate the mechanisms involved in the D-2-HG-induced impairment of mitochondrial respiration. D-2-HG significantly and selectively inhibited the activity of complex IV at concentrations as low as 0.5 mM (16%–44%) [Fig. 5D = $F_{(5,30)} = 44{,}51$, $P < 0.001$], with no effects on complexes I, II, II–III and SDH activities (Fig. 5A–C and E). Importantly, L-2-HG was not able to inhibit the activity of complex IV, indicating a selective inhibitory effect of the enantiomer D-2-HG on this respiratory chain activity.

3.5. D-2-HG significantly inhibits creatine kinase (CK) activity in cardiac cells

It can be seen in Fig. 6 that D-2-HG significantly inhibited CK activity (15%–42%) in cardiac cells from a concentration of 1 mM and higher [Fig. 6 = $F_{(5,30)} = 58{,}01$, $P < 0.001$], in contrast to 5 mM L-2-HG that caused no change of this activity. These data indicate that cellular ATP buffering may be compromised by D-2-HG.

3.6. D-2-HG significantly inhibits α-ketoglutarate dehydrogenase and citrate synthase activities in heart mitochondria of developing rats

Since glutamate-supported mitochondrial respiration was compromised by D-2-HG, we measured whether this metabolite could inhibit glutamate dehydrogenase (GDH) and α-ketoglutarate dehydrogenase (α-KGDH) activities, as well as other enzymes of the citric acid cycle including citrate synthase (CS) and malate dehydrogenase (MDH) in heart mitochondria. It can be seen in Fig. 7 that D-2-HG inhibited the activities of CS (23%) [Fig. 7D = $t_{(8)} = 3.797$, $P < 0.01$] and of a commercially purified α-KGDH from porcine heart (21%) [Fig. 7B = $F_{(2,24)} = 40.33$, $P < 0.001$], without changing the activities of GDH and MDH (Fig. 7A and E). These data indicate that D-2-HG impairs citric acid cycle activity.

The kinetic profile of the interaction of D-2-HG with a commercially purified α-KGDH from porcine heart was thereafter determined. Fig. 7C displays the Lineweaver-Burk double-reciprocal plot analyzed over a concentration range of substrate (α-ketoglutarate, 0.1–1 mM) and D-2-HG (1–5 mM). It can be seen in the figure that D-2-HG inhibits α-KGDH in a mixed fashion with a K_m of 0.074 ± 0.016 that increased up to 0.14 ± 0.037 mM, and a V_{max} of 183.9 ± 4.81 that decreased to 100.2 ± 13.5 nmol $min^{-1}.U^{-1}$, as the concentration of D-2-HG increased. In addition, the values of K_i (dissociation constant of the enzyme-inhibitor complex) and K_i' (dissociation constant of the enzyme-inhibitor-substrate complex) for the inhibition of α-KGDH activity by D-2-HG were 2.12 ± 0.61 mM and 6.62 ± 2.01 mM, respectively, suggesting that this organic acid preferentially binds to the enzyme instead of to the complex enzyme-substrate.

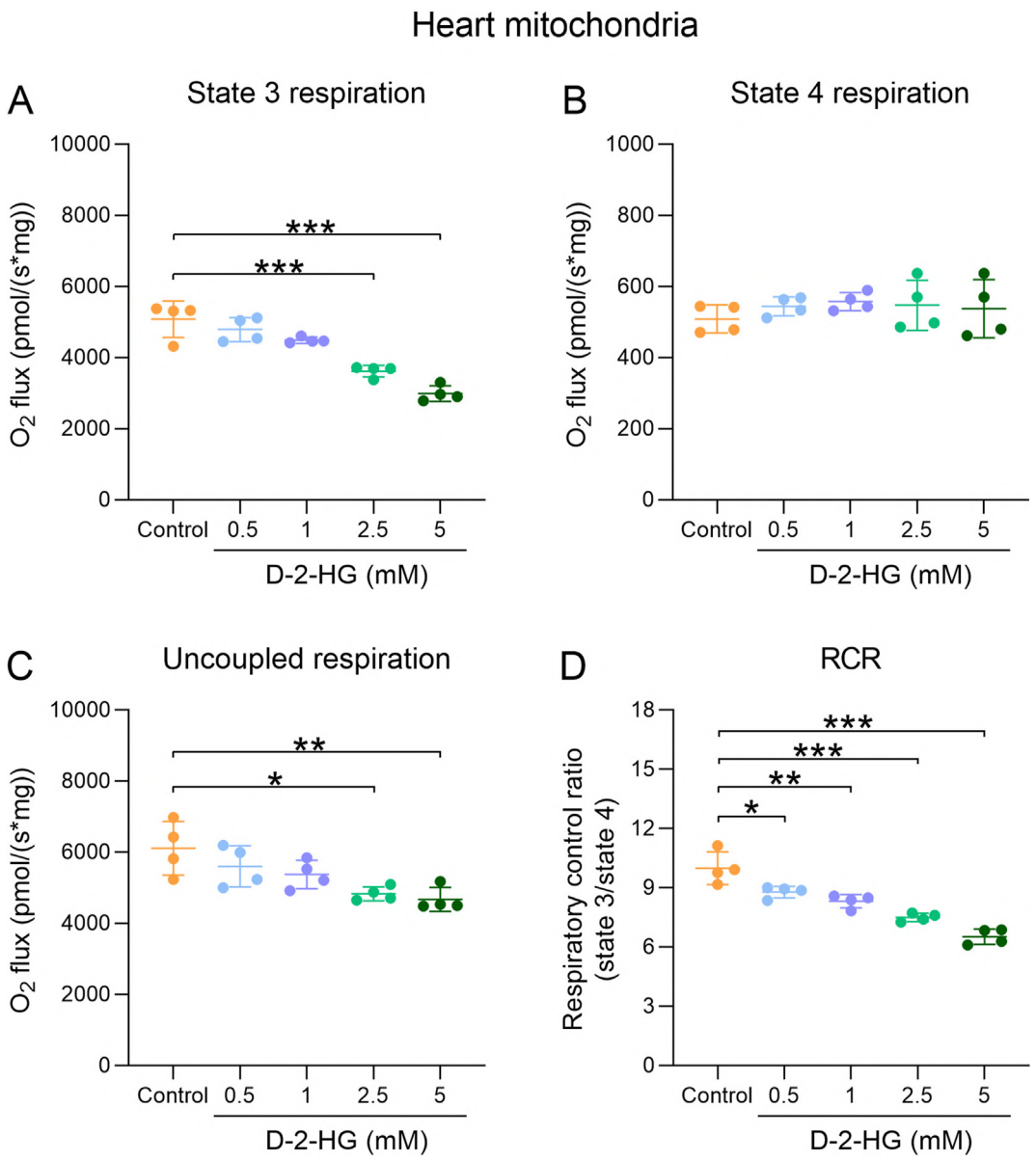

Fig. 1. D-2-HG impairs mitochondrial respiration in glutamate respiring purified mitochondria from heart of young rats. (A) State 3, (B) State 4, (C) uncoupled respiration and (D) respiratory control ratio (RCR). D-2-HG (0.5–5.0 mM) (experimental groups). Controls did not contain D-2-HG. Data are represented as means ± standard deviation for four independent experiments (animals) and were calculated as pmol O_2. s^{-1}. mg of protein^{-1}. *P < 0.05, **P < 0.01, ***P < 0.001, relatively to the control group (Tukey's multiple range test).

3.7. D-2-HG decreases Ca^{2+} retention capacity in heart mitochondria of developing rats

Additional experiments tested the influence of D-2-HG on the mitochondrial capacity to retain Ca^{2+} (Fig. 8). It can be seen in the figure that this metabolite significantly reduced this important mitochondrial function. Furthermore, D-2-HG-induced decrease of Ca^{2+} retention capacity was totally prevented by CsA, implying that mitochondrial permeability transition (MPT) pore opening was involved in this effect.

3.8. D-2-HG reduces viability of cardiac cells

Finally, we assessed the effects of D-2-HG on cell viability using the PI incorporation and the MTT assays. It was verified that 5 mM D-2-HG markedly increased the number of PI-positive cells (eight-fold) [Fig. 9 A-C = $t_{(9)} = 11.80$, $P < 0.001$] and significantly decreased formazan formation (25%) [Fig. 9D = $t_{(16)} = 9.812$, $P < 0.001$] in H9c2 cells, implying that this metabolite compromises cell viability.

4. Discussion

So far there is no therapy for D2HGA1 and D2HGA2 [6], implying the need for more investigation on the pathogenesis of these diseases. This is particularly true for the cardiac damage of D2HGA2, since most previous studies revealed *in vitro* and *in vivo* neurotoxic effects of D-2-HG, by disturbing redox homeostasis and bioenergetics [7–12], while the mechanisms underlying the cardiomyopathy characteristically observed in D2HGA2 remain unclear.

In this particular, dilated cardiomyopathy, cardiac hypertrophy and increased apoptosis associated with mitochondrial abnormalities and glycogen accumulation secondary to up-regulation of

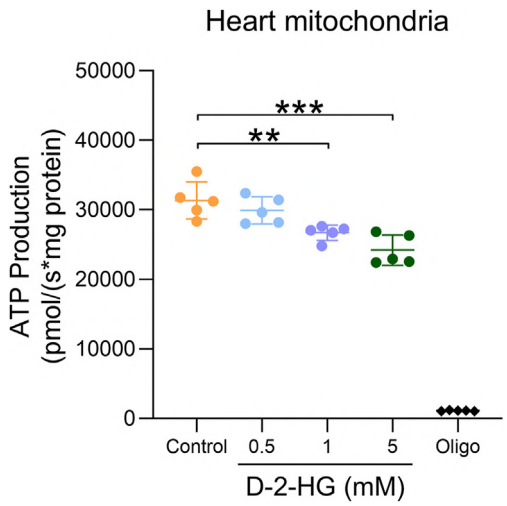

Fig. 2. D-2-HG decreases ATP production in heart mitochondrial preparations. D-2-HG (0.5–5.0 mM) (experimental groups). Controls did not contain D-2-HG. A positive control was performed using the ATP synthase inhibitor oligomycin A (1 g/mL). Data are represented as means ± standard deviation for five independent experiments (animals) and were expressed as pmol ATP. s^{-1}. mg of $protein^{-1}$. **P < 0.01, ***P < 0.001, relatively to the control group (Tukey's multiple range test).

genes involved in glycogen biosynthesis were found in cardiac cells in a transgenic D2HGA mouse model generated by activation of mutant IDH2, giving rise to elevated D-2-HG levels [14]. Another transgenic mouse model of D2HGA2 generated by introducing a gain-of-function mutation at the IDH2 gene also resulted in significantly elevated D-2-HG levels associated with severe cardiomyopathy, brain alterations, seizures and early mortality [13]. Importantly, silencing of IDH2 in mice with an inducible transgene or by a selective inhibitor of the human IDH2 mutant enzyme restored heart function and provided a survival benefit in the mutant mice, which was associated with lowering D-2HG levels, whereas treatment withdrawal resulted in deterioration of cardiac function [13,14]. Considering that the highest IDH2 mRNA and protein expression are found in heart tissue [13], it is conceivable that high D-2-HG levels induce cardiomyopathy. However, we cannot rule out that NADPH deprivation due to its consumption in the reaction αKG to D-2-HG by mutant IDH2 may also contribute to the cardiomyopathy in D2HGA2. This is in line with the observations that alterations of $NADP^+$/NADPH ratios may have deleterious effects on cardiac function [38].

In the present study we showed that D-2-HG markedly compromises mitochondrial bioenergetics in various preparations of heart of young rats and in cultivated H9c2 cells. We initially

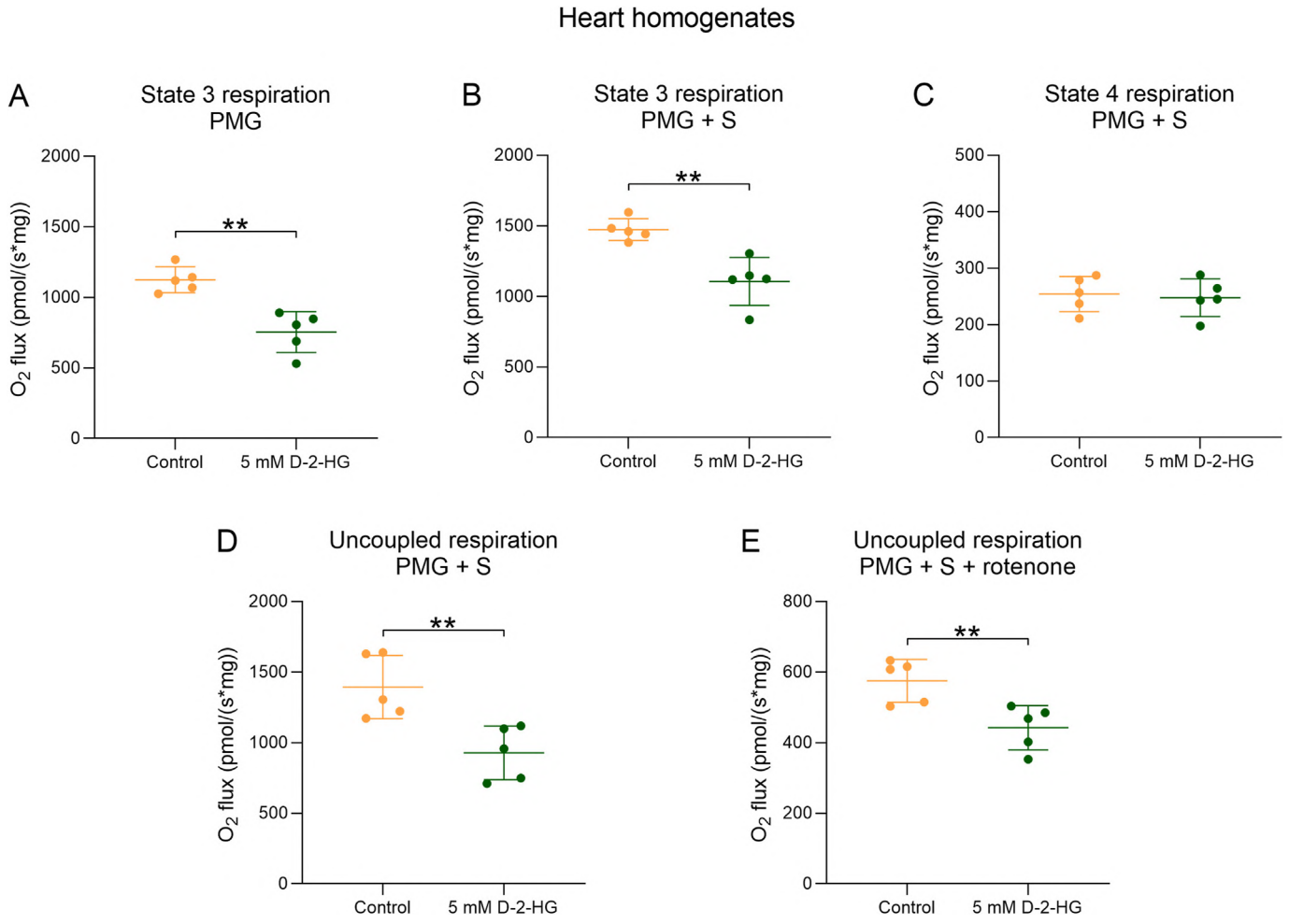

Fig. 3. D-2-HG compromises mitochondrial respiration in crude heart homogenates. (A and B) State 3, (C) state 4, and (D and E) uncoupled respiration. Pyruvate (P; 5 mM), malate (M; 0.5 mM) plus glutamate (G; 10 mM) (A) and succinate (S; 10 mM) (B–E) were used as substrates. Controls did not contain D-2-HG. Data are represented as means ± standard deviation for four independent experiments (animals) and were expressed as pmol O_2. s^{-1}. mg of $protein^{-1}$. *P < 0.05, **P < 0.01, relatively to the control group (Student's *t*-test for unpaired samples).

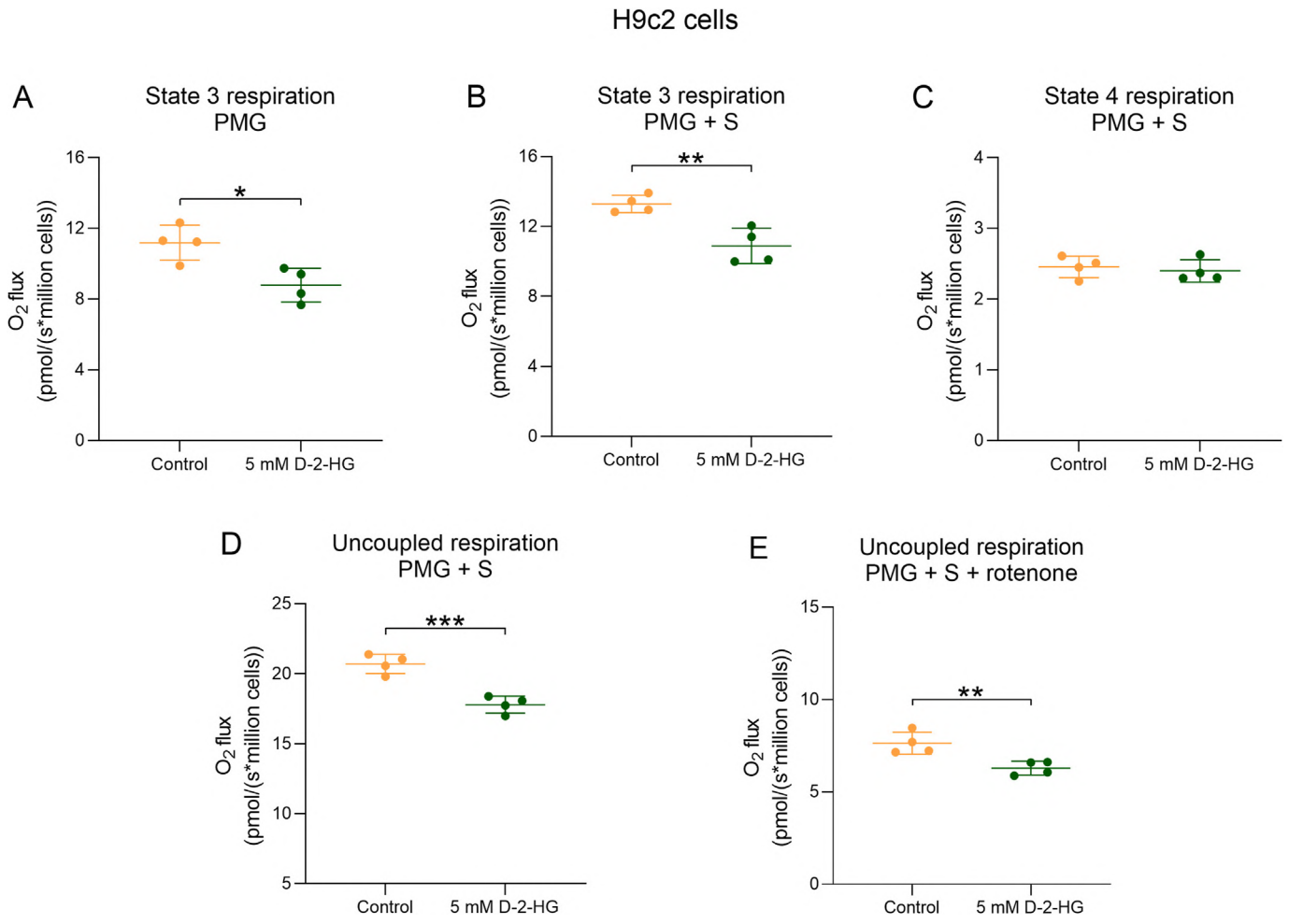

Fig. 4. D-2-HG impairs mitochondrial respiration in permeabilized cardiac cells (H9c2). Cells were permeabilized with digitonin (8 μM). (A and B) State 3, (C) state 4, and (D and E) uncoupled respiration. Pyruvate (P; 5 mM), malate (M; 0.5 mM) plus glutamate (G; 10 mM) (A) and succinate (S; 10 mM) (B–E) were used as substrates. Controls did not contain D-2-HG. Data are represented as means ± standard deviation for four independent experiments (N) and were expressed as pmol O_2. s^{-1}. million cells^{-1}. *P < 0.05, **P < 0.01, ***P < 0.001, relatively to the control group (Student's *t*-test for unpaired samples).

observed that D-2-HG induced a strong inhibition of state 3 (ADP-stimulated) and uncoupled (CCCP-stimulated) respiration, as well as a marked decrease of RCR and ATP production in heart mitochondria respiring with glutamate. D-2-HG also exerted a similar toxic effect on mitochondrial bioenergetics in crude heart homogenates and in intact cardiac cells, using both NADH-linked substrates (pyruvate, malate, and glutamate) and a $FADH_2$-linked substrate (succinate). In contrast, state 4 (resting respiration) was not changed in any of the experimental conditions utilized. These results indicate that D-2-HG impairs cellular bioenergetics homeostasis, acting as a potent metabolic inhibitor of mitochondrial respiration in purified heart mitochondria, as well as under conditions in which mitochondria were within an integrated cellular system that most closely resembles the *in vivo* condition (intact H9c2 cells and heart homogenates). It is emphasized that these experiments were performed with purified intact mitochondria. Although no specific mitochondrial D-2-HG transporter has been described, it is conceivable that D-2-HG transport is facilitated by one or more mitochondrial carriers because this organic acid is produced inside the mitochondrial matrix and must be released from this organelle to be found in the biological fluids of D2HGA patients [39]. The functionality of the mitochondrial respiratory chain complexes is critical for the production of ATP required to maintain the physiological functions of tissues with high energy demands such as the cardiac muscle [40]. Considering that D-2-HG caused a significant reduction of mitochondrial respiration, we evaluated whether this effect could be associated with an impairment of the respiratory chain. We observed that D-2-HG caused a marked reduction of cytochrome *c* oxidase activity (complex IV) in H9c2 cells, without altering the activity of the other respiratory complexes evaluated (I, II and II-III). This is in agreement with previous studies demonstrating *in vitro* and *in vivo* inhibition of complex IV mediated by D-2-HG in rat brain [7,9], skeletal muscle and heart [12], as well as in THP-1 cells (human monocytic cell line) [41]. In this particular, da Silva et al. [9] demonstrated through kinetic analysis that this metabolite inhibits complex IV activity in the brain of young rats by a non-competitive mechanism. Furthermore, Chan et al. [41] demonstrated that D-2-HG was able to inhibit the activity of purified cytochrome *c* oxidase, and through spectroscopic studies they hypothesized that the enzyme inhibition occurred by the binding of this metabolite to a site at or adjacent to the binuclear center formed by heme a3 and CuB, therefore interfering with oxygen reduction.

Noteworthy, a decrease in cellular energy production capacity due to a reduction of respiratory activity in glutamate-supported mitochondria may be related to inhibition of GDH or to a blockage of the citric acid cycle (CAC). Therefore, we evaluated the effects of D-2-HG on the activities of GDH and on the CAC enzymes

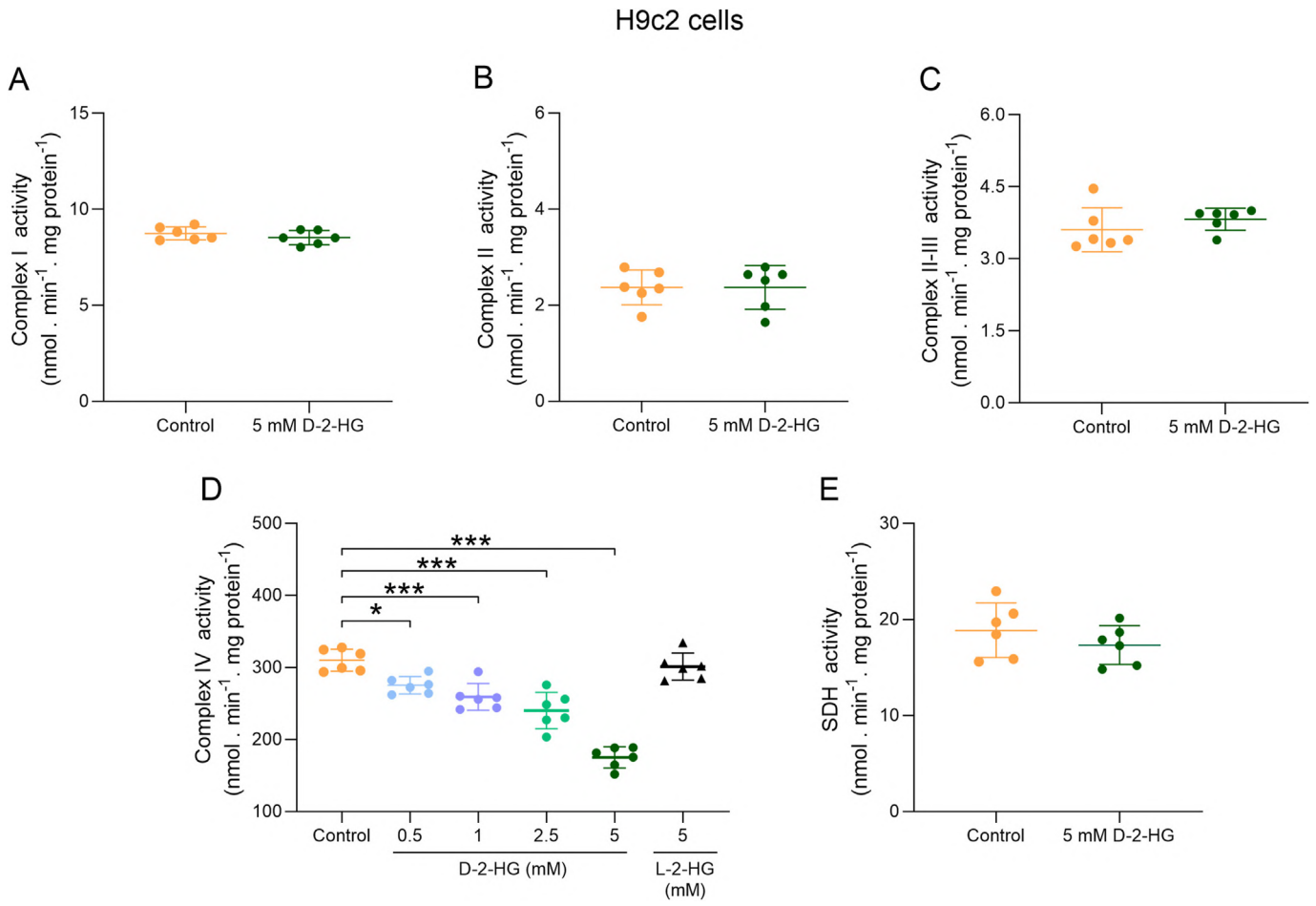

Fig. 5. D-2-HG inhibits cytochrome *c* oxidase (complex IV) activity in H9c2 cells. The activities of complexes I (A), II (B), II-III (C) and IV (D), as well as of SDH (E) were measured. H9c2 cells were pre-incubated for 30 min with D-2-HG (0.5–5 mM). Controls did not contain D-2-HG. L-2-HG (5 mM) effect on complex IV was also tested. Data are represented as means ± standard deviation for four to six independent experiments (N) and were expressed as nmol.min^{-1}.mg protein^{-1} or µmol.min^{-1}. mg protein^{-1}. *P < 0.05, ***P < 0.001, relatively to the control group (Student's *t*-test for unpaired samples or Tukey's multiple range test).

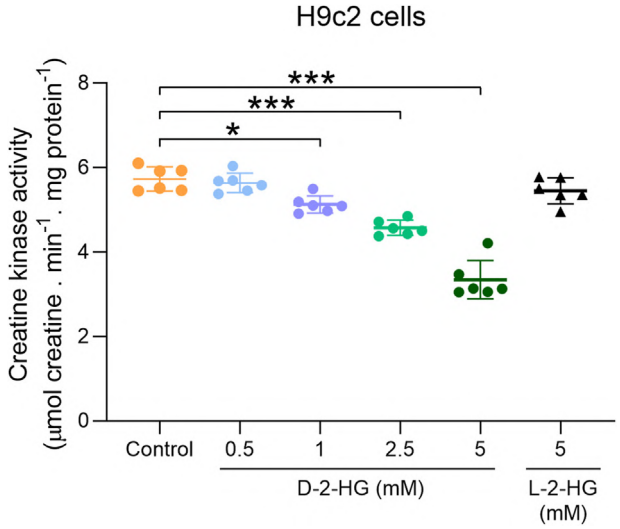

Fig. 6. D-2-HG inhibits the activity of creatine kinase in H9c2 cells. H9c2 cells were pre-incubated for 30 min with D-2-HG (0.5–5 mM). L-2-HG (5 mM) effect on creatine kinase activity was also tested. Controls did not contain D-2-HG. Data are represented as means ± standard deviation for four to six independent experiments (N) and were expressed as nmol.min^{-1}.mg protein^{-1} or µmol.min^{-1}. mg protein^{-1}. *P < 0.05, ***P < 0.001, relatively to the control group (Tukey's multiple range test).

CS, α-KGDH and MDH in heart mitochondria and SDH activity in cardiac cells. We found that D-2-HG caused a reduction in the activity of the enzymes CS and α-KGDH, which may potentially lead to a blockade of the CAC and consequent decrease of the supply of reduced coenzymes to the electron transport chain, possibly contributing to the metabolic inhibitor behavior of D-2-HG. It is also conceivable that D-2-HG-mediated inhibition of α-KGDH that was found to be mixed, may be related to the decreased mitochondrial respiration in glutamate respiring mitochondria. Therefore, the inability of α-KGDH to convert α-ketoglutarate (produced from glutamate by the action of GDH) to succinyl-CoA may result in a decreased flow of intermediates in the CAC. These findings may be associated with previous results demonstrating that D-2-HG caused a reduction of CO_2 production from acetate and glucose in rat heart and skeletal muscle, respectively, indicating a disruption of aerobic glycolysis and/or CAC activity in these tissues [12]. Our present results are also in agreement with the findings obtained by Wang and collaborators [13] showing that increased IDH2 activity leads to a depletion of alpha-ketoglutarate, suggesting the involvement of impaired citric acid cycle functions (compromised enzyme activities and/or anaplerosis) in their D2HGA mouse model.

On the other hand, creatine kinase (CK) activity plays a central role in the bioenergetics of cardiac cells to maintain cell ATP homeostasis by buffering and transferring high-energy phosphates,

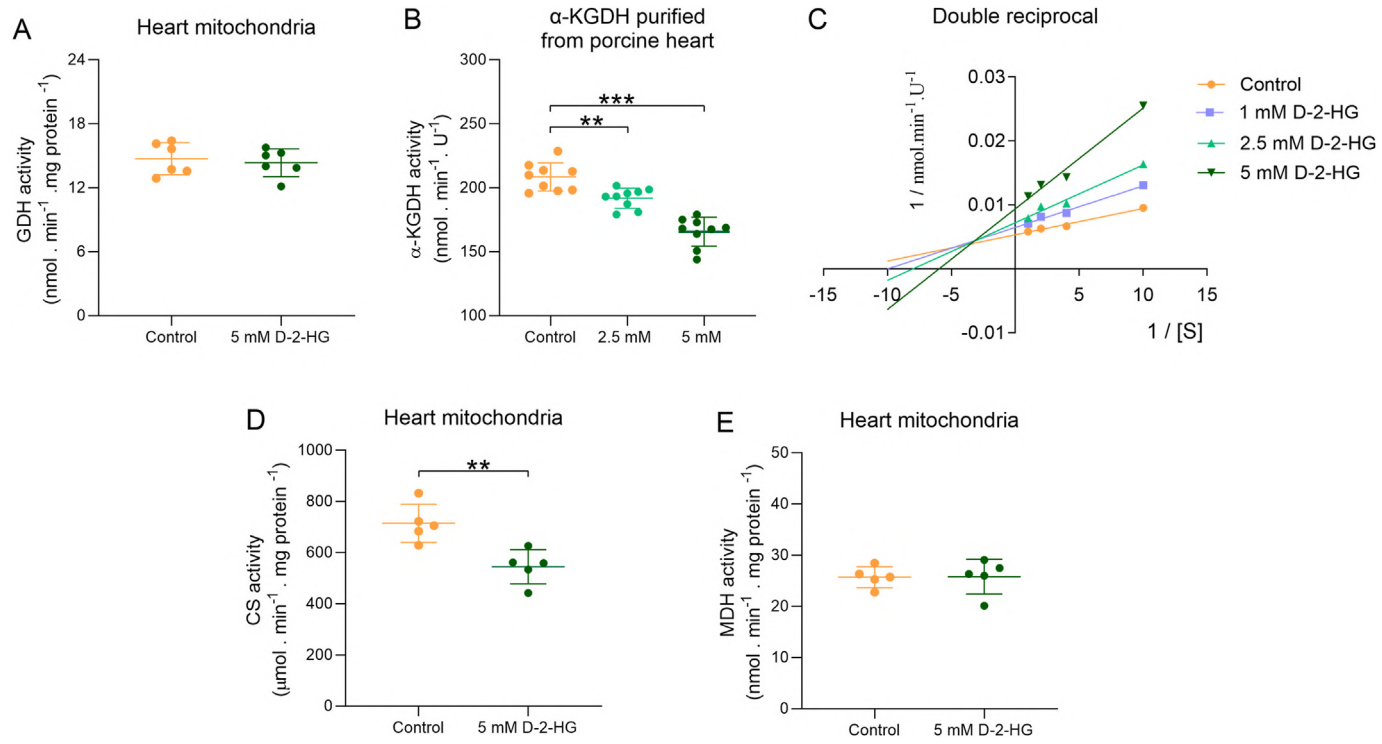

Fig. 7. D-2-HG inhibits the activities of α-ketoglutarate dehydrogenase (α-KGDH) and citrate synthase (CS). The activities of glutamate dehydrogenase (GDH) (A), citrate synthase (CS) (D) and malate dehydrogenase (MDH) (E) were performed in heart mitochondria (A, D and E), and for α-ketoglutarate dehydrogenase (α-KGDH) (B and C) a commercially purified porcine heart enzyme was used. Mitochondrial preparations or purified α-KGDH were pre-incubated for 30 min with D-2-HG (2.5–5 mM). Controls did not contain D-2-HG. Data are represented as means ± standard deviation for five to nine independent experiments performed in triplicate and expressed as µmol.min^{-1}. mg protein^{-1}, nmol.min^{-1}.mg protein^{-1} or nmol. min^{-1}. U^{-1}. (C) Kinetic analysis of α-KGDH inhibition by D-2-HG was also performed. The figure exhibits a double-reciprocal plot of α-KGDH for α-ketoglutarate (KG, 0.1–1 mM) [S] in the absence (controls ●) or presence of 1 (■), 2.5 (▲) and 5 (▼) mM D-2-HG, indicating a mixed profile of inhibition. The experiments were performed four times and the means used to create the graph. **P < 0.01, ***P < 0.001, relatively to the control group (Tukey's multiple range test or Student's *t*-test for unpaired samples).

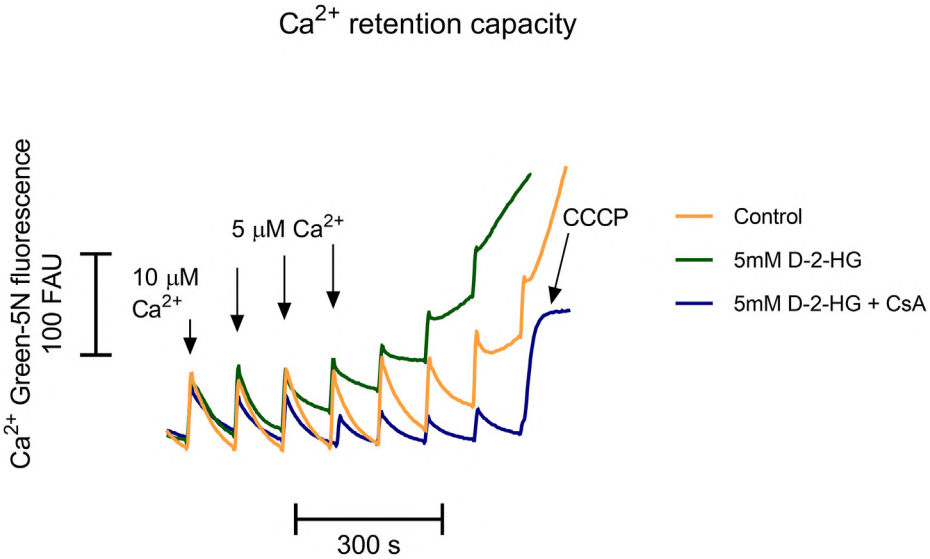

Fig. 8. D-2-HG reduces Ca^{2+} retention capacity in heart mitochondria of young rats. Glutamate (5 mM) was used as substrate. Controls were performed in the absence of D-2-HG. Mitochondrial preparations were first supplemented by 10 µM Ca^{2+} followed by consecutive additions of 5 µM Ca^{2+} every 2 min, as indicated by the arrows. Traces are representative of three independent experiments (animals) and were expressed as fluorescence arbitrary units (FAU).

preventing drastic fluctuations in cellular ATP/ADP concentrations [42]. We observed that D-2-HG inhibited CK activity in H9c2 cells, which allied to the other effects here observed on mitochondrial respiration may further aggravate cellular energy homeostasis. Furthermore, our present finding of D-2-HG-induced CK inhibition in H9c2 cells is in agreement with previous *in vitro* and *in vivo* studies demonstrating that D-2-HG causes CK inhibition in rat brain [7,10].

Another novel finding of the present study was that D-2-HG markedly reduced the capacity of heart mitochondria to retain

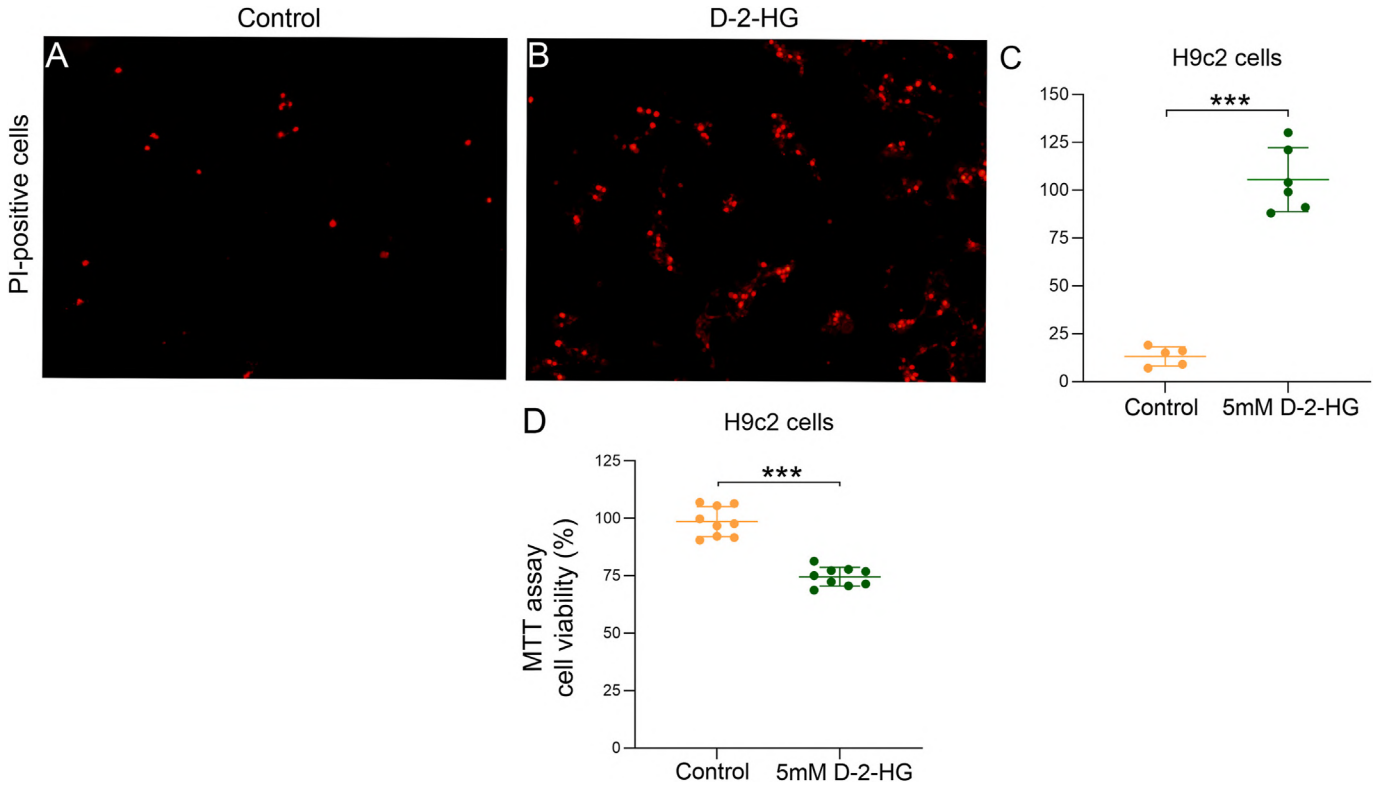

Fig. 9. D-2-HG compromises the viability of H9c2 cells. (A–C) For the propidium iodide (PI) assay, representative images were displayed from five to six independent experiments and data are represented as mean ± standard deviation. Quantification of PI-positive cells was performed at 100x magnification by using the mean of tree randomly selected fields. (D) For the MTT reduction assay, values are represented as means ± standard deviation for nine independent experiments and expressed as percentages of cell viability. The control group average in the MTT assay was assigned as 100% cell viability. ***P < 0.001, relatively to the control group (Student's *t*-test for unpaired samples).

Ca^{2+}, impairing therefore cellular Ca^{2+} homeostasis, which is vital to cardiomyocyte contractility [43,44]. This effect was probably linked to the opening of the mitochondrial permeability transition (MPT) pore, since cyclosporine A, a classical MPT inhibitor, totally prevented D-2-HG-induced reduction of Ca^{2+} retention capacity.

Overall, our data strongly indicate that D-2-HG disturbs mitochondrial bioenergetics in the heart. Mitochondrial normal functionality is very important to maintain critical heart functions such as the contractile force and the maintenance of internal Ca^{2+} stores, and this is evidenced by the fact that this organelle occupies about 30% of the mass of cardiomyocytes and is responsible for the production of more than 95% of the ATP required by this organ [15,45]. The high energy demand of cardiac muscle makes this tissue highly vulnerable to alterations of mitochondrial metabolism, as demonstrated in a variety of heart diseases that has been related to cardiac energy failure, including ischemia-reperfusion injury, cardiac hypertrophy, hypertension, atherosclerosis and heart failure [45–47].

Finally, in order to assess whether the bioenergetics dysfunction mediated by D-2-HG could compromise cell viability, we used the MTT and the PI incorporation assays in intact cardiac myoblasts. D-2-HG significantly decreased formazan formation (MTT assay) in H9c2 cells, indicating low dehydrogenase activities (this probe is closely linked to the activity of mitochondrial dehydrogenases) and/or to loss of cell viability [48]. D-2-HG also caused a significant increase in PI-positive cells, further supporting that this metabolite promotes cardiac cell death. The association between mitochondrial dysfunction and cell death was previously reported in a number of works evaluating pathophysiological mechanisms in heart diseases [45,49]. Of note, these results obtained in intact H9c2 cells may be explained by the possibility that D-2-HG is transported by a plasma membrane carrier in the heart, as was previously demonstrated to occur in renal cells and astrocytes where D-2-HG is carried by the sodium-dependent dicarboxylate transporter 3 (SLC13A3) and the organic anion transporters (SLC22A6 and SLC22A11), respectively [50].

Another point worth mentioning is that the L enantiomer of D-2HG, i.e., L-2-HG did not alter some bioenergetics parameters evaluated in the heart, indicating selective deleterious effects of D-2HG towards this tissue.

It should be also emphasized that previous observations obtained in transgenic mouse models of D2HGA2 revealed mitochondrial abnormalities and impairment of the citric acid cycle in the heart of the mutant mice [13,14]. Our present work performed in rats and H9c2 cells clarifies some D-2-HG-induced deleterious underlying mechanisms on important mitochondrial functions, which may possibly explain the mitochondrial anomalies and CAC intermediate alterations found in these D2HGA2 animals. We demonstrated for the first time that D-2-HG markedly inhibits critical enzyme activities of the CAC and electron transfer chain, besides compromising ATP production, intracellular energy transfer due to CK inhibition, as well as Ca^{2+} retention capacity in heart of developing rats. These damaging effects may possibly act synergistically reducing the viability of cardiac cells, as here demonstrated. It is therefore postulated that these pathomechanisms may contribute to the cardiomyopathy commonly observed in D2HGA2.

On the other hand, it is emphasized that some D2HGA patients excrete elevated quantities of lactate and citric acid cycle intermediates and dicarboxylic acids in the urine, suggesting a primary or functional mitochondrial dysfunction [51]. Our present investigation signalizes to a secondary mitochondrial dysfunction caused by the major metabolite that accumulates in this disorder.

At the present it is difficult to establish the pathophysiological importance of our findings since the concentrations of D-2-HG in cardiac tissue of D2HGA2 patients are still unknown. Although we may have used supra-physiological doses of D-2-HG in various assays, it is emphasized that 0.5–1.0 mM of this compound was shown to markedly disturb mitochondrial respiration, ATP production, and the activities of CK and cytochrome *c* oxidase. Furthermore, it is conceivable that intramitochondrial concentrations of D-2-HG are possibly higher than the levels found in plasma (around 757 μmol/L in D2HGA2 patients) since this metabolite is produced inside the mitochondria and the mitochondrial enzymes that generate D-2-HG are highly expressed in the cardiac tissue [52] (Human Protein Atlas, available from http://www.proteinatlas.org on October 29th, 2022).

5. Conclusions

In conclusion, the present data revealed various mitotoxic effects D-2-HG towards the heart, supporting the hypothesis that accumulation of this metabolite may represent a central event in the pathogenesis of the cardiomyopathy in D2HGA. We showed here that D-2-HG markedly disrupts fundamental mitochondrial functions and causes cardiac cell death. It seems desirable that our present results are confirmed in tissues (cultured fibroblasts) of D2HGA2 patients in order to further support the presumption that deregulation of mitochondrial energy and calcium homeostasis may be important pathomechanisms of heart damage, therefore contributing to the design of novel therapies aimed at improving mitochondrial dysfunction in this disease.

Author contributions

Conception of the work: RTR, SMW, AUA, MW. Resources: SMW, MW. Collection of data: RTR, ACR, RAM. Data analysis: RTR, ACR, RAM, RFC, AUA, MW. Writing - Original Draft: RTR, AUA, MW. Writing - Review & Editing: RFC, AUA, MW. Project administration and funding acquisition: MW. The manuscript has been approved by all authors.

Funding

This work was supported by grants from Conselho Nacional de Desenvolvimento Científico e Tecnológico [grant number 402440/2021-8], Fundação de Amparo à Pesquisa do Estado do Rio Grande do Sul (PRONEX II) [grant number 16/0465-0], and Fundação de Amparo à Pesquisa do Estado de São Paulo [grant number 17/17,728-8].

Declaration of competing interest

The authors declare that they have no known competing financial interests or personal relationships that could have appeared to influence the work reported in this paper.

References

[1] R.A. Chalmers, A.M. Lawson, R.W. Watts, A.S. Tavill, J.P. Kamerling, E. Hey, D. Ogilvie, D-2-hydroxyglutaric aciduria: case report and biochemical studies, J. Inherit. Metab. Dis. 3 (1980) 11–15, https://doi.org/10.1007/BF02312516.

[2] M. Kranendijk, E.A. Struys, K.M. Gibson, W.V. Wickenhagen, J.E. Abdenur, J. Buechner, E. Christensen, R.D. De Kremer, A. Errami, P. Gissen, W. Gradowska, E. Hobson, L. Islam, S.H. Korman, T. Kurczynski, B. Maranda, C. Meli, C. Rizzo, C. Sansaricq, F.K. Trefz, R. Webster, C. Jakobs, G.S. Salomons, Evidence for genetic heterogeneity in D-2-hydroxyglutaric aciduria, Hum. Mutat. 31 (2010) 279–283, https://doi.org/10.1002/humu.21186.

[3] M. Kranendijk, E.A. Struys, E. van Schaftingen, K.M. Gibson, W.A. Kanhai, M.S. van der Knaap, J. Amiel, N.R. Buist, A.M. Das, J.B. de Klerk, A.S. Feigenbaum, D.K. Grange, F.C. Hofstede, E. Holme, E.P. Kirk, S.H. Korman, E. Morava, A. Morris, J. Smeitink, R.N. Sukhai, H. Vallance, C. Jakobs, G.S. Salomons, IDH2 mutations in patients with D-2-hydroxyglutaric aciduria, Science 330 (2010) 336, https://doi.org/10.1126/science.1192632.

[4] M. Kranendijk, E.A. Struys, G.S. Salomons, M.S. van der Knaap, C. Jakobs, Progress in understanding 2-hydroxyglutaric acidurias, J. Inherit. Metab. Dis. 35 (2012) 571–587, https://doi.org/10.1007/s10545-012-9462-5.

[5] M. Wajner, S.I. Goodman, Disruption of mitochondrial homeostasis in organic acidurias: insights from human and animal studies, J. Bioenerg. Biomembr. (2011) 31–38, https://doi.org/10.1007/s10863-011-9324-0.

[6] M. Wajner, Neurological manifestations of organic acidurias, Nat. Rev. Neurol. 15 (2019) 253–271, https://doi.org/10.1038/s41582-019-0161-9.

[7] R.T. Ribeiro, B. Seminotti, Â. Zanatta, F.H. de Oliveira, A.U. Amaral, G. Leipnitz, M. Wajner, Neuronal death, glial reactivity, microglia activation, oxidative stress and bioenergetics impairment caused by intracerebroventricular administration of D-2-hydroxyglutaric acid to neonatal rats, Neuroscience 471 (2021) 115–132, https://doi.org/10.1016/J.NEUROSCIENCE.2021.07.024.

[8] M.S. da Rosa, B. Seminotti, A.U. Amaral, B. Parmeggiani, F.H. de Oliveira, G. Leipnitz, M. Wajner, Disruption of redox homeostasis and histopathological alterations caused by in vivo intrastriatal administration of D-2-hydroxyglutaric acid to young rats, Neuroscience 277 (2014) 281–293, https://doi.org/10.1016/j.neuroscience.2014.07.011.

[9] C.G. da Silva, C.A.J. Ribeiro, G. Leipnitz, C.S. Dutra-Filho, Â.T.S. Wyse, C.M.D. Wannmacher, J.J.F. Sarkis, C. Jakobs, M. Wajner, Inhibition of cytochrome c oxidase activity in rat cerebral cortex and human skeletal muscle by d-2-hydroxyglutaric acid in vitro, Biochim. Biophys. Acta (BBA) - Mol. Basis Dis. 1586 (2002) 81–91, https://doi.org/10.1016/S0925-4439(01)00088-6.

[10] C.G. da Silva, A.R.F. Bueno, P.F. Schuck, G. Leipnitz, C.A.J. Ribeiro, R.B. Rosa, C.S. Dutra Filho, A.T.S. Wyse, C.M.D. Wannmacher, M. Wajner, Inhibition of creatine kinase activity from rat cerebral cortex by D-2-hydroxyglutaric acid in vitro, Neurochem. Int. 44 (2004) 45–52, https://doi.org/10.1016/s0197-0186(03)00098-6.

[11] S. Kölker, V. Pawlak, B. Ahlemeyer, J.G. Okun, F. Hörster, E. Mayatepek, J. Krieglstein, G.F. Hoffmann, G. Köhr, NMDA receptor activation and respiratory chain complex V inhibition contribute to neurodegeneration in <scp>d</scp> -2-hydroxyglutaric aciduria, Eur. J. Neurosci. 16 (2002) 21–28, https://doi.org/10.1046/j.1460-9568.2002.02055.x.

[12] A. Latini, C.G. da Silva, G.C. Ferreira, P.F. Schuck, K. Scussiato, J.J. Sarkis, C.S. Dutra Filho, A.T.S. Wyse, C.M.D. Wannmacher, M. Wajner, Mitochondrial energy metabolism is markedly impaired by D-2-hydroxyglutaric acid in rat tissues, Mol. Genet. Metabol. 86 (2005) 188–199, https://doi.org/10.1016/j.ymgme.2005.05.002.

[13] F. Wang, J. Travins, Z. Lin, Y. Si, Y. Chen, J. Powe, S. Murray, D. Zhu, E. Artin, S. Gross, S. Santiago, M. Steadman, A. Kernytsky, K. Straley, C. Lu, A. Pop, E.A. Struys, E.E.W. Jansen, G.S. Salomons, M.D. David, C. Quivoron, V. Penard-Lacronique, K.S. Regan, W. Liu, L. Dang, H. Yang, L. Silverman, S. Agresta, M. Dorsch, S. Biller, K. Yen, Y. Cang, S.S.M. Su, S. Jin, A small molecule inhibitor of mutant IDH2 rescues cardiomyopathy in a D-2-hydroxyglutaric aciduria type II mouse model, J. Inherit. Metab. Dis. 39 (2016) 807–820, https://doi.org/10.1007/s10545-016-9960-y.

[14] E.A. Akbay, J. Moslehi, C.L. Christensen, S. Saha, J.H. Tchaicha, S.H. Ramkissoon, K.M. Stewart, J. Carretero, E. Kikuchi, H. Zhang, T.J. Cohoon, S. Murray, W. Liu, K. Uno, S. Fisch, K. Jones, S. Gurumurthy, C. Gliser, S. Choe, M. Keenan, J. Son, I. Stanley, J.A. Losman, R. Padera, R.T. Bronson, J.M. Asara, O. Abdel-Wahab, P.C. Amrein, A.T. Fathi, N.N. Danial, A.C. Kimmelman, A.L. Kung, K.L. Ligon, K.E. Yen, W.G. Kaelin, N. Bardeesy, K.-K. Wong, D-2-hydroxyglutarate produced by mutant IDH2 causes cardiomyopathy and neurodegeneration in mice, Genes Dev. 28 (2014) 479–490, https://doi.org/10.1101/gad.231233.113.

[15] J. Piquereau, F. Caffin, M. Novotova, C. Lemaire, V. Veksler, A. Garnier, R. Ventura-Clapier, F. Joubert, Mitochondrial dynamics in the adult cardiomyocytes: which roles for a highly specialized cell? Front. Physiol. 4 (2013) 102, https://doi.org/10.3389/fphys.2013.00102.

[16] K. Wang, Y. Xu, Q. Sun, J. Long, J. Liu, J. Ding, Mitochondria regulate cardiac contraction through ATP-dependent and independent mechanisms, Free Radic. Res. 52 (2018) 1256–1265, https://doi.org/10.1080/10715762.2018.1453137.

[17] J.N. Peoples, A. Saraf, N. Ghazal, T.T. Pham, J.Q. Kwong, Mitochondrial dysfunction and oxidative stress in heart disease, Exp. Mol. Med. 51 (2019) 1–13, https://doi.org/10.1038/s12276-019-0355-7.

[18] R. Ferranti, M.M. da Silva, A.J. Kowaltowski, Mitochondrial ATP-sensitive K + channel opening decreases reactive oxygen species generation, FEBS Lett. 536 (2003) 51–55, https://doi.org/10.1016/S0014-5793(03)00007-3.

[19] C. Cecatto, F.H. Hickmann, M.D.N. Rodrigues, A.U. Amaral, M. Wajner, Deregulation of mitochondrial functions provoked by long-chain fatty acid accumulating in long-chain 3-hydroxyacyl-CoA dehydrogenase and mitochondrial permeability transition deficiencies in rat heart - mitochondrial permeability transition pore opening a, FEBS J. 282 (2015) 4714–4726, https://doi.org/10.1111/febs.13526.

[20] M. Makrecka-Kuka, G. Krumschnabel, E. Gnaiger, High-resolution respirometry for simultaneous measurement of oxygen and hydrogen peroxide fluxes in permeabilized cells, tissue homogenate and isolated mitochondria, Biomolecules 5 (2015) 1319–1338, https://doi.org/10.3390/biom5031319.

[21] A.C. Roginski, A. Wajner, C. Cecatto, S.M. Wajner, R.F. Castilho, M. Wajner, A.U. Amaral, Disturbance of bioenergetics and calcium homeostasis provoked

by metabolites accumulating in propionic acidemia in heart mitochondria of developing rats, Biochim. Biophys. Acta (BBA) - Mol. Basis Dis. 1866 (2020), 165682, https://doi.org/10.1016/j.bbadis.2020.165682.
[22] E. Gnaiger, Capacity of oxidative phosphorylation in human skeletal muscle, Int. J. Biochem. Cell Biol. 41 (2009) 1837–1845, https://doi.org/10.1016/j.biocel.2009.03.013.
[23] C. Cecatto, A.U. Amaral, A. Wajner, S.M. Wajner, R.F. Castilho, M. Wajner, Disturbance of mitochondrial functions associated with permeability transition pore opening induced by cis-5-tetradecenoic and myristic acids in liver of adolescent rats, Mitochondrion 50 (2020) 1–13, https://doi.org/10.1016/j.mito.2019.09.008.
[24] J.J. Lemasters, C.R. Hackenbrock, Continuous measurement and rapid kinetics of ATP synthesis in rat liver mitochondria, mitoplasts and inner membrane vesicles determined by firefly-luciferase luminescence, Eur. J. Biochem. 67 (1976) 1–10, https://doi.org/10.1111/j.1432-1033.1976.tb10625.x.
[25] M.A. Maioli, D.E.C.V. Lemos, M. Guelfi, H.C.D. Medeiros, F. Riet-Correa, R.M.T. Medeiros, J.M. Barbosa-Filho, F.E. Mingatto, Mechanism for the uncoupling of oxidative phosphorylation by juliprosopine on rat brain mitochondria, Toxicon 60 (2012) 1355–1362, https://doi.org/10.1016/j.toxicon.2012.09.012.
[26] L.G.B. Michelini, C.E. Benevento, F.A. Rossato, E.S. Siqueira-Santos, R.F. Castilho, Effects of partial inhibition of respiratory complex I on H2O 2 production by isolated brain mitochondria in different respiratory states, Neurochem. Res. 39 (2014) 2419–2430, https://doi.org/10.1007/s11064-014-1446-4.
[27] J.C. Fischer, W. Ruitenbeek, J.A. Berden, J.M.F. Trijbels, J.H. Veerkamp, A.M. Stadhouders, R.C.A. Sengers, A.J.M. Janssen, Differential investigation of the capacity of succinate oxidation in human skeletal muscle, Clin. Chim. Acta 153 (1985) 23–36, https://doi.org/10.1016/0009-8981(85)90135-4.
[28] P. Rustin, D. Chretien, T. Bourgeron, B. Gérard, A. Rötig, J.M. Saudubray, A. Munnich, Biochemical and molecular investigations in respiratory chain deficiencies, Clin. Chim. Acta 228 (1994) 35–51, https://doi.org/10.1016/0009-8981(94)90055-8.
[29] G. Barrie Kitto, [19] Intra- and extramitochondrial malate dehydrogenases from chicken and tuna heart, Methods Enzymol. 13 (1969) 106–116, https://doi.org/10.1016/0076-6879(69)13023-2.
[30] D.R. Melo, S.R. Mirandola, N.A. Assunção, R.F. Castilho, Methylmalonate impairs mitochondrial respiration supported by NADH-linked substrates: involvement of mitochondrial glutamate metabolism, J. Neurosci. Res. 90 (2012) 1190–1199, https://doi.org/10.1002/jnr.23020.
[31] L. Tretter, V. Adam-Vizi, Inhibition of krebs cycle enzymes by hydrogen peroxide: a key role of α-ketoglutarate dehydrogenase in limiting NADH production under oxidative stress, J. Neurosci. 20 (2000) 8972–8979, https://doi.org/10.1523/jneurosci.20-24-08972.2000.
[32] P.A. Srere, [1] Citrate synthase. [EC 4.1.3.7. Citrate oxaloacetate-lyase (CoA-acetylating)], Methods Enzymol. 13 (1969) 3–11, https://doi.org/10.1016/0076-6879(69)13005-0.
[33] B.P. Hughes, A method for the estimation of serum creatine kinase and its use in comparing creatine kinase and aldolase activity in normal and pathological sera, Clin. Chim. Acta 7 (1962) 597–603, https://doi.org/10.1016/0009-8981(62)90137-7.
[34] A.P. Moura, B. Parmeggiani, M. Grings, L. de M. Alvorcem, R.M. Boldrini, A.P. Bumbel, M.M. Motta, B. Seminotti, M. Wajner, G. Leipnitz, Intracerebral Glycine administration impairs energy and redox homeostasis and induces glial reactivity in cerebral cortex of newborn rats, Mol. Neurobiol. 53 (2016) 5864–5875, https://doi.org/10.1007/s12035-015-9493-7.
[35] Â. Saito, R.F. Castilho, Inhibitory effects of adenine nucleotides on brain mitochondrial permeability transition, Neurochem. Res. 35 (2010) 1667–1674, https://doi.org/10.1007/s11064-010-0228-x.
[36] Â. Zanatta, M.D.N. Rodrigues, A.U. Amaral, D.G. Souza, A. Quincozes-Santos, M. Wajner, Ornithine and homocitrulline impair mitochondrial function, decrease antioxidant defenses and induce cell death in menadione-stressed rat cortical astrocytes: potential mechanisms of neurological dysfunction in HHH syndrome, Neurochem. Res. 41 (2016) 2190–2198, https://doi.org/10.1007/s11064-016-1933-x.
[37] O.H. Lowry, N.J. Rosebrough, A.L. Farr, R.J. Randall, Protein measurement with the Folin phenol reagent, J. Biol. Chem. 193 (1951) 265–275. http://www.ncbi.nlm.nih.gov/pubmed/14907713.
[38] J.R. Ussher, J.S. Jaswal, G.D. Lopaschuk, Pyridine nucleotide regulation of cardiac intermediary metabolism, Circ. Res. 111 (2012) 628–641, https://doi.org/10.1161/CIRCRESAHA.111.246371.
[39] M.K.M. Engqvist, C. Eßer, A. Maier, M.J. Lercher, V.G. Maurino, Mitochondrial 2-hydroxyglutarate metabolism, Mitochondrion 19 Pt B (2014) 275–281, https://doi.org/10.1016/J.MITO.2014.02.009.
[40] K. Ait-Aissa, S.C. Blaszak, G. Beutner, S.-W. Tsaih, G. Morgan, J.H. Santos, M.J. Flister, D.L. Joyce, A.K.S. Camara, D.D. Gutterman, A.J. Donato, G.A. Porter, A.M. Beyer, Mitochondrial oxidative phosphorylation defect in the heart of subjects with coronary artery disease, Sci. Rep. 9 (2019) 7623, https://doi.org/10.1038/s41598-019-43761-y.
[41] S.M. Chan, D. Thomas, M.R. Corces-Zimmerman, S. Xavy, S. Rastogi, W.-J. Hong, F. Zhao, B.C. Medeiros, D.A. Tyvoll, R. Majeti, Isocitrate dehydrogenase 1 and 2 mutations induce BCL-2 dependence in acute myeloid leukemia, Nat. Med. 21 (2015) 178–184, https://doi.org/10.1038/nm.3788.
[42] H. Hettling, J.H. van Beek, Analyzing the functional properties of the creatine kinase system with multiscale 'sloppy' modeling, PLoS Comput. Biol. 7 (2011), e1002130, https://doi.org/10.1371/journal.pcbi.1002130.
[43] I. Drago, D. de Stefani, R. Rizzuto, T. Pozzan, Mitochondrial Ca2+ uptake contributes to buffering cytoplasmic Ca2+ peaks in cardiomyocytes, Proc. Natl. Acad. Sci. USA 109 (2012) 12986–12991, https://doi.org/10.1073/pnas.1210718109.
[44] M. Luo, M.E. Anderson, Mechanisms of altered Ca 2+ handling in heart failure, Circ. Res. 113 (2013) 690–708, https://doi.org/10.1161/CIRCRESAHA.113.301651.
[45] P. Rosenberg, Mitochondrial dysfunction and heart disease, Mitochondrion 4 (2004) 621–628, https://doi.org/10.1016/j.mito.2004.07.016.
[46] D. Ramaccini, V. Montoya-Uribe, F.J. Aan, L. Modesti, Y. Potes, M.R. Wieckowski, I. Krga, M. Glibetić, P. Pinton, C. Giorgi, M.L. Matter, Mitochondrial function and dysfunction in dilated cardiomyopathy, Front. Cell Dev. Biol. 8 (2021), https://doi.org/10.3389/fcell.2020.624216.
[47] G. Siasos, V. Tsigkou, M. Kosmopoulos, D. Theodosiadis, S. Simantiris, N.M. Tagkou, A. Tsimpiktsioglou, P.K. Stampouloglou, E. Oikonomou, K. Mourouzis, A. Philippou, M. Vavuranakis, C. Stefanadis, D. Tousoulis, A.G. Papavassiliou, Mitochondria and cardiovascular diseases—from pathophysiology to treatment, Ann. Transl. Med. 6 (2018), https://doi.org/10.21037/atm.2018.06.21, 256–256.
[48] Y. Rai, R. Pathak, N. Kumari, D.K. Sah, S. Pandey, N. Kalra, R. Soni, B.S. Dwarakanath, A.N. Bhatt, Mitochondrial biogenesis and metabolic hyperactivation limits the application of MTT assay in the estimation of radiation induced growth inhibition, Sci. Rep. 8 (2018) 1531, https://doi.org/10.1038/s41598-018-19930-w.
[49] S.-B. Ong, A.B. Gustafsson, New roles for mitochondria in cell death in the reperfused myocardium, Cardiovasc. Res. 94 (2012) 190–196, https://doi.org/10.1093/cvr/cvr312.
[50] L. Bunse, S. Pusch, T. Bunse, F. Sahm, K. Sanghvi, M. Friedrich, D. Alansary, J.K. Sonner, E. Green, K. Deumelandt, M. Kilian, C. Neftel, S. Uhlig, T. Kessler, A. von Landenberg, A.S. Berghoff, K. Marsh, M. Steadman, D. Zhu, B. Nicolay, B. Wiestler, M.O. Breckwoldt, R. Al-Ali, S. Karcher-Bausch, M. Bozza, I. Oezen, M. Kramer, J. Meyer, A. Habel, J. Eisel, G. Poschet, M. Weller, M. Preusser, M. Nadji-Ohl, N. Thon, M.C. Burger, P.N. Harter, M. Ratliff, R. Harbottle, A. Benner, D. Schrimpf, J. Okun, C. Herold-Mende, S. Turcan, S. Kaulfuss, H. Hess-Stumpp, K. Bieback, D.P. Cahill, K.H. Plate, D. Hänggi, M. Dorsch, M.L. Suvà, B.A. Niemeyer, A. von Deimling, W. Wick, M. Platten, Suppression of antitumor T cell immunity by the oncometabolite (R)-2-hydroxyglutarate, Nat. Med. 24 (2018) 1192–1203, https://doi.org/10.1038/S41591-018-0095-6.
[51] M.S. van der Knaap, C. Jakobs, G.F. Hoffmann, M. Duran, A.C. Muntau, S. Schweitzer, R.I. Kelley, F. Parrot-Roulaud, J. Amiel, P. de Lonlay, D. Rabier, O. Eeg-Olofsson, D-2-hydroxyglutaric aciduria: further clinical delineation, J. Inherit. Metab. Dis. 22 (1999) 404–413, https://doi.org/10.1023/a:1005548005393.
[52] M. Uhlén, L. Fagerberg, B.M. Hallström, C. Lindskog, P. Oksvold, A. Mardinoglu, Å. Sivertsson, C. Kampf, E. Sjöstedt, A. Asplund, I.M. Olsson, K. Edlund, E. Lundberg, S. Navani, C.A.K. Szigyarto, J. Odeberg, D. Djureinovic, J.O. Takanen, S. Hober, T. Alm, P.H. Edqvist, H. Berling, H. Tegel, J. Mulder, J. Rockberg, P. Nilsson, J.M. Schwenk, M. Hamsten, K. von Feilitzen, M. Forsberg, L. Persson, F. Johansson, M. Zwahlen, G. von Heijne, J. Nielsen, F. Pontén, Tissue-based map of the human proteome, Science 347 (2015), https://doi.org/10.1126/Science.1260419/SUPPL_FILE/1260419_UHLEN.SM.PDF, 1979.

PARTE III: DISCUSSÃO

DISCUSSÃO

Indivíduos afetados pelas D-2-HGA e L-2-HGA, apresentam sintomatologia clínica predominantemente neurológica, incluindo crises epiléticas graves, hipotonia, atraso no desenvolvimento psicomotor e ataxia, bem como atrofia cerebral com hipo/desmielinização (leucodistrofia) e outras anormalidades cerebrais cujos mecanismos patogênicos são ainda pouco conhecidos (Kranendijk et al., 2012; Steenweg et al., 2009). Aproximadamente metade dos pacientes com a forma mais grave de D-2-HGA (tipo 2) também apresentam alterações cardíacas que podem os levar ao desfecho fatal nos primeiros anos de vida e cujos mecanismos são praticamente desconhecidos. Estudos prévios, particularmente *in vitro*, mas também *ex vivo*, utilizando cérebro de ratos jovens (ratos Wistar com 30 dias de vida) demonstraram efeitos deletérios dos metabólitos acumulados nessas doenças (D-2-HG e L-2-HG) sobre o metabolismo energético, homeostase redox, além de algumas alterações do sistema glutamatérgico (da Rosa et al., 2014; da Silva et al., 2002; Junqueira et al., 2004; Kölker et al., 2002; Latini et al., 2005, 2003b).

No entanto, como as manifestações clínicas dessas doenças podem ocorrer já no período perinatal ou no primeiro ano de vida dos afetados, é fundamental investigar o efeito desses ácidos orgânicos em modelos neonatais, mimetizando a situação nos pacientes em que o acumulo de D-2-HG e L-2-HG já ocorrem no nascimento ou mesmo antes. Nesse particular, um estudo recente de nosso grupo de pesquisa revelou que a administração *icv* de D-2-HG a ratos neonatos causou danos oxidativos aos lipídios, medido pelo aumento significativo nos níveis de malondialdeído (MDA), em estriado e córtex cerebral dos animais neonatos (Ribeiro et al., 2021). Também foi verificado que o D-2-HG aumentou a formação de grupamentos carbonila no córtex cerebral (dano oxidativo proteico) bem como a oxidação da 2',7' - diclorofluoresceína (DCFH) no córtex e no estriado, indicando aumento de EROs, nessas estruturas cerebrais, além de elevar as concentrações de nitratos e nitritos (parâmetro que avalia ERNs) no cérebro total. Finalmente, foi observado que o D-2-HG diminuiu as concentrações de GSH e elevou as atividades das enzimas antioxidantes SOD e CAT, indicando um provável mecanismo compensatório com aumento da transcrição gênica secundário a elevação das espécies reativas. Outros resultados interessantes desse trabalho foram as observações de que o dano oxidativo aos lipídeos e proteínas e o aumento da produção de espécies reativas induzido por D-2-HG foram prevenidos pelo pré-tratamento dos animais com o

antioxidante melatonina e o antagonista de receptores glutamatérgicos NMDA MK-801, indicando o envolvimento de espécies ativas e dos receptores NMDA nesses efeitos. O mesmo estudo mostrou ainda que além das alterações neuroquímicas, houve dano no córtex cerebral e estriado (menos intenso) com vacuolização e redução do número de neurônios sugestivo de morte neuronal, além de intensa reatividade.

Por outro lado, verificamos em um estudo anterior que a administração icv aguda do L-2-HG a ratos neonatos causa estresse oxidativo e algumas alterações patológicas, incluindo formação de vacúolos e edema cerebral mais intensamente no córtex cerebral dos animais (Ribeiro et al., 2018). Também foi verificado nesse estudo que a melatonina e o MK-801 preveniram a lipoperoxidação e a diminuição de GSH no córtex cerebral e estriado dos ratos neonatos.

Dessa forma, o primeiro objetivo da presente investigação foi estudar se a administração icv de L-2-HG poderia também comprometer a homeostase redox no cerebelo de ratos neonatos, que corresponde a uma estrutura cerebral com severas anormalidades na ressonância magnética nuclear de pacientes da L-2-HGA, resultando em ataxia, bastante comum nos pacientes afetados por essa doença (Gunduz et al., 2022). Enfatize-se que não há estudos *in vitro* ou *ex vivo* na literatura sobre ações deletérias do L-2-HG sobre o cerebelo em idade neonatal. Verificamos que a administração icv do L-2-HG à ratos neonatos aumentou significativamente a produção de espécies ativas, determinada pelo aumento da oxidação do DCFH, que reflete predominantemente EROs (Halliwell e Gutteridge, 2015), no cerebelo dos animais 6 horas após a injeção. Já que houve aumento da produção de espécies ativas, testamos se esse aumento poderia provocar dano oxidativo aos lipídico e verificamos que o L-2-HG causou um aumento significativo dos níveis de MDA (produto final de peroxidação de ácidos graxos insaturados, representando um bom marcador de lipoperoxidação) no cerebelo. Salienta-se que a lipoperoxidação pode afetar membranas lipídicas das células, resultando em alterações na organização das mesmas, bem como na fluidez e na permeabilidade, podendo prejudicar o transporte de íons e os processos metabólicos (Yadav e Ramana, 2013).

Com relação às defesas antioxidantes, verificamos que o L-2-HG causou uma diminuição significativa nas concentrações de GSH no cerebelo, que pode ser ocasionado por um maior consumo provocado pelo aumento da produção de radicais livres observado neste tecido. Tendo em vista que o GSH desempenha um papel fundamental na manutenção do estado redox intracelular por ser o antioxidante não enzimático mais abundante no cérebro e também ser um eficiente protetor de grupos sulfidrila, bem como um sequestrador de radicais livres, as concentrações desse antioxidante são utilizadas para avaliar a capacidade de um tecido em prevenir o dano oxidativo associado ao processo de produção de radicais livres (Halliwell, B., Gutteridge, 2015a), Assim, uma diminuição destas concentrações torna o cerebelo mais vulnerável ao dano oxidativo as suas biomoléculas, incluindo lipídeos.

Finalmente verificamos que a administração neonatal do L-2-HG provocou aumento significativo da atividade das enzimas GPx e SOD no cerebelo. Acreditamos que o aumento das atividades dessas enzimas tenha ocorrido devido à indução da expressão das mesmas a nível gênico por um mecanismo compensatório em resposta ao aumento na formação de espécies reativas, principalmente do radical superóxido e do peróxido de hidrogênio, mas essa hipótese requer estudos adicionais para que se possa estabelecer os mecanismos exatos que levaram ao aumento dessas atividades enzimáticas. Neste particular, é sabido que as EROs regulam a expressão de inúmeros genes, incluindo aqueles que codificam para enzimas antioxidantes por vias de sinalização específicas (Halliwell, B., Gutteridge, 2015a; Lakshminarayanan et al., 1998; Rushmore et al., 1991)..

Outros resultados que julgamos bastante importantes da presente investigação foram que o pré-tratamento dos ratos neonatos com a melatonina, uma hora antes da administração icv de L-2-HG, foi capaz de prevenir completamente, os efeitos pró-oxidantes do metabólito sobre o aumento dos níveis de MDA, formação de espécies ativas, pois normalizou o aumento da oxidação de DCFH, bem como a diminuição das concentrações de GSH. Esses resultados reforçam a hipótese de que o dano oxidativo lipídico, bem como a diminuição das defesas antioxidantes no cerebelo tenham sido causadas pela elevação da especialmente EROs, mais particularmente os radicais hidroxila e peroxil que sofrem ação “scavenger” da melatonina (Anisimov et al., 2006; Halliwell, B., Gutteridge, 2015c; Reiter et al., 2001). No entanto, o pré-tratamento com melatonina não foi capaz de normalizar o aumento das atividades da GPx e SOD mediada

pela injeção do metabólito, sugerindo que outras espécies reativas que não o superóxido e o peróxido de hidrogênio ou mesmo outros mecanismos estão evolvidos neste aumento de atividade das enzimas antioxidantes em resposta ao insulto pró-oxidante do L-2-HG.

O próximo passo de nossa investigação foi determinar se esse metabólito poderia alterar marcadores de dano cerebral no córtex e estriado, que também são lesados nos pacientes afetados por essa doença (Kranendijk et al., 2012; Weimar et al., 2013). Avaliamos os efeitos da administração icv de L-2-HG no período neonatal sobre marcadores de neurônios, astrócitos, micróglia e mielinização através de técnicas de imunofluorescência realizadas aos DPN15 e 75.

No que se refere a esses marcadores histoquímicos, a presente investigação mostrou pela primeira vez que a administração icv de L-2-HG em ratos neonatos causou efeitos de longa duração observados ao DPN15 e 75 dos animais, tais como perda neuronal (diminuição do número de células marcadas com NeuN), astrogliose (aumento de S100B e GFAP) e neuroinflamação (aumento de Iba1) no estriado e córtex cerebral.

A astrogliose, ou aumento da reatividade astrocitária, corresponde geralmente a uma condição desencadeada por dano ao SNC e caracterizada pela ativação e hipertrofia de astrócitos com aumento da expressão de marcadores astrocitários (S100B e GFAP), e, em casos graves, proliferação intensa dessas células (Anderson et al., 2014; Sofroniew e Vinters, 2010). Em condições fisiológicas, tais alterações astrocitárias têm o potencial de proteger os neurônios circundantes, mas em casos extremos os astrócitos podem perder funções essenciais, produzindo fatores potencialmente tóxicos, comprometendo e exacerbando o dano neuronal, como observado em diversas doenças neurodegenerativas (De Keyser et al., 2008; McGeer e McGeer, 2008; Nagele et al., 2004; Olivera-Bravo et al., 2011).

Já a diminuição significativa do número de células neurais marcadas com NeuN indica dano e/ou perda neuronal (Ünal-Çevik et al., 2004; Wolf et al., 1996). Enfatize-se que perda neuronal associada à astrogliose foi observada no cérebro de uma criança de 1 mês de idade com L-2-HGA (Chen et al., 1996). É possível, portanto, que esses achados histopatológicos possam ter sido devidos ao aumento nas concentrações cerebrais de L-2-HG.

Uma outra observação original do presente trabalho foi que a injeção neonatal de L-2-HG aumentou o conteúdo de Iba1 em ratos adolescentes e adultos, considerado um

excelente marcador de ativação da microglia durante processos inflamatórios (Hoogland et al., 2015; Sasaki et al., 2001). Enfatize-se que a ativação microglial pode levar à produção excessiva de citocinas pró-inflamatórias e radicais livres (Norden et al., 2016; Seminotti et al., 2019b; Wirths et al., 2010), e em seu conjunto levando à neuroinflamação.

Verificamos também que um aumento transitório dos níveis de L-2-HG no SNC no período perinatal alcançado pela injeção de L-2-HG desencadeou uma lesão duradoura da substância branca no córtex cerebral e estriado no DPN75, determinada pela diminuição da imunofluorescência das proteínas associadas a mielina MBP e CNPase, que poderia explicar a hipomielinização observada em pacientes e no modelo genético animal de L-2HGA (Gunduz et al., 2022; Jović et al., 2014; Kranendijk et al., 2012; Rzem et al., 2015; Topçu et al., 2005).

Um outro aspecto inédito de nosso estudo foi que essas alterações neuroquímicas de longa duração foram totalmente prevenidas (NeuN, MBP e CNPase) ou atenuadas (Iba1, GFAP, S100B) pelo pré-tratamento com o antioxidante melanonina. Portanto, considerando observações prévias demonstrando que o L-2-HG induz estresse oxidativo no córtex cerebral e estriado de ratos adolescentes e jovens (da Rosa et al., 2015; Latini et al., 2003a; Ribeiro et al., 2018), aliadas aos resultados da presente investigação, mostrando os efeitos benéficos da melatonina sobre as alterações imunohistopatológicas induzidas por esse ácido orgânico acumulado na L-2-HGA, sugerimos o envolvimento dessa condição patológica nos efeitos neurotóxicos provocados pela injeção neonatal de L-2-HG. Tomados em seu conjunto, acreditamos que a neurotoxicidade induzida por L-2-HG parece exigir uma interação celular múltipla e complexa que, após um desencadeamento inicial induzido por níveis cerebrais tóxicos de L-2-HG, se autoperpetua durante semanas, levando ao dano progressivo de neurônios, astrócitos e proteínas mielinizantes.

Por outro lado, tendo em vista que os pacientes afetados pela L-2-HGA apresentam atraso no desenvolvimento motor e cognitivo, bem como alterações motoras e de equilíbrio (ataxia), e que a doença progride de forma lenta e progressiva (Gunduz et al., 2022; Steenweg et al., 2010), resolvemos avaliar o neurodesenvolvimento, a motricidade e cognição dos animais, que receberam administração icv com L-2-HG no período neonatal, ao longo do seu desenvolvimento e na idade adulta. A avaliação de marcos do desenvolvimento neuromotor e cognitivo é de suma importância para aferir o

impacto de um dano perinatal em modelos animais experimentais (Horvath et al., 2015), podendo representar uma ferramenta essencial para rastrear o desenvolvimento dos animais pós-injeção com o L-2-HG e assim entender se nosso modelo químico é capaz de mimetizar os achados característicos da L-2-HGA. Assim, iniciamos por determinar os efeitos do L-2-HG sobre uma bateria de testes de neurodesenvolvimento ao longo das primeiras semanas de vida. Relativamente à abertura de olhos, verificamos que os animais L-2-HG tiveram um atraso de um dia na abertura total de ambos os olhos (DPN13), o que pode sugerir uma maturação do sistema visual prejudicada pela administração de L-2-HG (Guan et al., 2017; Katz e Shatz, 1996; Pecka et al., 2014).

Outros testes utilizados para estudar o desenvolvimento neuromotor dos ratos foram o endireitamento, teste de aversão à borda e geotaxia negativa no DPN7. Nossos dados mostram que os animais que receberam a injeção de L-2-HG apresentaram uma resposta sensório-motora deficiente, evidenciada por uma menor latência na realização de geotaxia negativa e endireitamento e uma pontuação diminuída no teste de aversão à borda. Também avaliamos se a administração de L-2-HG poderia causar distúrbios do desenvolvimento neuromotor associados à locomoção (teste de marcha) e força do tônus muscular (suspensão dos membros posteriores) no DPN7. A injeção icv de L-2-HG provocou uma diminuição acentuada da capacidade de marcha e da força muscular nos animais, o que está de acordo com as manifestações clínicas de alterações motoras observadas em pacientes com L-2HGA, onde se destaca a hipotonia, como um sintoma clássico de disfunção neurológica, sendo o achado mais prevalente nos estágios iniciais da doença (Kranendijk et al., 2012).

É importante ressaltar que o pré-tratamento com melatonina dos animais injetados com L-2-HG foi capaz de atenuar os déficits de neurodesenvolvimento na maioria dos testes aqui avaliados, denotando um efeito neuroprotetor desse antioxidante em nosso modelo experimental de L-2HGA. Nesse contexto, a melatonina tem sido amplamente empregada como agente neuroprotetor no combate ao estresse oxidativo, neuroinflamação e sinalização pró-apoptótica associada a diversas neuropatologias (Chitimus et al., 2020; Elsayed et al., 2021; Victor et al., 2021; Wakatsuki et al., 2001).

Déficits motores e cognitivos são características clínicas predominantes em pacientes com L-2-HGA e, à medida que a doença progride, a ataxia cerebelar e outros distúrbios motores tornam-se mais evidentes (Gunduz et al., 2022; Kranendijk et al., 2012; Steenweg et al., 2010). Neste estudo, verificamos que o L-2-HG causou déficit

motor no período neonatal, que persistiu na vida adulta, conforme verificado pela avaliação da função motora grosseira avaliada pelo teste do rota-rod e motricidade fina avaliada pelo teste de caminhada em escada no DPN45 dos animais. Nesse contexto, Gunduz et al (2022) correlacionaram movimentos irregulares e respostas somatossensoriais prejudicadas em pacientes com L-2-HGA com atrofia cerebelar. Assim, a perda acentuada de neurônios, reatividade glial e, principalmente, a desmielinização observada no córtex cerebral e estriado concomitante aos déficits motores mediados pela injeção icv de L-2-HG, demonstram o enorme potencial do nosso modelo para mimetizar os achados observados na L2HGA.

Observações em camundongos nocaute deficientes da enzima L-2-hidroxiglutarato desidrogenase (l2hgdh$^{-/-}$) revelaram lesões espongiformes da substância branca, mais acentuadamente nas regiões subcorticais e gânglios da base, e mais moderadas no córtex cerebral, cerebelo e hipocampo, bem como déficits cognitivos relacionados à evocação de memória de trabalho e de referência avaliadas pelos testes de labirinto em Y e labirinto aquático Morris, respectivamente (Rzem et al., 2015). Em consonância com os dados do modelo genético, também encontramos um comprometimento da memória de trabalho, verificado pelo protocolo de memória de trabalho do labirinto aquático de Morris, mas sem alterar a memória de referência. Diferente da memória de referência, que é dependente do hipocampo, a memória de trabalho é principalmente dependente de conexões neuronais associadas ao córtex pré-frontal e ao cerebelo (Stein, 2021). Nossa hipótese é que uma possível razão pela qual não identificamos deficiências na memória de referência de longo prazo pode estar envolvida com um baixo envolvimento hipocampal em nosso modelo químico de L2HGA. Finalmente, observamos que o pré-tratamento com melatonina foi capaz de prevenir completamente os distúrbios motores a longo prazo e atenuar os déficits cognitivos induzidos pela injeção icv de L-2-HG.

Considerando que as concentrações cerebrais de L-2-HG em pacientes com L-2-HGA ainda não são bem estabelecidas, existindo apenas um relato recente na literatura que demonstrou através do uso de técnica de espectroscopia por ressonância magnética, demonstrando que as concentrações intracerebrais do metabólito podem atingir valores acima de 4 mM (Anghileri et al., 2016), é concebível que dose utilizadas neste trabalho (0,750µmol/g de peso) seja condizente com as concentrações encontradas em pacientes com L-2-HGA. Cabe também ressaltar que o L-2-HG se acumula no cérebro dos

pacientes devido à produção local e pela dificuldade que os ácidos dicarboxílicos tem de sair do SNC por não haver transportadores efetivos para esses compostos deixarem o tecido cerebral (Sauer et al., 2010), exercendo dessa forma seus efeitos neurotóxicos.

Em conclusão, este é o primeiro relato mostrando que a administração *in vivo* de L-2-HG a ratos neonatos prejudica a homeostase redox no cerebelo logo após a injeção icv e que o distúrbio do estado redox dessa estrutura pode ser prevenido pelo potente antioxidante melatonina. Tendo em vista os dados aqui apresentados, aliados a estudos anteriores em modelos *in vitro* (Latini et al., 2003a) e *in vivo* (da Rosa et al., 2015, 2014; Ribeiro et al., 2018) em roedores, podemos presumir que um desequilíbrio da homeostase redox causado por concentrações elevadas de L-2-HG pode potencialmente contribuir, pelo menos em parte, para as alterações neurológicas que acomete os pacientes com L-2-HGA. Nesse particular, a presente investigação também demonstrou efeitos de longa duração nas principais estruturas cerebrais danificadas na L-2HGA (córtex cerebral e estriado), tais como perda neuronal, astrogliose, ativação da micróglia associada à neuroinflamação e alterações de mielinização que podem ser parcialmente secundárias ao estresse oxidativo, visto que a melatonina também preveniu ou atenuou a maioria dessas alterações imunhistoquímicas provocadas L-2-HG.

Por estas razões, é possível que os resultados da presente investigação (Figura 5), agindo sinergicamente com outros fatores intrínsecos (severidade das mutações patogênicas) e extrínsecos, podem potencialmente contribuir para explicar a fisiopatologia dos sintomas neurológicos e anormalidades cerebrais observadas nos pacientes afetados pela L-2-HGA. Caso nossos resultados neste modelo animal *in vivo* possam ser confirmados nos modelos nocaute dessas doenças e em tecidos (fibroblastos cultivados) de indivíduos afetados por L-2-HGA, é tentador especular que antioxidantes poderiam ser suplementados aos pacientes afetados como uma terapia adjuvante potencial para prevenir ou atenuar o dano oxidativo que parece estar atrelado à patologia desta doença.

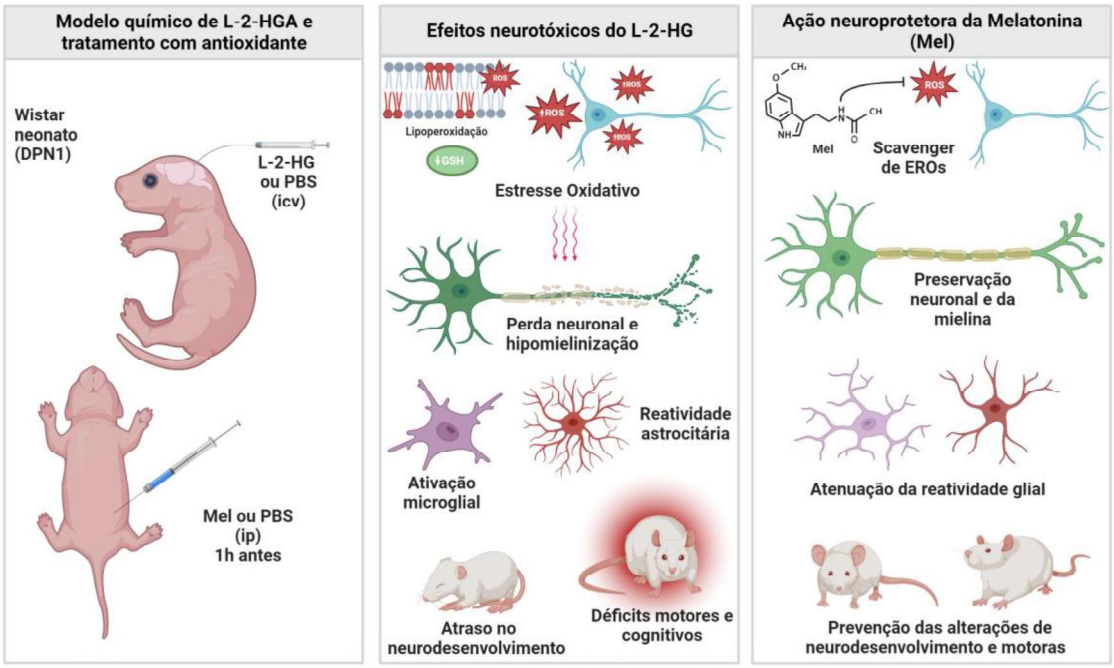

Figura 5. Mecanismos de neurotoxicidade medidos pelo L-2-HG. A administração intracerebroventricular do metabólito causa estresse oxidativo expressivo levando a dano neuronal, reatividade glial, hipomielinização e prejuízos no neurodesenvolvimento, atividade motora e cognição. A figura também mostra o papel neuroprotetor da melatonina (Mel) prevenindo os efeitos deletérios induzidos pelo L-2-HG.

A outra parte desse estudo objetivou avaliar os efeitos do D-2-HG, que se encontra bastante elevado na D-2-HGA, sobre funções mitocondriais críticas no coração de ratos adolescentes (30 dias de vida), uma vez que, pacientes com a D-2-HGA2 frequentemente desenvolvem cardiomiopatia que pode os levar à morte e que, por outro lado, os mecanismos precisos da cardiotoxicidade ainda são pouco conhecidos na D-2-HGA2. Nesse particular, convém salientar que pacientes afetados por D-2-HGA documentados excretam quantidades aumentadas de intermediários do ciclo de lactato e ácido cítrico ou ácidos dicarboxílicos, sugerindo uma disfunção mitocondrial primária ou funcional (van der Knaap et al., 1999a).

A hipótese de que o acúmulo de D-2-HG pode representar um fator determinante na cardiomiopatia que acomete pacientes com D-2-HGA2 é corroborada pelos estudos que demonstram que o uso de inibidores seletivos de IDH2 foram capazes de reduzir a produção de D-2-HG e, em paralelo, melhoraram as funções cardíacas e preveniram a cardiomiopatia em modelos de camundongos com D-2HGA2 (Akbay et al., 2014; Wang et al., 2016). No entanto, os mecanismos celulares subjacentes que levam ao dano cardíaco em D-2HGA2 permanecem pouco compreendidos.

Em nosso estudo, verificamos que o D-2-HG comprometeu marcadamente a bioenergética mitocondrial em várias preparações de coração de ratos em desenvolvimento, bem como em cardiomiócitos cultivados. Esse metabólito inibiu a respiração em mitocôndrias cardíacas purificadas, bem como em condições nas quais as mitocôndrias estavam dentro de um sistema celular integrado que mais se assemelha à condição *in vivo* (células H9c2 permeabilizadas e homogeneizados de coração). Também observamos que o D-2-HG inibiu acentuadamente a atividade da citocromo *c* oxidase (complexo IV) nas células H9c2, o que corrobora com estudos prévios realizados *in vitro* e *in vivo* em cérebro de ratos (da Silva et al., 2002; Ribeiro et al., 2021), músculo esquelético e coração (Latini et al., 2005), bem como em células THP-1 (linha celular monocítica humana) (Chan et al., 2015). Outro resultado interessante e original de nosso trabalho foi que o D-2-HG causou uma redução na atividade das enzimas citrato sintase e α-cetoglutarato desidrogenase, o que pode potencialmente levar a um bloqueio do CAC e subsequente diminuição do fornecimento de coenzimas reduzidas para a cadeia de transporte de elétrons, possivelmente contribuindo com o comportamento de inibidor metabólico de D-2-HG sobre a respiração mitocondrial. A inibição dessas atividades enzimáticas, mais especificamente da α-cetoglutarato desidrogenase, pode potencialmente explicar resultados anteriores demonstrando que o D-2-HG causou uma redução da produção de CO_2 a partir de acetato e de glicose no coração e músculo esquelético de ratos, respectivamente, indicando um comprometimento da glicólise aeróbica e/ou atividade do CAC nesses tecidos (Latini et al., 2005).

Observamos também que o D-2-HG inibiu a atividade da creatina cinase (CK) em células H9c2, o que aliado aos outros efeitos aqui observados na respiração mitocondrial, pode agravar ainda mais a homeostase energética celular. Além disso, nosso presente achado de inibição de CK induzida por D-2-HG em cardiomioblastos está de acordo com estudos anteriores *in vitro* e *in vivo* demonstrando que D-2-HG causa inibição de CK em cérebro de rato (da Silva et al., 2004; Ribeiro et al., 2021).

Outra observação original e importante do presente estudo foi que o D-2-HG reduziu acentuadamente a capacidade das mitocôndrias cardíacas de reter Ca^{2+}, prejudicando, portanto, a homeostase celular do Ca^{2+} que é vital para a contratilidade dos cardiomiócitos (Drago et al., 2012; Luo e Anderson, 2013). Este efeito foi provavelmente ligado à abertura do poro de transição de permeabilidade mitocondrial (PTP), uma vez

que a ciclosporina A, um inibidor clássico de MPT, impediu totalmente a redução da capacidade de retenção de Ca^{2+} induzida por D-2-HG.

Por fim, demonstramos que o D-2-HG diminuiu a viabilidade celular, determinada por ensaios de incorporação de MTT e PI em células H9c2 cultivadas. D-2-HG diminuiu significativamente a formação de formazan (ensaio do MTT), indicando baixa atividade de desidrogenases (esta sonda está intimamente ligada à atividade de desidrogenases mitocondriais) e/ou à perda de viabilidade celular (Rai et al., 2018). D-2-HG também causou um aumento significativo do número de células PI-positivas, apoiando ainda mais que este metabólito promove a morte celular ou ao menos lesão de membrana plasmática de células cardíacas. A associação entre disfunção mitocondrial e morte celular foi relatada anteriormente em vários trabalhos avaliando mecanismos fisiopatológicos em doenças cardíacas (Ong e Gustafsson, 2012; Rosenberg, 2004). Assim, nossos achados apontam para uma disfunção mitocondrial secundária causada pelo D-2-HG no coração, inibindo várias funções mitocondriais causadas pelo metabólito que mais se acumula neste distúrbio.

Concluindo, se os presentes resultados forem confirmados em tecidos (fibroblastos cultivados) de pacientes com D2HGA2, presume-se que os mecanismos patológicos aqui descritos (Figura 6) levando a disfunção mitocondrial possam estar relacionados com a cardiomiopatia dos pacientes afetados por essa doença e possam também contribuir para o desenvolvimento de novas terapias destinadas a melhorar a disfunção mitocondrial nesta doença, incluindo por exemplo agentes promotores da biogênese mitocondrial (agonistas PPAR, como o bezafibrato) ou agentes anapleróticos (trieptanoína) já utilizados em algumas doenças hereditárias do metabolismo intermediário (Dabner et al., 2021; Karunanidhi et al., 2022; Seminotti et al., 2022b; Shiraishi et al., 2021; Vockley et al., 2022, 2021). A trieptanoína por ser um triacilglicerol com cada ácido graxo contendo 7 carbonos, quando metabolizada gera duas acetil-Coa e um propionil-Coa por unidade de ácido graxo. Assim, a trieptonína serve como fonte de intermediários do CAC e consequentemente ajuda no combatendo a deficiência energética dos tecidos com alta demanda de acetil-Coa, como cérebro e coração (Vockley et al., 2022).

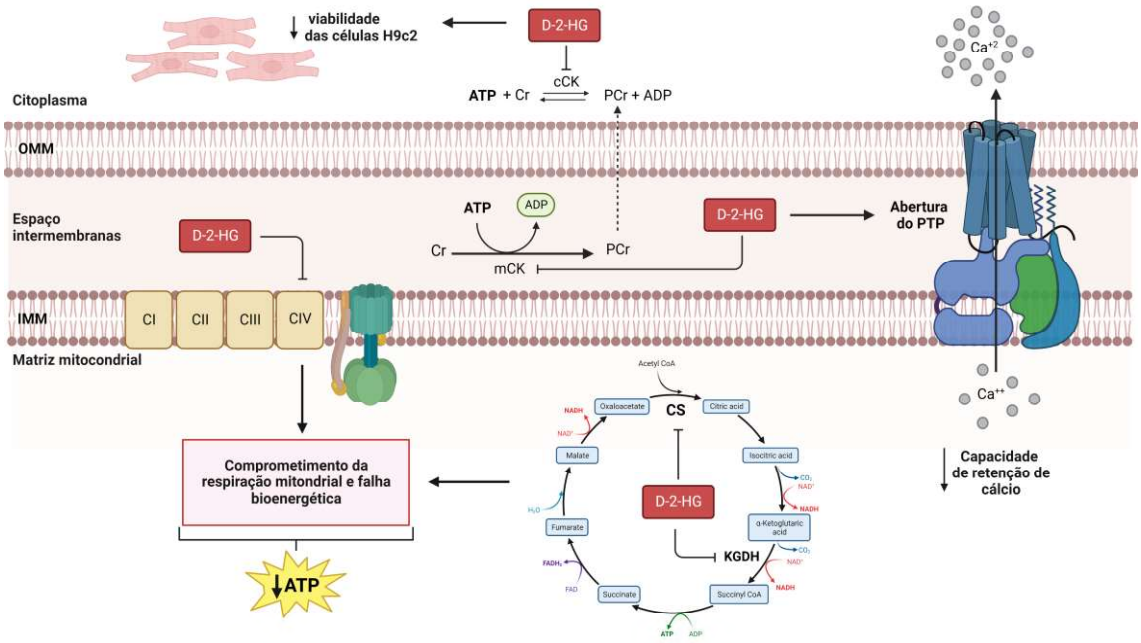

Figura 6. Mecanismos de mitotoxicidade provocados pelo ácido D-2-hidroxiglutárico (D-2-HG) no coração. A figura mostra os efeitos inibitórios de D-2-HG nas atividades da citocromo c oxidase (CIV), creatina quinase citosólica e mitocondrial (cCK e mCK), citrato sintase (CS) e α-cetoglutarato desidrogenase (KGDH), como bem como um comprometimento da respiração mitocondrial e produção de ATP. D-2-HG também diminuiu a capacidade de retenção de cálcio mitocondrial com o envolvimento da abertura do poro de transição de permeabilidade mitocondrial (PTP). Por fim, a viabilidade dos cardiomiócitos foi reduzida pelo D-2-HG possivelmente devido às ações sinérgicas de todos esses mecanismos de disfunção mitocondrial. Cr, creatina; IMM, membrana mitocondrial interna, OMM, membrana mitocondrial externa; PCr, fosfocreatina.

PARTE IV: CONCLUSÕES E PERSPECTIVAS

CONCLUSÕES

- A administração intracerebral de L-2-HG aumentou a produção de espécies reativas de oxigênio, provocou dano oxidativo lipídico e alterou as defesas antioxidantes no cerebelo de ratos neonatos 6 horas após a injeção. A maioria desses efeitos foi prevenida pelo potente antioxidante melatonina, implicando que a geração de espécies reativas pode estar subjacente ao estado redox celular alterado. Além disso, o L-2-HG foi capaz de induzir efeitos de longa duração (15 e 75 dias após a injeção), tais como perda neuronal (diminuição do número de células NeuN positivas), astrogliose (aumento das concentrações de GFAP e S100B), ativação microglial,/ neuroinflamação (aumento dos níveis da proteína Iba1) e distúrbios na mielinização (diminuição na concentração das proteínas de mielina MBP e CNPase) no córtex cerebral e estriado dos animais, cujos efeitos foram totalmente prevenidos ou atenuados pela melatonina, sugerindo que a produção aumentada de espécies ativas possa ter contribuído para essas alterações imunohistoquímicas. Atrasos no neurocomportamentais, bem como, déficits motores e cognitivos de ratos adultos mediados pelo L-2-HG foram atenuados ou prevenidos pelo pré-tratamento com melatonina, indicando a ação do estresse oxidativo nessas alterações comportamentais.
- Em resumo, a administração neonatal de L-2-HG, principal metabólito acumulado na L-2-HGA, provoca estresse oxidativo no cerebelo logo após a injeção, bem como diminuição da quantidade de neurônios, astrogliose, neuroinflamação e hipomielinização de longa duração e finalmente atraso do desenvolvimento neuromotor e déficit cognitivo nos

animais adultos (45 dias de vida) que foram provavelmente causados por estresse oxidativo, uma vez que o antioxidante melatonina foi capaz de prevenir essas alterações neurológicas.

- O D-2-HG comprometeu a respiração celular em preparações mitocondriais purificadas e homogeneizados brutos de coração de ratos jovens, bem como em células cardíacas cultivados *in vitro*.
- O D-2-HG inibiu a atividade das enzimas alfa-cetoglutarato desidrogenase, citrato sintase, creatina quinase e citocromo c oxidase (complexo IV da cadeia respiratória), bem como a produção de ATP.
- O D-2-HG comprometeu a capacidade de retenção de Ca 2+ mitocondrial em preparações mitocondriais do coração e em mioblastos H9c2, bem como a viabilidade de células H9c2 cultivadas (diminuição das concentrações de MTT e aumento da incorporação de iodeto de propídio). L-2HG não alterou alguns desses parâmetros (atividades do complexo IV e da creatina quinase) em preparações cardíacas, indicando um efeito inibitório seletivo do enantiômero D.
- Em conclusão, presume-se que o D-2-HG prejudica funções mitocondriais essenciais para a viabilidade celular no coração (bioenergética e a capacidade de retenção de Ca 2+), podendo esses mecanismos patológicos estarem potencialmente envolvidos na cardiomiopatia comumente observada na D2HGA2.

PERSPECTIVAS

- Avaliar funções mitocondriais (respiração celular, fosforilação oxidativa, e retenção mitocondrial de cálcio) e homeostase redox no modelo nocaute de acidúria D-2-hydroxiglutárica no coração e cérebro dos animais ao longo do desenvolvimento.
- Avaliar funções mitocondriais (respiração celular, fosforilação oxidativa e retenção mitocondrial de cálcio) e homeostase redox no modelo nocaute de acidúria L-2-hydroxiglutárica no cérebro dos animais ao longo do desenvolvimento.
- Avaliar funções mitocondriais (respiração celular, fosforilação oxidativa e retenção mitocondrial de cálcio) e homeostase redox em fibroblastos cultivados de pacientes afetados pelas acidúrias D-2-hydroxiglutárica tipo 1 e 2 e acidúria L-2-hydroxiglutárica.
- Avaliar os efeitos do tratamento com bezafibrato (30 ou 100 mg/kg/dia em animais; 10μM em células), triheptanoína (2,5 ou 4 g/kg/dia em animais; 144 mM em células) sobre as possíveis alterações detectadas nos animais nocaute com acidúria D-2-hydroxiglutárica, bem como em células (fibroblastos) de pacientes.
- Avaliar os efeitos do tratamento com BEZ (30 ou 100 mg/kg/dia) ou do antagonista de receptores glutamatérgicos NMDA MK-801 sobre alterações da homeostase energética e mitocondrial, histopatológicas, imunohistoquímicas e comportamentais provocadas pela administração de D-2-HG em córtex cerebral e estriado de ratos eutanasiados 7 dias após a injeção.

- Estudar os efeitos in vitro e *ex vivo* do D-2-HG e do L-2-HG sobre parâmetros do sistema glutamatérgico (captação e liberação de glutamato, expressão de receptores e transportadores glutatergicos, influxo de cálcio e atividade da enzima glutamina sintetase) em cérebro de ratos ao longo do desenvolvimento, tendo em vista a similaridade desses metabólitos com o glutamato.

REFERÊNCIAS

Adam-Vizi, V., Starkov, A.A., 2010. Calcium and mitochondrial reactive oxygen species generation: how to read the facts. J Alzheimers Dis 20 Suppl 2. https://doi.org/10.3233/JAD-2010-100465

Akbay, E.A., Moslehi, J., Christensen, C.L., Saha, S., Tchaicha, J.H., Ramkissoon, S.H., Stewart, K.M., Carretero, J., Kikuchi, E., Zhang, H., Cohoon, T.J., Murray, S., Liu, W., Uno, K., Fisch, S., Jones, K., Gurumurthy, S., Gliser, C., Choe, S., Keenan, M., Son, J., Stanley, I., Losman, J.A., Padera, R., Bronson, R.T., Asara, J.M., Abdel-Wahab, O., Amrein, P.C., Fathi, A.T., Danial, N.N., Kimmelman, A.C., Kung, A.L., Ligon, K.L., Yen, K.E., Kaelin, W.G., Bardeesy, N., Wong, K.-K., 2014. D-2-hydroxyglutarate produced by mutant IDH2 causes cardiomyopathy and neurodegeneration in mice. Genes Dev 28, 479–490. https://doi.org/10.1101/gad.231233.113

Amaral, A.U., Seminotti, B., da Silva, J.C., de Oliveira, F.H., Ribeiro, R.T., Vargas, C.R., Leipnitz, G., Santamaría, A., Souza, D.O., Wajner, M., 2018. Induction of Neuroinflammatory Response and Histopathological Alterations Caused by Quinolinic Acid Administration in the Striatum of Glutaryl-CoA Dehydrogenase Deficient Mice. Neurotox Res 33, 593–606. https://doi.org/10.1007/S12640-017-9848-0

Anderson, M.A., Ao, Y., Sofroniew, M. V., 2014. Heterogeneity of reactive astrocytes. Neurosci Lett 565, 23–29. https://doi.org/10.1016/j.neulet.2013.12.030

Anghileri, E., Bertolino, N., Salsano, E., Antelmi, L., Carpinelli, P., Castellotti, B., Zucca, I., Gellera, C., Bisogno, R., Caccia, C., Cuccarini, V., 2016. In-vivo brain H1-MR-Spectroscopy identification and quantification of 2-hydroxyglutarate in L-2-Hydroxyglutaric aciduria. Brain Res 1648, 506–511. https://doi.org/10.1016/j.brainres.2016.08.013

Anisimov, V.N., Popovich, I.G., Zabezhinski, M.A., Anisimov, S. V, Vesnushkin, G.M., Vinogradova, I.A., 2006. Melatonin as antioxidant, geroprotector and anticarcinogen. Biochim Biophys Acta 1757, 573–89. https://doi.org/10.1016/j.bbabio.2006.03.012

Aratani, Y., Miura, N., Ohno, N., Suzuki, K., 2012. [Role of neutrophil-derived reactive oxygen species in host defense and inflammation]. Med Mycol J 53, 123–8.

Baines, C.P., Kaiser, R.A., Purcell, N.H., Blair, N.S., Osinska, H., Hambleton, M.A., Brunskill, E.W., Sayen, M.R., Gottlieb, R.A., Dorn, G.W., Bobbins, J., Molkentin, J.D., 2005. Loss of cyclophilin D reveals a critical role for mitochondrial permeability transition in cell death. Nature 434, 658–662. https://doi.org/10.1038/NATURE03434

Barbot, C., Fineza, I., Diogo, L., Maia, M., Melo, J., Guimarães, A., Pires, M.M., Cardoso, M.L., Vilarinho, L., 1997. L-2-Hydroxyglutaric aciduria: Clinical, biochemical and magnetic resonance imaging in six Portuguese pediatric patients. Brain Dev 19, 268–273. https://doi.org/10.1016/S0387-7604(97)00574-3

Barth, P.G., Wanders, R.J.A., Scholte, H.R., Abeling, N., Jakobs, C., Schutgens, R.B.H., Vreken, P., 1998. L-2-hydroxyglutaric aciduria and lactic acidosis. J Inherit Metab Dis 21, 251–254. https://doi.org/10.1023/A:1005316121584

Basso, E., Fante, L., Fowlkes, J., Petronilli, V., Forte, M.A., Bernardi, P., 2005. Properties of the permeability transition pore in mitochondria devoid of Cyclophilin D. J Biol Chem 280, 18558–18561. https://doi.org/10.1074/JBC.C500089200

Baughman, J.M., Perocchi, F., Girgis, H.S., Plovanich, M., Belcher-Timme, C.A., Sancak, Y., Bao, X.R., Strittmatter, L., Goldberger, O., Bogorad, R.L., Koteliansky, V., Mootha, V.K., 2011. Integrative genomics identifies MCU as an essential component of the mitochondrial calcium uniporter. Nature 476, 341–345. https://doi.org/10.1038/NATURE10234

Beaudet, A.L., Scriver, C.R., Sly, W.S., Valle, D., 2014. Genetics, Biochemistry, and Molecular Bases of Variant Human Phenotypes, in: Beaudet, A.L., Vogelstein, B., Kinzler, K.W., Antonarakis, S.E., Ballabio, A., Gibson, K.M., Mitchell, G. (Eds.), The Online Metabolic and Molecular Bases of Inherited Disease. The McGraw-Hill Companies, Inc., New York, NY.

Bernardi, P., 2013. The mitochondrial permeability transition pore: a mystery solved? Front Physiol 4. https://doi.org/10.3389/FPHYS.2013.00095

Bernardi, P., von Stockum, S., 2012. The permeability transition pore as a Ca(2+) release channel: new answers to an old question. Cell Calcium 52, 22–27. https://doi.org/10.1016/J.CECA.2012.03.004

Bock, F.J., Tait, S.W.G., 2020. Mitochondria as multifaceted regulators of cell death. Nat Rev Mol Cell Biol 21, 85–100. https://doi.org/10.1038/S41580-019-0173-8

Carter, S.F., Herholz, K., Rosa-Neto, P., Pellerin, L., Nordberg, A., Zimmer, E.R., 2019. Astrocyte Biomarkers in Alzheimer's Disease. Trends Mol Med 25, 77–95. https://doi.org/10.1016/j.molmed.2018.11.006

Cecatto, C., Amaral, A.U., Wajner, A., Wajner, S.M., Castilho, R.F., Wajner, M., 2020. Disturbance of mitochondrial functions associated with permeability transition pore opening induced by cis-5-tetradecenoic and myristic acids in liver of adolescent rats. Mitochondrion 50, 1–13. https://doi.org/10.1016/J.MITO.2019.09.008

Chalmers, R.A., Purkiss, P., Watts, R.W., Lawson, A.M., 1980. Screening for organic acidurias and amino acidopathies in newborns and children. J Inherit Metab Dis 3, 27–43.

Chalmers,RA and Lawson, A., 1983. Organic acids in man: analytical chemistry, biochemistry, and diagnosis of the organic acidurias. Arch Dis Child 58, 240. https://doi.org/10.1136/adc.58.3.240-c

Chan, A., Seguin, R., Magnus, T., Papadimitriou, C., Toyka, K. v., Antel, J.P., Gold, R., 2003. Phagocytosis of apoptotic inflammatory cells by microglia and its therapeutic implications: Termination of CNS autoimmune inflammation and modulation by interferon-beta. Glia 43, 231–242. https://doi.org/10.1002/glia.10258

Chan, S.M., Thomas, D., Corces-Zimmerman, M.R., Xavy, S., Rastogi, S., Hong, W.-J., Zhao, F., Medeiros, B.C., Tyvoll, D.A., Majeti, R., 2015. Isocitrate dehydrogenase 1 and 2 mutations induce BCL-2 dependence in acute myeloid leukemia. Nat Med 21, 178–184. https://doi.org/10.1038/nm.3788

Chen, E., Nyhan, W.L., Jakobs, C., Greco, C.M., Barkovich, A.J., Cox, V.A., Packman, S., 1996. L-2-Hydroxyglutaric aciduria: neuropathological correlations and first report of severe

neurodegenerative disease and neonatal death. J Inherit Metab Dis 19, 335–343. https://doi.org/10.1007/BF01799264

Chitimus, D.M., Popescu, M.R., Voiculescu, S.E., Panaitescu, A.M., Pavel, B., Zagrean, L., Zagrean, A.M., 2020. Melatonin's Impact on Antioxidative and Anti-Inflammatory Reprogramming in Homeostasis and Disease. Biomolecules 2020, Vol. 10, Page 1211 10, 1211. https://doi.org/10.3390/BIOM10091211

Cipolla-Neto, J., Amaral, F.G. do, 2018. Melatonin as a Hormone: New Physiological and Clinical Insights. Endocr Rev 39, 990–1028. https://doi.org/10.1210/er.2018-00084

Colombo, E., Farina, C., 2016. Astrocytes: Key Regulators of Neuroinflammation. Trends Immunol 37, 608–620. https://doi.org/10.1016/J.IT.2016.06.006

Crompton, M., 1999. The mitochondrial permeability transition pore and its role in cell death. Biochem J 341 (Pt 2), 233–249. https://doi.org/10.1042/0264-6021:3410233

da Rosa, M.S., João Ribeiro, C.A., Seminotti, B., Teixeira Ribeiro, R., Umpierrez Amaral, A., de Moura Coelho, D., de Oliveira, F.H., Leipnitz, G., Wajner, M., 2015. In vivo intracerebral administration of L-2-hydroxyglutaric acid provokes oxidative stress and histopathological alterations in striatum and cerebellum of adolescent rats. Free Radic Biol Med 83, 201–213. https://doi.org/10.1016/j.freeradbiomed.2015.02.008

da Rosa, M.S., Seminotti, B., Amaral, A.U., Parmeggiani, B., de Oliveira, F.H., Leipnitz, G., Wajner, M., 2014. Disruption of redox homeostasis and histopathological alterations caused by in vivo intrastriatal administration of D-2-hydroxyglutaric acid to young rats. Neuroscience 277, 281–293. https://doi.org/10.1016/j.neuroscience.2014.07.011

da Silva, C.G., Bueno, A.R.F., Schuck, P.F., Leipnitz, G., Ribeiro, C.A.J., Rosa, R.B., Dutra Filho, C.S., Wyse, A.T.S., Wannmacher, C.M.D., Wajner, M., 2004. Inhibition of creatine kinase activity from rat cerebral cortex by D-2-hydroxyglutaric acid in vitro. Neurochem Int 44, 45–52. https://doi.org/10.1016/s0197-0186(03)00098-6

da Silva, C.G., Bueno, A.R.F., Schuck, P.F., Leipnitz, G., Ribeiro, C.A.J., Wannmacher, C.M.D., Wyse, A.T.S., Wajner, M., 2003. L-2-Hydroxyglutaric acid inhibits mitochondrial creatine kinase activity from cerebellum of developing rats. International Journal of Developmental Neuroscience 21, 217–224. https://doi.org/10.1016/S0736-5748(03)00035-2

da Silva, C.G., Ribeiro, C.A.J., Leipnitz, G., Dutra-Filho, C.S., Wyse, Â.T.S., Wannmacher, C.M.D., Sarkis, J.J.F., Jakobs, C., Wajner, M., 2002. Inhibition of cytochrome c oxidase activity in rat cerebral cortex and human skeletal muscle by d-2-hydroxyglutaric acid in vitro. Biochimica et Biophysica Acta (BBA) - Molecular Basis of Disease 1586, 81–91. https://doi.org/10.1016/S0925-4439(01)00088-6

da Silva, J.C., Amaral, A.U., Cecatto, C., Wajner, A., dos Santos Godoy, K., Ribeiro, R.T., de Mello Gonçalves, A., Zanatta, Â., da Rosa, M.S., Loureiro, S.O., Vargas, C.R., Leipnitz, G., de Souza, D.O.G., Wajner, M., 2017. α-Ketoadipic Acid and α-Aminoadipic Acid Cause Disturbance of Glutamatergic Neurotransmission and Induction of Oxidative Stress In Vitro in Brain of Adolescent Rats. Neurotox Res 32, 276–290. https://doi.org/10.1007/s12640-017-9735-8

Dabner, L., Pieles, G.E., Steward, C.G., Hamilton-Shield, J.P., Ness, A.R., Rogers, C.A., Bucciarelli-Ducci, C., Greenwood, R., Ellis, L., Sheehan, K., Reeves, B.C., 2021. Treatment of Barth Syndrome by Cardiolipin Manipulation (CARDIOMAN) With Bezafibrate: Protocol for a Randomized Placebo-Controlled Pilot Trial Conducted in the Nationally Commissioned Barth Syndrome Service. JMIR Res Protoc 10, e22533. https://doi.org/10.2196/22533

de Almeida, M.M.A., Watson, A.E.S., Bibi, S., Dittmann, N.L., Goodkey, K., Sharafodinzadeh, P., Galleguillos, D., Nakhaei-Nejad, M., Kosaraju, J., Steinberg, N., Wang, B.S., Footz, T., Giuliani, F., Wang, J., Sipione, S., Edgar, J.M., Voronova, A., 2022. Fractalkine enhances oligodendrocyte regeneration and remyelination in a demyelination mouse model. Stem Cell Reports. https://doi.org/10.1016/J.STEMCR.2022.12.001

De Keyser, J., Mostert, J.P., Koch, M.W., 2008. Dysfunctional astrocytes as key players in the pathogenesis of central nervous system disorders. J Neurol Sci 267, 3–16. https://doi.org/10.1016/j.jns.2007.08.044

de Stefani, D., Raffaello, A., Teardo, E., Szabó, I., Rizzuto, R., 2011. A forty-kilodalton protein of the inner membrane is the mitochondrial calcium uniporter. Nature 476, 336–340. https://doi.org/10.1038/NATURE10230

Delanty, N., Dichter, M.A., 1998. Oxidative injury in the nervous system. Acta Neurol Scand 98, 145–53.

Drago, I., de Stefani, D., Rizzuto, R., Pozzan, T., 2012. Mitochondrial Ca2+ uptake contributes to buffering cytoplasmic Ca2+ peaks in cardiomyocytes. Proceedings of the National Academy of Sciences 109, 12986–12991. https://doi.org/10.1073/pnas.1210718109

Dulamea, A.O., 2017. The contribution of oligodendrocytes and oligodendrocyte progenitor cells to central nervous system repair in multiple sclerosis: perspectives for remyelination therapeutic strategies. Neural Regen Res 12, 1939–1944. https://doi.org/10.4103/1673-5374.221146

Duncan, G.J., Simkins, T.J., Emery, B., 2021. Neuron-Oligodendrocyte Interactions in the Structure and Integrity of Axons. Front Cell Dev Biol 9, 460. https://doi.org/10.3389/FCELL.2021.653101/BIBTEX

Duran, M., Kamerling, J.P., Bakker, H.D., van Gennip, A.H., Wadman, S.K., 1980. L-2-Hydroxyglutaric aciduria: an inborn error of metabolism? J Inherit Metab Dis 3, 109–12.

Elsayed, N.A., Boyer, T.M., Burd, I., 2021. Fetal Neuroprotective Strategies: Therapeutic Agents and Their Underlying Synaptic Pathways. Front Synaptic Neurosci 13, 33. https://doi.org/10.3389/FNSYN.2021.680899/BIBTEX

Faas, M.M., de Vos, P., 2020. Mitochondrial function in immune cells in health and disease. Biochim Biophys Acta Mol Basis Dis 1866. https://doi.org/10.1016/J.BBADIS.2020.165845

Fernandez-Castaneda, A., Gaultier, A., 2016. Adult oligodendrocyte progenitor cells - multifaceted regulators of the CNS in health and disease. Brain Behav Immun 57, 1. https://doi.org/10.1016/J.BBI.2016.01.005

Figueira, T.R., Barros, M.H., Camargo, A.A., Castilho, R.F., Ferreira, J.C.B., Kowaltowski, A.J., Sluse, F.E., Souza-Pinto, N.C., Vercesi, A.E., 2013. Mitochondria as a source of reactive

oxygen and nitrogen species: from molecular mechanisms to human health. Antioxid Redox Signal 18, 2029–2074. https://doi.org/10.1089/ARS.2012.4729

Fu, R., Shen, Q., Xu, P., Luo, J.J., Tang, Y., 2014. Phagocytosis of microglia in the central nervous system diseases. Mol Neurobiol 49, 1422–1434. https://doi.org/10.1007/S12035-013-8620-6

Fulton, D., Paez, P.M., Campagnoni, A.T., 2010. The multiple roles of myelin protein genes during the development of the oligodendrocyte. ASN Neuro 2, 25–37. https://doi.org/10.1042/AN20090051

Giacci, M.K., Bartlett, C.A., Smith, N.M., Iyer, K.S., Toomey, L.M., Jiang, H., Guagliardo, P., Kilburn, M.R., Fitzgerald, M., 2018. Oligodendroglia Are Particularly Vulnerable to Oxidative Damage after Neurotrauma In Vivo. The Journal of Neuroscience 38, 6491. https://doi.org/10.1523/JNEUROSCI.1898-17.2018

Gibson, K.M., Craigen, W., Herman, G.E., Jakobs, C., 1993a. D-2-hydroxyglutaric aciduria in a newborn with neurological abnormalities: a new neurometabolic disorder? J Inherit Metab Dis 16, 497–500.

Gibson, K.M., ten Brink, H.J., Schor, D.S., Kok, R.M., Bootsma, A.H., Hoffmann, G.F., Jakobs, C., 1993b. Stable-isotope dilution analysis of D- and L-2-hydroxyglutaric acid: application to the detection and prenatal diagnosis of D- and L-2-hydroxyglutaric acidemias. Pediatr Res 34, 277–80. https://doi.org/10.1203/00006450-199309000-00007

Gregersen, N., Ingerslev, J., Rasmussen, K., 1977. Low molecular weight organic acids in the urine of the newborn. Acta Paediatr Scand 66, 85–9.

Guan, W., Cao, J.-W., Liu, L.-Y., Zhao, Z.-H., Fu, Y., Yu, Y.-C., 2017. Eye opening differentially modulates inhibitory synaptic transmission in the developing visual cortex. Elife 6. https://doi.org/10.7554/ELIFE.32337

Guerreiro, G., Faverzani, J., Moura, A.P., Volfart, V., Gome dos Reis, B., Sitta, A., Gonzalez, E.A., de Lima Rosa, G., Coitinho, A.S., Baldo, G., Wajner, M., Vargas, C.R., 2021. Protective effects of L-carnitine on behavioral alterations and neuroinflammation in striatum of glutaryl-COA dehydrogenase deficient mice. Arch Biochem Biophys 709. https://doi.org/10.1016/J.ABB.2021.108970

Gulcin, İ., Buyukokuroglu, M.E., Kufrevioglu, O.I., 2003. Metal chelating and hydrogen peroxide scavenging effects of melatonin. J Pineal Res 34, 278–281. https://doi.org/10.1034/j.1600-079X.2003.00042.x

Gunduz, A., Aktuglu-Zeybek, A.C., Tezer, D., Enver, E.O., Zubarioglu, T., Kiykim, E., E. Kiziltan, M., 2022. Postural tremor in L-2-hydroxyglutaric aciduria is associated with cerebellar atrophy. Neurol Sci 43, 2051–2058. https://doi.org/10.1007/S10072-021-05555-X

Halliwell, B., 2006. Reactive Species and Antioxidants. Redox Biology Is a Fundamental Theme of Aerobic Life. Plant Physiol 141, 312–322. https://doi.org/10.1104/pp.106.077073

Halliwell, B., Gutteridge, J., 2015a. Oxygen: boon yet bane, in: Free Radicals in Biology and Medicine. Oxford University Press Inc., New York, NY, pp. 1–29.

Halliwell, B., Gutteridge, J., 2015b. Antioxidants from the diet, in: Free Radicals in Biology and Medicine. Oxford University Press Inc., New York, NY, pp. 153–197.

Halliwell, B., Gutteridge, J., 2015c. Antioxidant defenses synthesized in vivo, in: Free Radicals in Biology and Medicine. Oxford University Press Inc., New York, NY, pp. 77–151.

Halliwell, B., Gutteridge, J.M.C., 2015. Oxidative stress and redox regulation: adaptation, damage, repair, senescence, and death, in: Free Radicals in Biology and Medicine. Oxford University Press, New York, NY, pp. 199–2083. https://doi.org/10.1093/acprof:oso/9780198717478.001.0001

Hamann, I., Petroll, K., Grimm, L., Hartwig, A., Klotz, L.-O., 2014. Insulin-like modulation of Akt/FoxO signaling by copper ions is independent of insulin receptor. Arch Biochem Biophys 558, 42–50. https://doi.org/10.1016/j.abb.2014.06.004

Han, H., Myllykoski, M., Ruskamo, S., Wang, C., Kursula, P., 2013. Myelin-specific proteins: a structurally diverse group of membrane-interacting molecules. Biofactors 39, 233–241. https://doi.org/10.1002/BIOF.1076

Hines, D.J., Hines, R.M., Mulligan, S.J., Macvicar, B.A., 2009. Microglia processes block the spread of damage in the brain and require functional chloride channels. Glia 57, 1610–1618. https://doi.org/10.1002/GLIA.20874

Hoek, J.B., Rydstrom, J., 1988. Physiological roles of nicotinamide nucleotide transhydrogenase. Biochem J 254, 1–10. https://doi.org/10.1042/BJ2540001

Hoffmann, G.F., von Kries, R., Klose, D., Lindner, M., Schulze, A., Muntau, A.C., R�schinger, W., Liebl, B., Mayatepek, E., Roscher, A.A., 2004. Frequencies of inherited organic acidurias and disorders of mitochondrial fatty acid transport and oxidation in Germany. Eur J Pediatr 163, 76–80. https://doi.org/10.1007/s00431-003-1246-3

Hoogland, I.C.M., Houbolt, C., van Westerloo, D.J., van Gool, W.A., van de Beek, D., 2015. Systemic inflammation and microglial activation: Systematic review of animal experiments. J Neuroinflammation 12, 1–13. https://doi.org/10.1186/S12974-015-0332-6/TABLES/5

Horvath, G., Reglődi, D., Farkas, J., Vadasz, G., Mammel, B., Kvarik, T., Bodzai, G., Kiss-Illes, B., Farkas, D., Matkovits, A., Manavalan, S., Gaszner, B., Tamas, A., Kiss, P., 2015. Perinatal positive and negative influences on the early neurobehavioral reflex and motor development. Adv Neurobiol 10, 149–167. https://doi.org/10.1007/978-1-4939-1372-5_8

Hovens, I.B., Nyakas, C., Schoemaker, R.G., 2014. A novel method for evaluating microglial activation using ionized calcium-binding adaptor protein-1 staining: cell body to cell size ratio. Neuroimmunol Neuroinflamm 1, 82–88. https://doi.org/10.4103/2347-8659.139719

Hughes, E.G., Kang, S.H., Fukaya, M., Bergles, D.E., 2013. Oligodendrocyte progenitors balance growth with self-repulsion to achieve homeostasis in the adult brain. Nat Neurosci 16, 668–676. https://doi.org/10.1038/NN.3390

Irani, K., 2000. Oxidant signaling in vascular cell growth, death, and survival : a review of the roles of reactive oxygen species in smooth muscle and endothelial cell mitogenic and apoptotic signaling. Circ Res 87, 179–83.

Javadov, S., Kozlov, A. v., Camara, A.K.S., 2020. Mitochondria in Health and Diseases. Cells 9. https://doi.org/10.3390/CELLS9051177

Jović, N.J., Kosać, A., Koprivšek, K., 2014. L-2-hydroxyglutaric aciduria: A case report. Srp Arh Celok Lek 142, 337–341. https://doi.org/10.2298/SARH1406337J

Junqueira, D., Brusque, A.M., Porciúncula, L.O., Rotta, L.N., Frizzo, M.E.S., Wyse, A.T.S., Wannmacher, C.M.D., Souza, D.O., Wajner, M., 2004. In vitro effects of D-2-hydroxyglutaric acid on glutamate binding, uptake and release in cerebral cortex of rats. J Neurol Sci 217, 189–194. https://doi.org/10.1016/j.jns.2003.10.005

Junqueira, D., Brusque, A.M., Porciúncula, L.O., Rotta, L.N., Ribeiro, C.A.J., Frizzo, M.E.S., Dutra Filho, C.S., Wannmacher, C.M.D., Wyse, A.T.S., Souza, D.O., Wajner, M., 2003. Effects of L-2-hydroxyglutaric acid on various parameters of the glutamatergic system in cerebral cortex of rats. Metab Brain Dis 18, 233–243. https://doi.org/10.1023/A:1025559200816

Karunanidhi, A., Van't Land, C., Rajasundaram, D., Grings, M., Vockley, J., Mohsen, A., 2022. Medium branched chain fatty acids improve the profile of tricarboxylic acid cycle intermediates in mitochondrial fatty acid β-oxidation deficient cells: A comparative study. J Inherit Metab Dis 45, 541–556. https://doi.org/10.1002/jimd.12480

Katz, L.C., Shatz, C.J., 1996. Synaptic Activity and the Construction of Cortical Circuits. Science (1979) 274, 1133–1138. https://doi.org/10.1126/SCIENCE.274.5290.1133

Kölker, S., Pawlak, V., Ahlemeyer, B., Okun, J.G., Hörster, F., Mayatepek, E., Krieglstein, J., Hoffmann, G.F., Köhr, G., 2002. NMDA receptor activation and respiratory chain complex V inhibition contribute to neurodegeneration in D-2-hydroxyglutaric aciduria. European Journal of Neuroscience 16, 21–28. https://doi.org/10.1046/j.1460-9568.2002.02055.x

Kowaltowski, A.J., Castilho, R.F., Vercesi, A.E., 2001. Mitochondrial permeability transition and oxidative stress. FEBS Lett 495, 12–15. https://doi.org/10.1016/S0014-5793(01)02316-X

Kranendijk, M., Salomons, G.S., Gibson, K.M., Van Schaftingen, E., Jakobs, C., Struys, E.A., 2011. A lymphoblast model for IDH2 gain-of-function activity in d-2-hydroxyglutaric aciduria type II: Novel avenues for biochemical and therapeutic studies. Biochim Biophys Acta Mol Basis Dis 1812, 1380–1384. https://doi.org/10.1016/j.bbadis.2011.08.006

Kranendijk, M., Struys, E.A., Gibson, K.M., Wickenhagen, W. V., Abdenur, J.E., Buechner, J., Christensen, E., De Kremer, R.D., Errami, A., Gissen, P., Gradowska, W., Hobson, E., Islam, L., Korman, S.H., Kurczynski, T., Maranda, B., Meli, C., Rizzo, C., Sansaricq, C., Trefz, F.K., Webster, R., Jakobs, C., Salomons, G.S., 2010a. Evidence for genetic heterogeneity in D-2-hydroxyglutaric aciduria. Hum Mutat 31, 279–283. https://doi.org/10.1002/humu.21186

Kranendijk, M., Struys, E.A., Salomons, G.S., van der Knaap, M.S., Jakobs, C., 2012. Progress in understanding 2-hydroxyglutaric acidurias. J Inherit Metab Dis 35, 571–587. https://doi.org/10.1007/s10545-012-9462-5

Kranendijk, M., Struys, E.A., van Schaftingen, E., Gibson, K.M., Kanhai, W.A., van der Knaap, M.S., Amiel, J., Buist, N.R., Das, A.M., de Klerk, J.B., Feigenbaum, A.S., Grange, D.K., Hofstede, F.C., Holme, E., Kirk, E.P., Korman, S.H., Morava, E., Morris, A., Smeitink, J., Sukhai, R.N., Vallance, H., Jakobs, C., Salomons, G.S., 2010b. IDH2 mutations in patients with D-2-hydroxyglutaric aciduria. Science 330, 336. https://doi.org/10.1126/science.1192632

Kreutzberg, G.W., 1996. Microglia: a sensor for pathological events in the CNS. Trends Neurosci 19, 312–318. https://doi.org/10.1016/0166-2236(96)10049-7

Kwon, H.S., Koh, S.H., 2020. Neuroinflammation in neurodegenerative disorders: the roles of microglia and astrocytes. Translational Neurodegeneration 2020 9:1 9, 1–12. https://doi.org/10.1186/S40035-020-00221-2

Lakshminarayanan, V., Drab-Weiss, E.A., Roebuck, K.A., 1998. H2O2 and tumor necrosis factor-alpha induce differential binding of the redox-responsive transcription factors AP-1 and NF-kappaB to the interleukin-8 promoter in endothelial and epithelial cells. J Biol Chem 273, 32670–8.

Latini, A., da Silva, C.G., Ferreira, G.C., Schuck, P.F., Scussiato, K., Sarkis, J.J., Dutra Filho, C.S., Wyse, A.T.S., Wannmacher, C.M.D., Wajner, M., 2005. Mitochondrial energy metabolism is markedly impaired by D-2-hydroxyglutaric acid in rat tissues. Mol Genet Metab 86, 188–199. https://doi.org/10.1016/j.ymgme.2005.05.002

Latini, A., Scussiato, K., Borba Rosa, R., Leipnitz, G., Llesuy, S., Belló-Klein, A., Dutra-Filho, C.S., Wajner, M., 2003a. Induction of oxidative stress by L-2-hydroxyglutaric acid in rat brain. J Neurosci Res 74, 103–110. https://doi.org/10.1002/jnr.10735

Latini, A., Scussiato, K., Rosa, R.B., Llesuy, S., Belló-Klein, A., Dutra-Filho, C.S., Wajner, M., 2003b. D-2-hydroxyglutaric acid induces oxidative stress in cerebral cortex of young rats. European Journal of Neuroscience 17, 2017–2022. https://doi.org/10.1046/j.1460-9568.2003.02639.x

Lee, J., Gravel, M., Zhang, R., Thibault, P., Braun, P.E., 2005. Process outgrowth in oligodendrocytes is mediated by CNP, a novel microtubule assembly myelin protein. J Cell Biol 170, 661–673. https://doi.org/10.1083/JCB.200411047

Lehninger, A.L., Vercesi, A., Bababunmi, E.A., 1978. Regulation of Ca2+ release from mitochondria by the oxidation-reduction state of pyridine nucleotides. Proc Natl Acad Sci U S A 75, 1690–1694. https://doi.org/10.1073/PNAS.75.4.1690

Lenz, K.M., Nelson, L.H., 2018. Microglia and beyond: Innate immune cells as regulators of brain development and behavioral function. Front Immunol 9, 698. https://doi.org/10.3389/FIMMU.2018.00698/BIBTEX

Liu, X., Kim, C.N., Yang, J., Jemmerson, R., Wang, X., 1996. Induction of apoptotic program in cell-free extracts: requirement for dATP and cytochrome c. Cell 86, 147–157. https://doi.org/10.1016/S0092-8674(00)80085-9

Luo, M., Anderson, M.E., 2013. Mechanisms of Altered Ca 2+ Handling in Heart Failure. Circ Res 113, 690–708. https://doi.org/10.1161/CIRCRESAHA.113.301651

Maciel, E.N., Kowaltowski, A.J., Schwalm, F.D., Rodrigues, J.M., Souza, D.O., Vercesi, A.E., Wajner, M., Castilho, R.F., 2004. Mitochondrial permeability transition in neuronal damage promoted by Ca2+ and respiratory chain complex II inhibition. J Neurochem 90, 1025–1035. https://doi.org/10.1111/J.1471-4159.2004.02565.X

Mayatepek, E., Hoffmann, G.F., Baumgartner, R., Schulze, A., Jakobs, C., Trefz, F.K., Bremer, H.J., 1996. Atypical vitamin B12-unresponsive methylmalonic aciduria in sibship with severe progressive encephalomyelopathy: a new genetic disease? Eur J Pediatr 155, 398–403.

McGeer, P.L., McGeer, E.G., 2008. Glial reactions in Parkinson's disease. Movement Disorders 23, 474–483. https://doi.org/10.1002/mds.21751

Mirandola, S.R., Melo, D.R., Saito, Â., Castilho, R.F., 2010. 3-nitropropionic acid-induced mitochondrial permeability transition: comparative study of mitochondria from different tissues and brain regions. J Neurosci Res 88, 630–639. https://doi.org/10.1002/JNR.22239

Motavaf, M., Piao, X., 2021. Oligodendrocyte Development and Implication in Perinatal White Matter Injury. Front Cell Neurosci 15, 444. https://doi.org/10.3389/FNCEL.2021.764486/BIBTEX

Moura, A.P., Parmeggiani, B., Gasparotto, J., Grings, M., Fernandez Cardoso, G.M., Seminotti, B., Moreira, J.C.F., Gelain, D.P., Wajner, M., Leipnitz, G., 2018. Glycine Administration Alters MAPK Signaling Pathways and Causes Neuronal Damage in Rat Brain: Putative Mechanisms Involved in the Neurological Dysfunction in Nonketotic Hyperglycinemia. Mol Neurobiol 55, 741–750. https://doi.org/10.1007/s12035-016-0319-z

Moura, A.P., Parmeggiani, B., Grings, M., Alvorcem, L. de M., Boldrini, R.M., Bumbel, A.P., Motta, M.M., Seminotti, B., Wajner, M., Leipnitz, G., 2016. Intracerebral Glycine Administration Impairs Energy and Redox Homeostasis and Induces Glial Reactivity in Cerebral Cortex of Newborn Rats. Mol Neurobiol 53, 5864–5875. https://doi.org/10.1007/s12035-015-9493-7

Nagele, R.G., Wegiel, Jerzy, Venkataraman, V., Imaki, H., Wang, K.-C., Wegiel, Jarek, 2004. Contribution of glial cells to the development of amyloid plaques in Alzheimer's disease. Neurobiol Aging 25, 663–74. https://doi.org/10.1016/j.neurobiolaging.2004.01.007

Nave, K.A., 2010. Myelination and support of axonal integrity by glia. Nature 468, 244–252. https://doi.org/10.1038/NATURE09614

Nelson, D.L., Cox, M.M., 2017. Lehninger Principles of Biochemistry, 7th ed.

Nicholls, D.G., Ferguson, S., 2013. Bioenergetics, Bioenergetics: Fourth Edition. Elsevier. https://doi.org/10.1016/C2010-0-64902-9

Norden, D.M., Trojanowski, P.J., Villanueva, E., Navarro, E., Godbout, J.P., 2016. Sequential activation of microglia and astrocyte cytokine expression precedes increased iba-1 or GFAP immunoreactivity following systemic immune challenge. Glia 64, 300–316. https://doi.org/10.1002/GLIA.22930

Nunnari, J., Suomalainen, A., 2012. Mitochondria: In Sickness and in Health. Cell 148, 1145. https://doi.org/10.1016/J.CELL.2012.02.035

Oksanen, M., Lehtonen, S., Jaronen, M., Goldsteins, G., Hämäläinen, R.H., Koistinaho, J., 2019. Astrocyte alterations in neurodegenerative pathologies and their modeling in human induced pluripotent stem cell platforms. Cell Mol Life Sci 76, 2739–2760. https://doi.org/10.1007/S00018-019-03111-7

Olivera-Bravo, S., Fernández, A., Sarlabós, M.N., Rosillo, J.C., Casanova, G., Jiménez, M., Barbeito, L., 2011. Neonatal astrocyte damage is sufficient to trigger progressive striatal degeneration in a rat model of glutaric acidemia-I. PLoS One 6, e20831. https://doi.org/10.1371/journal.pone.0020831

Olivera-Bravo, S., Ribeiro, C.A.J., Isasi, E., Trías, E., Leipnitz, G., Díaz-Amarilla, P., Woontner, M., Beck, C., Goodman, S.I., Souza, D., Wajner, M., Barbeito, L., 2015. Striatal neuronal death mediated by astrocytes from the Gcdh−/− mouse model of glutaric acidemia type I. Hum Mol Genet 24, 4504–4515. https://doi.org/10.1093/hmg/ddv175

Ong, S.-B., Gustafsson, A.B., 2012. New roles for mitochondria in cell death in the reperfused myocardium. Cardiovasc Res 94, 190–196. https://doi.org/10.1093/cvr/cvr312

Onishi, M., Yamano, K., Sato, M., Matsuda, N., Okamoto, K., 2021. Molecular mechanisms and physiological functions of mitophagy. EMBO J 40. https://doi.org/10.15252/EMBJ.2020104705

Pan, X., Liu, J., Nguyen, T., Liu, C., Sun, J., Teng, Y., Fergusson, M.M., Rovira, I.I., Allen, M., Springer, D.A., Aponte, A.M., Gucek, M., Balaban, R.S., Murphy, E., Finkel, T., 2013. The physiological role of mitochondrial calcium revealed by mice lacking the mitochondrial calcium uniporter. Nat Cell Biol 15, 1464–1472. https://doi.org/10.1038/NCB2868

Pecka, M., Han, Y., Sader, E., Mrsic-Flogel, T.D., 2014. Experience-Dependent Specialization of Receptive Field Surround for Selective Coding of Natural Scenes. Neuron 84, 457–469. https://doi.org/10.1016/j.neuron.2014.09.010

Pendin, D., Greotti, E., Pozzan, T., 2014. The elusive importance of being a mitochondrial Ca(2+) uniporter. Cell Calcium 55, 139–145. https://doi.org/10.1016/J.CECA.2014.02.008

Pieri, C., Marra, M., Moroni, F., Recchioni, R., Marcheselli, F., 1994. Melatonin: A peroxyl radical scavenger more effective than vitamin E. Life Sci 55, PL271–PL276. https://doi.org/10.1016/0024-3205(94)00666-0

Popov, L.D., 2020. Mitochondrial biogenesis: An update. J Cell Mol Med 24, 4892. https://doi.org/10.1111/JCMM.15194

Rai, Y., Pathak, R., Kumari, N., Sah, D.K., Pandey, S., Kalra, N., Soni, R., Dwarakanath, B.S., Bhatt, A.N., 2018. Mitochondrial biogenesis and metabolic hyperactivation limits the application of MTT assay in the estimation of radiation induced growth inhibition. Sci Rep 8, 1531. https://doi.org/10.1038/s41598-018-19930-w

Ramos, J.M.P., Bussi, C., Gaviglio, E.A., Arroyo, D.S., Baez, N.S., Rodriguez-Galan, M.C., Iribarren, P., 2017. Type I IFNs Are Required to Promote Central Nervous System Immune Surveillance through the Recruitment of Inflammatory Monocytes upon Systemic Inflammation. Front Immunol 8. https://doi.org/10.3389/FIMMU.2017.01666

Rashed, M., Ozand, P.T., al Aqeel, A., Gascon, G.G., 1994. Experience of King Faisal Specialist Hospital and Research Center with Saudi organic acid disorders. Brain Dev 16 Suppl, 1–6.

Rasola, A., Bernardi, P., 2011. Mitochondrial permeability transition in Ca(2+)-dependent apoptosis and necrosis. Cell Calcium 50, 222–233. https://doi.org/10.1016/J.CECA.2011.04.007

Reiter, R.J., Mayo, J.C., Tan, D.-X., Sainz, R.M., Alatorre-Jimenez, M., Qin, L., 2016. Melatonin as an antioxidant: under promises but over delivers. J Pineal Res 61, 253–278. https://doi.org/10.1111/jpi.12360

Reiter, R.J., Tan, D.X., Manchester, L.C., Qi, W., 2001. Biochemical reactivity of melatonin with reactive oxygen and nitrogen species: a review of the evidence. Cell Biochem Biophys 34, 237–56. https://doi.org/10.1385/CBB:34:2:237

Reiter, R.J., Tan, D.-X., Rosales-Corral, S., Manchester, L.C., 2013. The universal nature, unequal distribution and antioxidant functions of melatonin and its derivatives. Mini Rev Med Chem 13, 373–84. https://doi.org/10.2174/1389557511313030006

Ribeiro, R.T., Seminotti, B., Zanatta, Â., de Oliveira, F.H., Amaral, A.U., Leipnitz, G., Wajner, M., 2021. Neuronal Death, Glial Reactivity, Microglia Activation, Oxidative Stress and Bioenergetics Impairment Caused by Intracerebroventricular Administration of D-2-hydroxyglutaric Acid to Neonatal Rats. Neuroscience 471, 115–132. https://doi.org/10.1016/J.NEUROSCIENCE.2021.07.024

Ribeiro, R.T., Zanatta, Â., Amaral, A.U., Leipnitz, G., de Oliveira, F.H., Seminotti, B., Wajner, M., 2018. Experimental Evidence that In Vivo Intracerebral Administration of L-2-Hydroxyglutaric Acid to Neonatal Rats Provokes Disruption of Redox Status and Histopathological Abnormalities in the Brain. Neurotox Res 33, 681–692. https://doi.org/10.1007/s12640-018-9874-6

Rizzuto, R., de Stefani, D., Raffaello, A., Mammucari, C., 2012. Mitochondria as sensors and regulators of calcium signalling. Nat Rev Mol Cell Biol 13, 566–578. https://doi.org/10.1038/NRM3412

Rosenberg, P., 2004. Mitochondrial dysfunction and heart disease. Mitochondrion 4, 621–628. https://doi.org/10.1016/j.mito.2004.07.016

Rushmore, T.H., Morton, M.R., Pickett, C.B., 1991. The antioxidant responsive element. Activation by oxidative stress and identification of the DNA consensus sequence required for functional activity. J Biol Chem 266, 11632–9.

Rzem, R., Achouri, Y., Marbaix, E., Schakman, O., Wiame, E., Marie, S., Gailly, P., Vincent, M.F., Veiga-Da-cunha, M., van Schaftingen, E., 2015. A mouse model of L-2-hydroxyglutaric aciduria, a disorder of metabolite repair. PLoS One 10. https://doi.org/10.1371/journal.pone.0119540

Rzem, R., Veiga-Da-Cunha, M., Noël, G., Goffette, S., Nassogne, M.C., Tabarki, B., Schöller, C., Marquardt, T., Vikkula, M., van Schaftingen, E., 2004. A gene encoding a putative FAD-dependent L-2-hydroxyglutarate dehydrogenase is mutated in L-2-hydroxyglutaric aciduria. Proc Natl Acad Sci U S A 101, 16849–16854. https://doi.org/10.1073/PNAS.0404840101

Samuraki, M., Komai, K., Hasegawa, Y., Kimura, M., Yamaguchi, S., Terada, N., Yamada, M., 2008. A successfully treated adult patient with L-2-hydroxyglutaric aciduria. Neurology 70, 1051–1052. https://doi.org/10.1212/01.WNL.0000287141.90944.95

Sasaki, Y., Ohsawa, K., Kanazawa, H., Kohsaka, S., Imai, Y., 2001. Iba1 Is an Actin-Cross-Linking Protein in Macrophages/Microglia. Biochem Biophys Res Commun 286, 292–297. https://doi.org/10.1006/BBRC.2001.5388

Sauer, S.W., Opp, S., Mahringer, A., Kamiński, M.M., Thiel, C., Okun, J.G., Fricker, G., Morath, M.A., Kölker, S., 2010. Glutaric aciduria type I and methylmalonic aciduria: Simulation of cerebral import and export of accumulating neurotoxic dicarboxylic acids in in vitro

models of the blood–brain barrier and the choroid plexus. Biochimica et Biophysica Acta (BBA) - Molecular Basis of Disease 1802, 552–560. https://doi.org/10.1016/j.bbadis.2010.03.003

Seminotti, B., Brondani, M., Ribeiro, R.T., Leipnitz, G., Wajner, M., 2022a. Disturbance of Mitochondrial Dynamics, Endoplasmic Reticulum-Mitochondria Crosstalk, Redox Homeostasis, and Inflammatory Response in the Brain of Glutaryl-CoA Dehydrogenase-Deficient Mice: Neuroprotective Effects of Bezafibrate. Mol Neurobiol 59, 4839–4853. https://doi.org/10.1007/S12035-022-02887-3

Seminotti, B., Brondani, M., Ribeiro, R.T., Leipnitz, G., Wajner, M., 2022b. Disturbance of Mitochondrial Dynamics, Endoplasmic Reticulum-Mitochondria Crosstalk, Redox Homeostasis, and Inflammatory Response in the Brain of Glutaryl-CoA Dehydrogenase-Deficient Mice: Neuroprotective Effects of Bezafibrate. Mol Neurobiol 59, 4839–4853. https://doi.org/10.1007/s12035-022-02887-3

Seminotti, B., da Silva, J.C., Ribeiro, R.T., Leipnitz, G., Wajner, M., 2019a. Free Radical Scavengers Prevent Argininosuccinic Acid-Induced Oxidative Stress in the Brain of Developing Rats: a New Adjuvant Therapy for Argininosuccinate Lyase Deficiency? Mol Neurobiol. https://doi.org/10.1007/s12035-019-01825-0

Seminotti, B., Zanatta, Â., Ribeiro, R.T., da Rosa, M.S., Wyse, A.T.S., Leipnitz, G., Wajner, M., 2019b. Disruption of Brain Redox Homeostasis, Microglia Activation and Neuronal Damage Induced by Intracerebroventricular Administration of S-Adenosylmethionine to Developing Rats. Mol Neurobiol 56, 2760–2773. https://doi.org/10.1007/s12035-018-1275-6

Shiraishi, H., Yamada, K., Egawa, K., Ishige, M., Ochi, F., Watanabe, A., Kawakami, S., Kuzume, K., Watanabe, K., Sameshima, K., Nakamagoe, K., Tamaoka, A., Asahina, N., Yokoshiki, S., Kobayashi, K., Miyakoshi, T., Oba, K., Isoe, T., Hayashi, H., Yamaguchi, S., Sato, N., 2021. Efficacy of bezafibrate for preventing myopathic attacks in patients with very long-chain acyl-CoA dehydrogenase deficiency. Brain Dev 43, 214–219. https://doi.org/10.1016/J.BRAINDEV.2020.07.019

Simons, M., Nave, K.A., 2015. Oligodendrocytes: Myelination and Axonal Support. Cold Spring Harb Perspect Biol 8. https://doi.org/10.1101/CSHPERSPECT.A020479

Smith, J.A., Das, A., Ray, S.K., Banik, N.L., 2012. Role of pro-inflammatory cytokines released from microglia in neurodegenerative diseases. Brain Res Bull 87, 10–20. https://doi.org/10.1016/J.BRAINRESBULL.2011.10.004

Sofroniew, M. v., 2009. Molecular dissection of reactive astrogliosis and glial scar formation. Trends Neurosci 32, 638–647. https://doi.org/10.1016/J.TINS.2009.08.002

Sofroniew, M. V, Vinters, H. V, 2010. Astrocytes: biology and pathology. Acta Neuropathol 119, 7–35. https://doi.org/10.1007/s00401-009-0619-8

Southorn, P.A., Powis, G., 1988. Free radicals in medicine. I. Chemical nature and biologic reactions. Mayo Clin Proc 63, 381–9.

Starkov, A.A., 2010. The molecular identity of the mitochondrial Ca2+ sequestration system. FEBS J 277, 3652–3663. https://doi.org/10.1111/J.1742-4658.2010.07756.X

Steenweg, M.E., Jakobs, C., Errami, A., van Dooren, S.J.M., Adeva Bartolomé, M.T., Aerssens, P., Augoustides-Savvapoulou, P., Baric, I., Baumann, M., Bonafé, L., Chabrol, B., Clarke, J.T.R., Clayton, P., Coker, M., Cooper, S., Falik-Zaccai, T., Gorman, M., Hahn, A., Hasanoglu, A., King, M.D., de Klerk, H.B.C., Korman, S.H., Lee, C., Meldgaard Lund, A., Mejaski-Bosnjak, V., Pascual-Castroviejo, I., Raadhyaksha, A., Rootwelt, T., Roubertie, A., Ruiz-Falco, M.L., Scalais, E., Schimmel, U., Seijo-Martinez, M., Suri, M., Sykut-Cegielska, J., Trefz, F.K., Uziel, G., Valayannopoulos, V., Vianey-Saban, C., Vlaho, S., Vodopiutz, J., Wajner, M., Walter, J., Walter-Derbort, C., Yapici, Z., Zafeiriou, D.I., Spreeuwenberg, M.D., Celli, J., den Dunnen, J.T., van der Knaap, M.S., Salomons, G.S., 2010. An overview of L-2-hydroxyglutarate dehydrogenase gene (L2HGDH) variants: a genotype-phenotype study. Hum Mutat 31, 380–390. https://doi.org/10.1002/humu.21197

Steenweg, M.E., Salomons, G.S., Yapici, Z., Uziel, G., Scalais, E., Zafeiriou, D.I., Ruiz-Falco, M.L., Mejaški-Bošnjak, V., Augoustides-Savvopoulou, P., Wajner, M., Walter, J., Verhoeven-Duif, N.M., Struys, E.A., Jakobs, C., van der Knaap, M.S., 2009. l-2-Hydroxyglutaric Aciduria: Pattern of MR Imaging Abnormalities in 56 Patients1. https://doi.org/10.1148/radiol.2513080647 251, 856–865. https://doi.org/10.1148/RADIOL.2513080647

Stein, H., 2021. Why Does the Neocortex Need the Cerebellum for Working Memory? The Journal of Neuroscience 41, 6368. https://doi.org/10.1523/JNEUROSCI.0701-21.2021

Struys, E.A., Jansen, E.E.W., Verhoeven, N.M., Jakobs, C., 2004. Measurement of urinary D- and L-2-hydroxyglutarate enantiomers by stable-isotope-dilution liquid chromatography-tandem mass spectrometry after derivatization with diacetyl-L-tartaric anhydride. Clin Chem 50, 1391–5. https://doi.org/10.1373/clinchem.2004.033399

Švidrnoch, M., Přibylka, A., Bekárek, V., Ševčík, J., Smolka, V., Maier, V., 2016. Enantioseparation of d,l-2-hydroxyglutaric acid by capillary electrophoresis with tandem mass spectrometry—Fast and efficient tool for d- and l-2-hydroxyglutaracidurias diagnosis. J Chromatogr A 1467, 383–390. https://doi.org/10.1016/j.chroma.2016.05.095

Tanveer, A., Virji, S., Andreeva, L., Totty, N.F., Hsuan, J.J., Ward, J.M., Crompton, M., 1996. Involvement of cyclophilin D in the activation of a mitochondrial pore by Ca2+ and oxidant stress. Eur J Biochem 238, 166–172. https://doi.org/10.1111/J.1432-1033.1996.0166Q.X

Topçu, M., Aydin, Ö.F., Yalçinkaya, C., Haliloğlu, G., Aysun, S., Anlar, B., Topaloğlu, H., Turanli, G., Yalnizoğlu, D., Kesimer, M., Coşkun, T., 2005. L-2-hydroxyglutaric aciduria: a report of 29 patients. Turk J Pediatr 47, 1–7.

Topçu, M., Jobard, F., Halliez, S., Coskun, T., Yalçinkayal, C., Gerceker, F.O., Wanders, R.J.A., Prud'homme, J.F., Lathrop, M., Özguc, M., Fischer, J., 2004. L-2-Hydroxyglutaric aciduria: identification of a mutant gene C14orf160, localized on chromosome 14q22.1. Hum Mol Genet 13, 2803–2811. https://doi.org/10.1093/HMG/DDH300

Tzakos, A., Kursula, P., Troganis, A., Theodorou, V., Tselios, T., Svarnas, C., Matsoukas, J., Apostolopoulos, V., Gerothanassis, I., 2005. Structure and function of the myelin proteins: current status and perspectives in relation to multiple sclerosis. Curr Med Chem 12, 1569–1587. https://doi.org/10.2174/0929867054039026

Ünal-Çevik, I., Kilinç, M., Gürsoy-Özdemir, Y., Gurer, G., Dalkara, T., 2004. Loss of NeuN immunoreactivity after cerebral ischemia does not indicate neuronal cell loss: A cautionary note. Brain Res 1015, 169–174. https://doi.org/10.1016/J.BRAINRES.2004.04.032

van der Knaap, M.S., Jakobs, C., Hoffmann, G.F., Duran, M., Muntau, A.C., Schweitzer, S., Kelley, R.I., Parrot-Roulaud, F., Amiel, J., de Lonlay, P., Rabier, D., Eeg-Olofsson, O., 1999a. D-2-hydroxyglutaric aciduria: further clinical delineation. J Inherit Metab Dis 22, 404–13. https://doi.org/10.1023/a:1005548005393

van der Knaap, M.S., Jakobs, C., Hoffmann, G.F., Nyhan, W.L., Renier, W.O., Smeitink, J.A.M., Catsman-Berrevoets, C.E., Hjalmarson, O., Vallance, H., Sugita, K., Bowe, C.M., Herrin, J.T., Craigen, W.J., Buist, N.R.M., Brookfield, D.S.K., Chalmers, R.A., 1999b. D-2-Hydroxyglutaric aciduria: biochemical marker or clinical disease entity? Ann Neurol 45, 111–9. https://doi.org/10.1002/1531-8249(199901)45:1<111::AID-ART17>3.0.CO;2-N

Victor, S., Rocha-Ferreira, E., Rahim, A., Hagberg, H., Edwards, D., 2021. New possibilities for neuroprotection in neonatal hypoxic-ischemic encephalopathy. European Journal of Pediatrics 2021 181:3 181, 875–887. https://doi.org/10.1007/S00431-021-04320-8

Vockley, J., Burton, B., Berry, G., Longo, N., Phillips, J., Sanchez-Valle, A., Chapman, K., Tanpaiboon, P., Grunewald, S., Murphy, E., Lu, X., Cataldo, J., 2021. Effects of triheptanoin (UX007) in patients with long-chain fatty acid oxidation disorders: Results from an open-label, long-term extension study. J Inherit Metab Dis 44, 253–263. https://doi.org/10.1002/jimd.12313

Vockley, J., Enns, G.M., Ramirez, A.N., Bedrosian, C.L., Reineking, B., Lu, X., Ray, K., Rahman, S., Marsden, D., 2022. Response to triheptanoin therapy in critically ill patients with LC-FAOD: Report of patients treated through an expanded access program. Mol Genet Metab 136, 152–162. https://doi.org/10.1016/j.ymgme.2022.04.001

Wajner, M., 2019. Neurological manifestations of organic acidurias. Nat Rev Neurol 15, 253–271. https://doi.org/10.1038/s41582-019-0161-9

Wajner, M., Vargas, C.R., Funayama, C., Fernandez, A., Elias, M.L.C., Goodman, S.I., Jakobs, C., van der Knaap, M.S., 2002. D-2-hydroxyglutaric aciduria in a patient with a severe clinical phenotype and unusual MRI findings. J Inherit Metab Dis 25, 28–34. https://doi.org/10.1023/A:1015165212965/METRICS

Wakatsuki, A., Okatani, Y., Shinohara, K., Ikenoue, N., Fukaya, T., 2001. Melatonin protects against ischemia/reperfusion-induced oxidative damage to mitochondria in fetal rat brain. J Pineal Res 31, 167–172. https://doi.org/10.1034/J.1600-079X.2001.310211.X

Wall, S.B., Oh, J.-Y., Diers, A.R., Landar, A., 2012. Oxidative Modification of Proteins: An Emerging Mechanism of Cell Signaling. Front Physiol 3, 369. https://doi.org/10.3389/fphys.2012.00369

Wang, C., Neugebauer, U., Bürck, J., Myllykoski, M., Baumgärtel, P., Popp, J., Kursula, P., 2011. Charge Isomers of Myelin Basic Protein: Structure and Interactions with Membranes, Nucleotide Analogues, and Calmodulin. PLoS One 6, e19915. https://doi.org/10.1371/JOURNAL.PONE.0019915

Wang, F., Travins, J., Lin, Z., Si, Y., Chen, Y., Powe, J., Murray, S., Zhu, D., Artin, E., Gross, S., Santiago, S., Steadman, M., Kernytsky, A., Straley, K., Lu, C., Pop, A., Struys, E.A., Jansen, E.E.W., Salomons, G.S., David, M.D., Quivoron, C., Penard-Lacronique, V., Regan, K.S., Liu, W., Dang, L., Yang, H., Silverman, L., Agresta, S., Dorsch, M., Biller, S., Yen, K., Cang, Y., Su, S.S.M., Jin, S., 2016. A small molecule inhibitor of mutant IDH2 rescues cardiomyopathy in a D-2-hydroxyglutaric aciduria type II mouse model. J Inherit Metab Dis 39, 807–820. https://doi.org/10.1007/s10545-016-9960-y

Wang, F., Yang, Y.J., Yang, N., Chen, X.J., Huang, N.X., Zhang, J., Wu, Y., Liu, Z., Gao, X., Li, T., Pan, G.Q., Liu, S.B., Li, H.L., Fancy, S.P.J., Xiao, L., Chan, J.R., Mei, F., 2018. Enhancing Oligodendrocyte Myelination Rescues Synaptic Loss and Improves Functional Recovery after Chronic Hypoxia. Neuron 99, 689-701.e5. https://doi.org/10.1016/J.NEURON.2018.07.017

Webb, R., Hughes, M.G., Thomas, A.W., Morris, K., 2017. The Ability of Exercise-Associated Oxidative Stress to Trigger Redox-Sensitive Signalling Responses. Antioxidants (Basel) 6, 63. https://doi.org/10.3390/antiox6030063

Weimar, C., Schlamann, M., Krägeloh-Mann, I., Schöls, L., 2013. L-2 hydroxyglutaric aciduria as a rare cause of leukencephalopathy in adults. Clin Neurol Neurosurg 115, 765–766. https://doi.org/10.1016/j.clineuro.2012.06.040

Wirths, O., Breyhan, H., Marcello, A., Cotel, M.C., Brück, W., Bayer, T.A., 2010. Inflammatory changes are tightly associated with neurodegeneration in the brain and spinal cord of the APP/PS1KI mouse model of Alzheimer's disease. Neurobiol Aging 31, 747–757. https://doi.org/10.1016/J.NEUROBIOLAGING.2008.06.011

Wolf, H.K., Buslei, R., Schmidt-Kastner, R., Schmidt-Kastner, P.K., Pietsch, T., Wiestler, O.D., Blümcke, I., 1996. NeuN: a useful neuronal marker for diagnostic histopathology. J Histochem Cytochem 44, 1167–1171. https://doi.org/10.1177/44.10.8813082

Yadav, U.C.S., Ramana, K. V, 2013. Regulation of NF-κB-induced inflammatory signaling by lipid peroxidation-derived aldehydes. Oxid Med Cell Longev 2013, 690545. https://doi.org/10.1155/2013/690545

Yang, I., Han, S.J., Kaur, G., Crane, C., Parsa, A.T., 2010. The Role of Microglia in Central Nervous System Immunity and Glioma Immunology. J Clin Neurosci 17, 6. https://doi.org/10.1016/J.JOCN.2009.05.006

Yilmaz, K., 2009. Riboflavin treatment in a case with l-2-hydroxyglutaric aciduria. European Journal of Paediatric Neurology 13, 57–60. https://doi.org/10.1016/j.ejpn.2008.01.003

Young, K.M., Psachoulia, K., Tripathi, R.B., Dunn, S.J., Cossell, L., Attwell, D., Tohyama, K., Richardson, W.D., 2013. Oligodendrocyte dynamics in the healthy adult CNS: evidence for myelin remodeling. Neuron 77, 873–885. https://doi.org/10.1016/J.NEURON.2013.01.006

Zago, E.B., Castilho, R.F., Vercesi, A.E., 2000. The redox state of endogenous pyridine nucleotides can determine both the degree of mitochondrial oxidative stress and the solute selectivity of the permeability transition pore. FEBS Lett 478, 29–33. https://doi.org/10.1016/S0014-5793(00)01815-9

Zoratti, M., Szabò, I., 1995. The mitochondrial permeability transition. Biochim Biophys Acta 1241, 139–176. https://doi.org/10.1016/0304-4157(95)00003-A